ISSN 1881-7815 Online ISSN 1881-7823

BST
BioScience Trends

Volume 6, Number 4
August, 2012

IRCA
BSSA

IACMHR

www.biosciencetrends.com

BST
BioScience Trends

ISSN: 1881-7815
Online ISSN: 1881-7823
CODEN: BTIRCZ
Issues/Year: 6
Language: English
Publisher: IACMHR Co., Ltd.

BioScience Trends is one of a series of peer-reviewed journals of the International Research and Cooperation Association for Bio & Socio-Sciences Advancement (IRCA-BSSA) Group and is published bimonthly by the International Advancement Center for Medicine & Health Research Co., Ltd. (IACMHR Co., Ltd.) and supported by the IRCA-BSSA and Shandong University China-Japan Cooperation Center for Drug Discovery & Screening (SDU-DDSC).

BioScience Trends devotes to publishing the latest and most exciting advances in scientific research. Articles cover fields of life science such as biochemistry, molecular biology, clinical research, public health, medical care system, and social science in order to encourage cooperation and exchange among scientists and clinical researchers.

BioScience Trends publishes Original Articles, Brief Reports, Reviews, Policy Forum articles, Case Reports, News, and Letters on all aspects of the field of life science. All contributions should seek to promote international collaboration.

Editorial Board

Editorial Office

Pearl City Koishikawa 603,
2-4-5 Kasuga, Bunkyo-ku,
Tokyo 112-0003, Japan
Tel: +81-3-5840-8764
Fax: +81-3-5840-8765
E-mail: office@biosciencetrends.com

BioScience Trends

Editorial and Head Office

Pearl City Koishikawa 603, 2-4-5 Kasuga, Bunkyo-ku,
Tokyo 112-0003, Japan

Tel: +81-3-5840-8764, Fax: +81-3-5840-8765
E-mail: office@biosciencetrends.com
URL: www.biosciencetrends.com

Editorial Board Members

CONTENTS

Volume 6, Number 4, 2012

Brief Reports

Original Articles

CONTENTS (*Continued*)

(This journal was partially supported by a Grant-in-Aid for Scientific Research from Japan Society for the Promotion of Science.)

Brief Report

DOI: 10.5582/bst.2012.v6.4.153

Des-γ-carboxy prothrombin and c-Met were concurrently and extensively expressed in hepatocellular carcinoma and associated with tumor recurrence

Jianjun Gao[1,*], Xiaobin Feng[2,*], Yoshinori Inagaki[3], Peipei Song[1], Norihiro Kokudo[1], Kiyoshi Hasegawa[1], Yasuhiko Sugawara[1], Wei Tang[1,]**

[1] *Hepato-Biliary-Pancreatic Surgery Division, Department of Surgery, Graduate School of Medicine, The University of Tokyo, Tokyo, Japan;*
[2] *Institute of Hepatobiliary Surgery, Southwest Hospital, Third Military Medical University, Chongqing, China;*
[3] *The Laboratory of Microbiology, Graduate School of Pharmaceutical Sciences, The University of Tokyo, Tokyo, Japan.*

Summary **The aim of this study was to investigate co-expression of des-γ-carboxy prothrombin (DCP) and c-Met in hepatocellular carcinoma (HCC) and its significance in predicting tumor recurrence after surgical resection. Immunohistochemical techniques were used to examine DCP and c-Met expression in HCC samples collected from 153 patients. DCP and c-Met staining were observed in tumor areas in 63.4% (97/153) and 66.7% (102/153) of patients, respectively, and these figures are markedly higher than the rates at which adjacent nontumorous areas tested positive of 13.1% (20/154) and 28.8% (44/153). Furthermore, DCP and c-Met were consistently present or absent in HCC regions in 51.0% (78/153) and 20.9% (32/153) of patients, in adjacent nontumorous regions in 7.2% (11/153) and 65.4% (100/153) of patients, and in whole regions including HCC and adjacent nontumorous regions in 58.2% (89/153) and 19.6% (30/153) of patients. These results indicate that DCP and c-Met usually appeared or disappeared in HCC in a parallel manner. c-Met was found to be related to tumor recurrence in patients with HCC. When combined with DCP, c-Met is more effective at predicting non-recurrence of HCC than c-Met alone. Expression of neither DCP nor c-Met in HCC regions and adjacent regions signified a low rate of tumor recurrence after surgical resection. Results of the current study suggested that DCP and c-Met are commonly and concurrently expressed in HCC and their absence is associated with a low risk of tumor recurrence.**

Keywords: Des-γ-carboxy prothrombin (DCP), hepatocellular carcinoma (HCC), c-Met, histochemical expression, DCP/c-Met signal pathway, recurrence

1. Introduction

Hepatocellular carcinoma (HCC) is a severe condition that is found worldwide. Eastern Asian countries such as Japan and China are areas where HCC is highly prevalent due to serious hepatitis C virus (HCV)/ hepatitis B virus (HBV) infection in the population (*1,2*). Therapeutic regimens including liver transplantation, surgical resection, and local-regional therapy such as transarterial chemoembolization (TACE) play a major role in HCC management. Although these treatments as well as diagnostic modalities and clinical screening have made great progress in recent years, HCC continues to have a dismal prognosis, with 5-year recurrence at 40-70% due to invasion and metastasis prior to treatment (*3*). Therefore, a key step would be to explore prognostic factors to help distinguish patients with a high or low risk of recurrence and then adopt an appropriate approach for surveillance and treatment of this disease.

* Both contributed equally to this work.

** *Address correspondence to:*
Dr. Wei Tang, Hepato-Biliary-Pancreatic Surgery Division, Department of Surgery, Graduate School of Medicine, The University of Tokyo, 7-3-1 Hongo, Bunkyo-ku, Tokyo, Japan.
E-mail: TANG-SUR@h.u-tokyo.ac.jp

The *c-Met* proto-oncogene was originally identified as a transforming gene activated after *in vitro* treatment of a human osteosarcoma cell line with a chemical carcinogen, *N*-methyl-*N'*-nitro-*N*-nitrosoguanidine (*4*). Molecular cloning studies revealed that it encodes a protein tyrosine kinase that is now known as the cell surface receptor for hepatocyte growth factor (HGF) (*5*). Activation of the c-Met signaling pathway is involved in diverse cellular responses such as mitogenesis, motogenesis, or morphogenesis depending on the particular cell type and the microenvironment (*6*). Expression of c-Met in HCC was reported to be linked to an unfavorable clinicopathologic status, including a high proliferation index, low degree of differentiation, and vascular invasion and metastasis (*3,7-11*). In addition, a high level of c-Met is correlated with a poor prognosis, including risk of tumor recurrence and short survival time (*3,12-14*). These studies suggest that c-Met might serve as a prognostic factor for HCC. That said, previous studies found that HGF, the natural ligand of c-Met, was not expressed or activated in normal liver tissue and was often absent in human HCC tissues (*8,9,15,16*). HCC tissues that are positive for HGF have a rather homogeneous HGF signal that is not correlated with the histological grade or other morphological features (*8*). These results seem to suggest that activation of the c-Met signal transduction pathway seems to depend on factors other than HGF in HCC pathology. Thus far, the potential factors that trigger c-Met signal transduction and contribute to the initiation and progression of HCC are, at least in part, largely unknown.

Recent studies by the current authors and other researchers found that des-γ-carboxy prothrombin (DCP), an abnormal cytokine secreted by HCC cells, was involved in the activation and regulation of downstream pathways of the c-Met signaling system *in vitro* and in animal studies (*17-20*). Thus, whether or not DCP and c-Met are co-expressed in human HCC and whether their co-expression is correlated with tumor recurrence are questions of great interest. The present study focuses on the expression profiles of DCP and c-Met in human HCC tissues and explores their clinical prognostic value in predicting tumor recurrence.

2. Materials and Methods

2.1. *Patients*

Liver tissue samples were collected from 153 patients (123 males and 30 females; median age of 63 years; range of 19-81 years) with a single primary HCC nodule. These patients underwent surgical resection at the Hepato-Biliary-Pancreatic Surgery Division, Department of Surgery, Graduate School of Medicine, The University of Tokyo, between January 2005 and December 2007. The study was approved by the Ethics Committee of The University of Tokyo.

2.2. *Immunohistochemical staining*

Sections (4-μm thick) were obtained from archival formalin-fixed, paraffin-embedded tissue blocks, deparaffinized with a xylene solution and dehydrated through a graded series of ethanol solutions. Endogenous peroxidase was inactivated through administration of 0.3% hydrogen peroxide/methanol for 30 min. After microwave irradiation, the slides were incubated with blocking serum at room temperature for 30 min. The sections were then incubated with the primary anti-DCP monoclonal antibody (MU-3, 1:900 dilution; Eisai, Tokyo, Japan) for 60 min at room temperature. After the sections were incubated with biotinylated secondary antibody for 60 min, detection of DCP was achieved by the biotin streptavidin-peroxidase complex method using a commercial kit (Histofine SAB-PO kit; Nichirei, Tokyo, Japan). 3,3'-diaminobenzidine was used as the chromogen and hematoxylin was used as a counterstain. Sections that had not been subjected to primary antibody incubation served as a negative control to monitor background staining. The percentage of stained cancer cells out of the total number of cancer cells was determined in 10 random microscopic fields of each tissue sample, or using the entire area, if the tissue sample comprised fewer than 10 fields. Samples in which more than 10% of carcinoma cells were stained were defined as positive (*21,22*).

2.3. *Statistical analysis*

Statview 5.0J (Abacus Concepts, Berkeley, CA, USA) statistical software was used for data analysis. A χ^2 test was used to evaluate the relationship between DCP/c-Met expression and tumor recurrence. $p < 0.05$ was considered statistically significant.

3. Results and Discussion

3.1. *DCP and c-Met expression profiles in HCC and surrounding non-cancerous liver tissues*

DCP and c-Met expression in HCC and adjacent nontumorous liver tissues were determined using immunohistochemistry. Immunohistochemical staining for DCP indicated that 97 patients (97/153, 63.4%) were positive for DCP staining in cancerous tissues (Table 1). Of these 97 patients, 82 were positive for DCP staining only in HCC tissues and 15 were positive for DCP staining in both tumorous tissues and adjacent nontumorous tissues. DCP expression was detected in adjacent noncancerous tissues in 20 patients (20/153, 13.1%). A significant difference ($p < 0.01$) in DCP positivity was noted in HCC tissues compared to adjacent nontumorous tissues. The c-Met expression profile was also observed in HCC

specimens collected in the present study (Table 1). In total, 102 patients (102/153, 66.7%) were found to have c-Met-staining tumors; c-Met was detected in HCC tissues alone in 66 patients and in both HCC and surrounding nontumorous liver tissues in 36. Expression of c-Met in adjacent nontumorous tissues was noted in a markedly smaller number of patients (44/153, 28.8%) compared to that in tumorous tissues ($p < 0.01$). The expression profiles of DCP and c-Met noted in the present study indicated that HCC tissues are prone to express DCP and c-Met and implied that abnormally elevated expression of these two molecules in HCC tissues may play a role in HCC development and progression.

3.2. *Co-existence of DCP and c-Met in HCC*

One aim of the current study was to investigate whether DCP and c-Met co-existed in the liver tissues of patients with HCC. Specifically, the correlation between the presence of DCP and the presence of c-Met was analyzed in three matched groups: *i*) cancerous tissue producing DCP and cancerous tissue expressing c-Met; *ii*) adjacent non-cancerous tissue producing DCP and adjacent noncancerous tissue expressing c-Met; and *iii*) whole tissue (either cancerous or adjacent noncancerous tissue) producing DCP and whole tissue expressing c-Met. In each matched group, the patients were divided into four categories according to the presence or absence of DCP and c-Met, *i.e.* DCP positive and c-Met-positive patients, DCP-negative and c-Met-negative patients, DCP-positive and c-Met-negative patients, and DCP-negative and c-Met-positive patients.

For the first matched group, 78 patients (78/153, 51.0%) had co-existence of DCP and c-Met while 43 patients (43/153, 28.1%) had expression of only one of the two molecules, either DCP or c-Met, in HCC regions (Table 2). Of the 97 patients with cancerous tissues that were stained with DCP antibody, 78 (78/97, 80.3%) were found to have c-Met expression in tumor regions. Similarly, 76.5% of patients had DCP expression in HCC regions among the patients that were found positive for c-Met in tumor areas. These results suggested that the existence of DCP was usually accompanied by the presence of c-Met in tumorous tissue. The percentage of consistent expression of DCP and c-Met (71.9%) was markedly higher than that of inconsistent expression (28.1%) ($p < 0.0001$). In the second matched group, *i.e.* DCP and c-Met in adjacent noncancerous liver tissues, 100 patients (accounting for 65.4% of all patients) displayed no staining for the two molecules. In the group with noncancerous tissues that were not stained with DCP antibody, c-Met expression was not observed in the same area in 75.1% of specimens. Coincidentally, the group with no c-Met staining in adjacent noncancerous tissues had a negative rate of DCP staining in noncancerous areas of 91.7%. A parallel relationship between DCP and c-Met was also apparent in the adjacent nontumorous liver tissues of patients with HCC ($p = 0.0054$). Finally, co-expression of DCP and c-Met was analyzed in whole tissue, including cancerous and adjacent non-cancerous areas. Eighty-nine specimens (89/153, 58.2%) concurrently expressed DCP and c-Met while thirty (30/153, 19.6%) expressed neither DCP nor c-Met. Collectively, consistent expression of DCP and c-Met in whole tissues existed in 77.8% of patients, revealing a relationship between the existence of DCP and c-Met in patients with HCC ($p < 0.0001$). All of these results indicated that the existence of DCP and c-Met was parallel in tumor tissues, adjacent nontumorous tissues, and whole tissues of HCC samples investigated in this study (Figure 1).

Table 1. DCP and c-Met expression in cancerous tissues and adjacent noncancerous tissues

Sub-group	DCP *n* (percent)	c-Met *n* (percent)
C(+)NC(+)	15 (9.8%)	36 (23.5%)
C(+)NC(–)	82 (53.6%)	66 (43.1%)
C(–)NC(+)	5 (3.3%)	8 (5.2%)
C(–)NC(–)	51 (33.3%)	43 (28.1%)
Total cases	153	153
C(+)	97 (63.4%)	102 (66.7%)
NC (+)	20 (13.1%)	44 (28.8%)

C: cancerous tissues; NC: adjacent noncancerous tissues.

Table 2. Correlation analysis of DCP and c-Met expression in HCC specimens

Sub-group	DCP_c↔$c\text{-}Met_c$	DCP_{nc}↔$c\text{-}Met_{nc}$	DCP_w↔$c\text{-}Met_w$
DCP(+)c-Met(+) cases	78 (51.0%)	11 (7.2%)	89 (58.2%)
DCP(–)c-Met(–) cases	32 (20.9%)	100 (65.4%)	30 (19.6%)
DCP(+)c-Met(–) cases	19 (12.4%)	9 (5.9%)	13 (8.5%)
DCP(–)c-Met(+) cases	24 (15.7%)	33 (21.6%)	21 (13.7%)
Total cases	153	153	153
p value	< 0.0001	0.0054	< 0.0001

DCP_c: DCP in cancerous tissue; $c\text{-}Met_c$: c-Met in cancerous tisse; DCP_{nc}: DCP in adjacent noncancerous tissue; $c\text{-}Met_{nc}$: c-Met in adjacent noncancerous tissue; DCP_w: DCP in whole tissue, including cancerous tissue and adjacent noncancerous issue; $c\text{-}Met_w$: c-Met in whole tissue, including cancerous tissue and adjacent noncancerous issue.

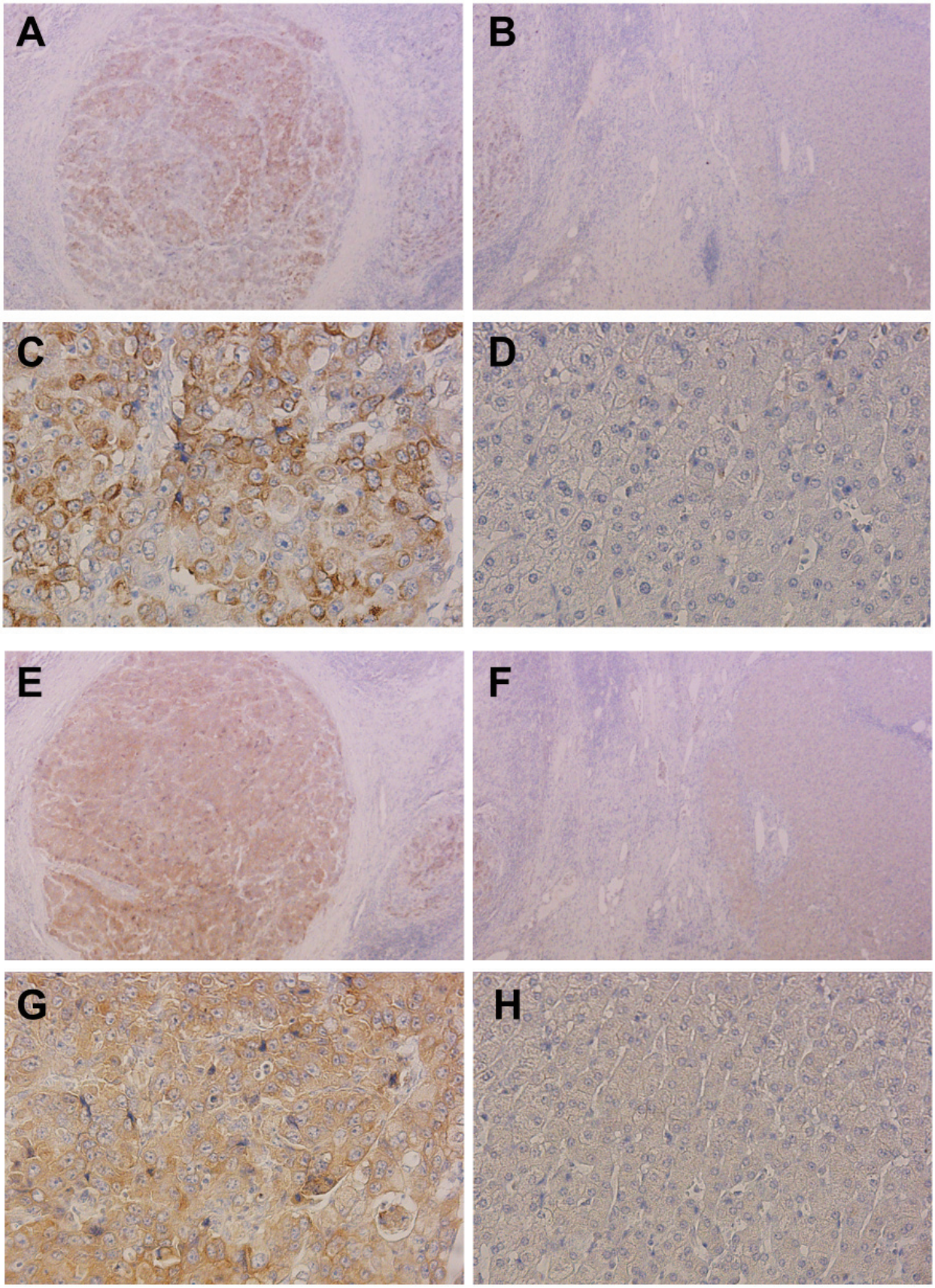

Figure 1. A representative case of DCP and c-Met staining in HCC and adjacent noncancerous tissue. HCC specimens from one patient were examined for DCP (**A**-**D**) and c-Met (**E**-**F**) expression, respectively. HCC nodule displayed immunoreactions for both DCP (**A** and **C**) and c-Met (**E** and **G**) while adjacent nontumorous liver tissue (the right area of HCC nodule) showed neither DCP (**B** and **D**) nor c-Met (**F** and **H**) immunoreactivity. Staining of DCP and c-Met was localized to both cytoplasm and cell membrane, as shown in **C** and **G**. **A**, **B**, **E**, and **F**, original magnification ×40; **C**, **D**, **G**, and **H**, original magnification ×200.

3.3. *Influence of DCP/c-Met expression on HCC recurrence*

As recurrence is a common behavior of HCC after treatment with surgical excision, the influence of DCP and/or c-Met expression on HCC recurrence was examined. The role of c-Met alone in predicting HCC recurrence was first examined. HCC recurrence was noted in 49 of 102 patients (48.0%) when c-Met was detected in tumors, whereas the group without c-Met in tumor areas had a clearly lower recurrence rate of 27.5% (14/51) (p = 0.0147) (Figure 2). When the patients were grouped according to whether c-Met was expressed in whole tissue, *i.e.* either tumorous tissue or adjacent nontumorous tissue, significant differences in recurrence rates were noted in the two groups. Patients in the c-Met-positive group were more susceptible to recurrence, at a rate of 46.4% (51/110), compared to the c-Met-negative group with a recurrence rate of 27.9% (12/43) (p = 0.0371) (Figure 2). Next, the combined role of c-Met and DCP in differentiating HCC recurrence was examined. Patients with c-Met and/or DCP in HCC and adjacent nontumorous tissues were found to have a recurrence rate of 47.2% (58/123), which is similar to that in the group positive for c-Met alone as noted above. However, patients with neither c-Met nor DCP in tumors and adjacent nontumorous tissues had a lower recurrence rate of 16.7% than patients without no c-Met (Figure 2). These results indicated that the combination of c-Met and DCP is more efficient than c-Met alone in distinguishing a low risk of recurrence in patients with HCC. Absence of c-Met and DCP in tumors and adjacent nontumorous tissues was associated with a low HCC recurrence.

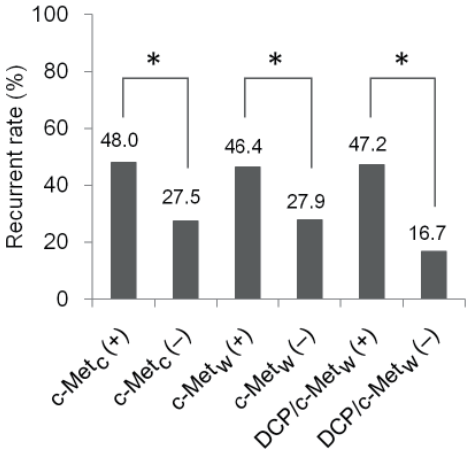

Figure 2. Tumor recurrence rates in different groups in relation to DCP/c-Met presence or absence. c-Met$_c$: c-Met in cancerous tissue; c-Met$_w$: c-Met in whole tissue, including cancerous and adjacent noncancerous tissue; DCP/c-Met$_w$: DCP and/or c-Met in whole tissue, including cancerous and adjacent noncancerous tissue. * $p < 0.05$.

The current study determined the expression of DCP and c-Met in human HCC samples and investigated their clinical value in predicting tumor recurrence. Results revealed that DCP and c-Met were expressed in HCC tissues in 63.4% and 66.7% of patients but were only observed in adjacent nontumorous tissues in 13.1% and 28.8% of patients, respectively. In addition to their extensive presence in HCC tissues, DCP and c-Met were usually concurrently expressed. This form of expression of DCP and c-Met was found to be related to tumor recurrence. Absence of DCP and c-Met in HCC and adjacent nontumorous tissues indicated a low risk of HCC recurrence. These results suggest that abnormal expression of DCP and c-Met in the liver tissues of patients with HCC are associated with tumor behavior.

DCP is an abnormal prothrombin that lacks the ability to interact with other coagulation factors (*23,24*). Its production was found to be related to decreased activity of γ-glutamyl carboxylase in hepatic cells, abnormal vitamin K metabolism, and overexpression of prothrombin precursor in hepatic cells (*25-27*). Currently, serous DCP is used as a diagnostic marker for HCC in Japan, South Korea, and Indonesia (*28-30*). Recent molecular biological studies of DCP have revealed the usefulness of this molecule as a diagnostic marker as well as its significant role in cancer progression. DCP has two kringle domains similar to those in HGF and both are considered necessary for HGF to bind with c-Met (*31*). Research has proven that DCP can bind with the surface receptor c-Met and result in c-Met phosphorylation (*31*). The current authors previously found that DCP can activate c-Met and induce matrix metalloproteinase activity in HCC cells, thus promoting the migration and invasion of HCC cells *in vitro* (*32*). The possible interaction between DCP and c-Met in human HCC was evident in the results of the present study, *i.e.* they existed extensively and concurrently in HCC tissues. Thus, DCP may trigger the c-Met signal transduction pathway, promoting HCC cells invasion and metastasis that always lead to tumor recurrence. This speculation may explain why absence of DCP and c-Met in HCC signifies a low risk of tumor recurrence as was noted in the present study.

In conclusion, this study provided evidence that DCP and c-Met usually coexist in HCC and their absence was associated with a low risk of tumor recurrence. Further studies are still needed to clarify their relationship to clinicopathological features of HCC and the prognosis for patients with HCC.

Acknowledgement

This project was supported by Grants-in-Aid from the Ministry of Education, Science, Sports, and Culture of Japan.

References

1. Miki D, Ochi H, Hayes CN, Aikata H, Chayama K. Hepatocellular carcinoma: Towards personalized medicine. Cancer Sci. 2012; 103:846-850.
2. Jemal A, Bray F, Center MM, Ferlay J, Ward E, Forman D. Global cancer statistics. CA Cancer J Clin. 2011; 61:69-90.
3. Ke AW, Shi GM, Zhou J, Wu FZ, Ding ZB, Hu MY, Xu Y, Song ZJ, Wang ZJ, Wu JC, Bai DS, Li JC, Liu KD, Fan J. Role of overexpression of CD151 and/or c-Met in predicting prognosis of hepatocellular carcinoma. Hepatology. 2009; 49:491-503.
4. Cooper CS, Park M, Blair DG, Tainsky MA, Huebner K, Croce CM, Vande Woude GF. Molecular cloning of a new transforming gene from a chemically transformed human cell line. Nature. 1984; 311:29-33.
5. Naldini L, Vigna E, Narsimhan RP, Gaudino G, Zarnegar R, Michalopoulos GK, Comoglio PM. Hepatocyte growth factor (HGF) stimulates the tyrosine kinase activity of the receptor encoded by the proto-oncogene *c-MET*. Oncogene. 1991; 6:501-504.
6. Gao J, Inagaki Y, Song P, Qu X, Kokudo N, Tang W. Targeting c-Met as a promising strategy for the treatment of hepatocellular carcinoma. Pharmacol Res. 2012; 65:23-30.
7. Suzuki K, Hayashi N, Yamada Y, Yoshihara H, Miyamoto Y, Ito Y, Ito T, Katayama K, Sasaki Y, Ito A, et al. Expression of the c-met protooncogene in human hepatocellular carcinoma. Hepatology. 1994; 20:1231-1236.
8. D'Errico A, Fiorentino M, Ponzetto A, Daikuhara Y, Tsubouchi H, Brechot C, Scoazec JY, Grigioni WF. Liver hepatocyte growth factor does not always correlate with hepatocellular proliferation in human liver lesions: Its specific receptor c-met does. Hepatology. 1996; 24:60-64.
9. Ueki T, Fujimoto J, Suzuki T, Yamamoto H, Okamoto E. Expression of hepatocyte growth factor and its receptor c-met proto-oncogene in hepatocellular carcinoma. Hepatology. 1997; 25:862-866.
10. Osada S, Kanematsu M, Imai H, Goshima S. Clinical significance of serum HGF and c-Met expression in tumor tissue for evaluation of properties and treatment of hepatocellular carcinoma. Hepatogastroenterology. 2008; 55:544-549.
11. Okano J, Shiota G, Kawasaki H. Expression of hepatocyte growth factor (HGF) and HGF receptor (c-met) proteins in liver diseases: An immunohistochemical study. Liver. 1999; 19:151-159.
12. Wang ZL, Liang P, Dong BW, Yu XL, Yu de J. Prognostic factors and recurrence of small hepatocellular carcinoma after hepatic resection or microwave ablation: A retrospective study. J Gastrointest Surg. 2008; 12:327-337.
13. Wu FS, Zheng SS, Wu LJ, Ding W, Ma ZM, Wang ZM, Teng LS, Zhao WH. Study on the prognostic value of hepatocyte growth factor and c-met for patients with hepatocellular carcinoma. Zhonghua Wai Ke Za Zhi. 2006; 44:603-608.
14. Gao JJ, Inagaki Y, Xue X, Qu XJ, Tang W. c-Met: A potential therapeutic target for hepatocellular carcinoma. Drug Discov Ther. 2011; 5:2-11.
15. Kinoshita T, Tashiro K, Nakamura T. Marked increase of HGF mRNA in non-parenchymal liver cells of rats treated with hepatotoxins. Biochem Biophys Res Commun. 1989; 165:1229-1234.
16. Noguchi O, Enomoto N, Ikeda T, Kobayashi F, Marumo F, Sato C. Gene expressions of c-met and hepatocyte growth factor in chronic liver disease and hepatocellular carcinoma. J Hepatol. 1996; 24:286-292.
17. Gao FJ, Cui SX, Chen MH, Cheng YN, Sun LR, Ward SG, Kokudo N, Tang W, Qu XJ. Des-gamma-carboxy prothrombin increases the expression of angiogenic factors in human hepatocellular carcinoma cells. Life Sci. 2008; 83:815-820.
18. Wang SB, Cheng YN, Cui SX, Zhong JL, Ward SG, Sun LR, Chen MH, Kokudo N, Tang W, Qu XJ. Des-gamma-carboxy prothrombin stimulates human vascular endothelial cell growth and migration. Clin Exp Metastasis. 2009; 26:469-477.
19. Ma M, Qu XJ, Mu GY, Chen MH, Cheng YN, Kokudo N, Tang W, Cui SX. Vitamin K2 inhibits the growth of hepatocellular carcinoma *via* decrease of des-gamma-carboxy prothrombin. Chemotherapy. 2009; 55:28-35.
20. Inagaki Y, Qi F, Gao J, Qu X, Hasegawa K, Sugawara Y, Tang W, Kokudo N. Effect of c-Met inhibitor SU11274 on hepatocellular carcinoma cell growth. Biosci Trends. 2011; 5:52-56.
21. Inagaki Y, Xu HL, Hasegawa K, Aoki T, Beck Y, Sugawara Y, Tang W, Kokudo N. Des-gamma-carboxyprothrombin in patients with hepatocellular carcinoma and liver cirrhosis. J Dig Dis. 2011; 12:481-488.
22. Jiao B, Zhang YH, Cheng YN, Gao JJ, Zhang QZ. A low-dose combination of valsartan and low molecular weight heparin better improved glomerular permeability than did high-dose monotherapy in rats with diabetic nephropathy. Drug Discov Ther. 2011; 5:119-124.
23. Tang W, Kokudo N, Sugawara Y, Guo Q, Imamura H, Sano K, Karako H, Qu X, Nakata M, Makuuchi M. Des-gamma-carboxyprothrombin expression in cancer and/or non-cancer liver tissues: Association with survival of patients with resectable hepatocellular carcinoma. Oncol Rep. 2005; 13:25-30.
24. Tang W, Miki K, Kokudo N, Sugawara Y, Imamura H, Minagawa M, Yuan LW, Ohnishi S, Makuuchi M. Des-gamma-carboxy prothrombin in cancer and non-cancer liver tissue of patients with hepatocellular carcinoma. Int J Oncol. 2003; 22:969-975.
25. Shah DV, Engelke JA, Suttie JW. Abnormal prothrombin in the plasma of rats carrying hepatic tumors. Blood. 1987; 69:850-854.
26. Okuda H, Obata H, Nakanishi T, Furukawa R, Hashimoto E. Production of abnormal prothrombin (des-gamma-carboxy prothrombin) by hepatocellular carcinoma. A clinical and experimental study. J Hepatol. 1987; 4:357-363.
27. Ono M, Ohta H, Ohhira M, Sekiya C, Namiki M. Measurement of immunoreactive prothrombin, des-gamma-carboxy prothrombin, and vitamin K in human liver tissues: Overproduction of immunoreactive prothrombin in hepatocellular carcinoma. Am J Gastroenterol. 1990; 85:1149-1154.
28. Tateishi R, Enooku K, Shiina S, Koike K. Tumor markers for hepatocellular carcinoma. Nihon Rinsho. 2012; 70:821-827.
29. Bachtiar I, Kheng V, Wibowo GA, Gani RA, Hasan I, Sanityoso A, Budhihusodo U, Lelosutan SA, Martamala R, Achwan WA, Soemoharjo S, Sulaiman A, Lesmana LA, Tai S. Alpha-1-acid glycoprotein as potential

biomarker for alpha-fetoprotein-low hepatocellular carcinoma. BMC Res Notes. 2010; 3:319.
30. Choi J, Park Y, Kim JH, Kim HS. Evaluation of automated serum des-gamma-carboxyprothrombin (DCP) assays for detecting hepatocellular carcinoma. Clin Biochem. 2011; 44:1464-1468.
31. Suzuki M, Shiraha H, Fujikawa T, Takaoka N, Ueda N, Nakanishi Y, Koike K, Takaki A, Shiratori Y. Des-gamma-carboxy prothrombin is a potential autologous growth factor for hepatocellular carcinoma. J Biol Chem. 2005; 280:6409-6415.
32. Yue P, Gao ZH, Xue X, Cui SX, Zhao CR, Yuan Y, Yin Z, Inagaki Y, Kokudo N, Tang W, Qu XJ. Des-gamma-carboxyl prothrombin induces matrix metalloproteinase activity in hepatocellular carcinoma cells by involving the ERK1/2 MAPK signalling pathway. Eur J Cancer. 2011; 47:1115-1124.

(Received July 7, 2012; Revised July 26, 2012; Accepted August 1, 2012)

Brief Report

DOI: 10.5582/bst.2012.v6.4.160

Lipase, protease, and biofilm as the major virulence factors in staphylococci isolated from acne lesions

Jongkon Saising[1,2], Sudarat Singdam[1], Metta Ongsakul[1], Supayang Piyawan Voravuthikunchai[1,2,*]

[1] *Department of Microbiology, Faculty of Science, Prince of Songkla University, Hat Yai, Songkhla, Thailand;*
[2] *Natural Products Research Center, Faculty of Science, Prince of Songkla University, Hat Yai, Songkhla, Thailand.*

Summary **Staphylococci involve infections in association with a number of bacterial virulence factors. Extracellular enzymes play an important role in staphylococcal pathogenesis. In addition, biofilm is known to be associated with their virulence. In this study, 149 staphylococcal isolates from acne lesions were investigated for their virulence factors including lipase, protease, and biofilm formation. Coagulase-negative staphylococci were demonstrated to present lipase and protease activities more often than coagulase-positive staphylococci. A microtiter plate method (quantitative method) and a Congo red agar method (qualitative method) were comparatively employed to assess biofilm formation. In addition, biofilm forming ability was commonly detected in a coagulase-negative group (97.7%, microtiter plate method and 84.7%, Congo red agar method) more frequently than in coagulase-positive organisms (68.8%, microtiter plate method and 62.5%, Congo red agar method). This study clearly confirms an important role for biofilm in coagulase-negative staphylococci which is of serious concern as a considerable infectious agent in patients with acnes and implanted medical devices. The Congo red agar method proved to be an easy method to quickly detect biofilm producers. Sensitivity of the Congo red agar method was 85.54% and 68.18% and accuracy was 84.7% and 62.5% in coagulase-negative and coagulase-positive staphylococci, respectively, while specificity was 50% in both groups. The results clearly demonstrated that a higher percentage of coagulase-negative staphylococci isolated from acne lesions exhibited lipase and protease activities, as well as biofilm formation, than coagulase-positive staphylococci.**

Keywords: Biofilm, lipase, protease, staphylococci, acne

1. Introduction

Staphylococcus has been considered to be a major public health issue because it can cause both health-associated and community-associated infections, with considerable morbidity and even mortality. The infections are either minor such as infections of skin and soft tissues or more serious systemic infections including endocarditis, osteomyelitis, and septic shock syndrome (*1*). Staphylococcal infections are caused mainly by strains that have already colonized parts of the human body, making the colonized persons a reservoir for the spread of the organisms (*2*).

The organisms are one of the microorganisms commonly isolated from acne lesions (*3*). The skin environment contains lipids, polysaccharides, proteins, and a variety of mixed polymers. The skin microbiota produces a range of extracellular enzymes that degrade these polymers. Proteolytic, lipolytic, and esterolytic activities are frequently detected among various exo-enzymatic activities of staphylococci (*4,5*). The presence of oleic acid released from the hydrolysis of serum lipids by staphylococcal lipase could be pathologically important (*6*). On the other hand, protease is thought to be involved in host tissue invasion (*7*). This enzyme can interact with the host defense mechanisms and tissue components (*8*).

Additionally, the ability to form biofilm is one

**Address correspondence to:*
Dr. Supayang PiyawanVoravuthikunchai, Natural Products Research Center and Department of Microbiology, Faculty of Science, Prince of Songkla University, Hat Yai, Songkhla 90112, Thailand.
E-mail: supayang.v@psu.ac.th

of the known staphylococcal virulence factors. The formation of biofilm involves two stages: (*i*) initial adhesion of bacterial cells to the host cell surface and (*ii*) the formation of a multilayered cell cluster surrounded by an extracellular polysaccharide matrix (*9*). The production of the exopolysaccharide matrix has been suggested to prevent the access of antibiotics to the bacterial cells embedded in the community (*10*). Treatment of staphylococcal infections is becoming difficult due to increased antibiotic resistance. Many reports indicated that antibiotic resistance in biofilm forming cells increased when compared to that in the planktonic growth phase (*11-13*). Consequently, there is a need to identify virulent strains by detecting their ability to produce biofilm. Detection of staphylococcal virulence factors may be a necessary step for prevention, control, and treatment of the infections. This may lead to more effective infection control practices, decreasing colonization, and development of vaccines and new or improved antimicrobial agents (*7*). Data on clinical isolates from various infection sites such as atopic dermatitis, conjunctiva, blood and infected devices have documented staphylococcal virulence factors including lipase, protease, and biofilm (*14-16*). In contrast, there has been limited information on virulence factors of staphylococci isolated from acne lesions.

In this study, a large collection of staphylococcal isolates from acne lesions was investigated for their enzyme activities including lipase and protease. In addition, biofilm formation, another important virulence factor, was assessed using a qualitative Congo red agar method, compared to a quantitative microtiter plate method used as the standard method.

2. Materials and Methods

2.1. *Bacterial isolates*

A total of 149 staphylococcal isolates from acne lesions were characterized according to Bergey's Manual of Systematic Bacteriology (*17*) including their characteristic macroscopic colony appearance, Gram-staining, production of acid from mannitol salt agar (Merck, Darmstadt, Germany), catalase activity and coagulase tests. They were further classified as 85 isolates of coagulase-negative and 64 isolates of coagulase-positive staphylococci. All cultures were maintained on tryticase soy broth (TSB, Difco, Becton Dickinson, Sparks, MD, USA) containing 20% glycerol (Vidhyasom, Bangkok, Thailand) at –80°C. *Staphylococcus aureus (S. aureus)* ATCC 25923 was included as a reference strain.

2.2. *Screening for lipase activity*

Nutrient Agar (NA, Difco) containing 1% tributyrin (Fluka, Buchs, Germany) was used to study lipolytic activity. The isolates were subcultured on tryticase soy agar (TSA, Difco) and incubated at 37°C for 24 h. They were inoculated on tributyrin agar plates and incubated at 37°C for 72 h. The presence of clear zones was taken as an indication of positive lipase activity.

2.3. *Screening for protease activity*

Nutrient agar supplemented with 2% casein (Sigma, Steinhelm, Germany) was used to screen for protease activity. The isolates were subcultured on TSA and incubated at 37°C for 24 h. They were inoculated on casein agar plates and incubated at 37°C for 24 h. The isolates producing opalescent zones around the colony were identified as protease positive.

2.4. *Detection of biofilm formation by the microtiter plate method*

Quantitative assessment of biofilm formation using the microtiter plate method was carried out according to the protocol (*18*). Briefly, an overnight culture grown in TSB supplemented with 0.25% glucose (Univar, Auckland, New Zealand) was adjusted to a McFarland standard No. 0.5 and diluted 100-fold. One hundred µL of bacterial suspension was transferred to a 96-well microtiter plate (Corning, New York, USA), 100 µL of TSB supplemented with 0.25% glucose was added, and incubated at 37°C for 24 h. After incubation, the broth was discarded from each well and washed twice with phosphate buffered saline to remove non-adherent cells. After airdrying, the wells were stained with 0.1% crystal violet (Merck) for 30 min, washed with water, and air dried before 200 µL of dimethyl sulfoxide (Merck) was added. The absorbance was measured at 595 nm with a microtiter plate reader (Bio Tek, Winooski, USA). All strains were classified into the following categories: non-adherent, weakly, moderately, and strongly adherent based on the optical density of bacterial films (*19*).

2.5. *Detection of biofilm formation by the Congo red agar method*

Qualitative evaluation of biofilm producers using the Congo red agar method to detect slime production was performed as previously described (*20*). The medium is comprised of brain heart infusion broth (Difco) 37 g/L, sucrose (Univar) 50 g/L, Congo red (Fluka) 0.8 g/L and agar (Merck) 10 g/L. Inoculated plates were incubated at 37°C for 24 h. Slime producing strains presented black colonies while non producing strains developed red colonies. The scale of colony color evaluation was assessed as follows: very black and black colonies were biofilm producing strains, almost black colonies were weak biofilm producers while very red to Bordeaux colonies were considered as non-biofilm producing

strains (*21,22*).

2.6. *Statistical analysis*

Parameters including sensitivity, specificity, positive predictive value, negative predictive value, and accuracy of the Congo red agar method were determined by the analysis of a 2 × 2 table. The microtiter plate method was used as the standard method.

3. Results and Discussion

Lipase and protease enzymes have been demonstrated in staphylococci associated with infection. About 17% of coagulase-negative staphylococci isolated from infectious processes of newborns revealed lipase activity (*22*). Other workers reported 97% of *S. aureus* from the colonized skin of patients with acute-phase atopic dermatitis exhibited protease activity (*14*). In this study, 100% of coagulase-negative (85 isolates) produced lipase enzymes. Of 64 coagulase-positive staphylococci, only 42 isolates (65.6%) were lipase positive. Fifty six (65.9%) coagulase-negative and 17 (26.6%) coagulase-positive staphylococci demonstrated protease activity. *S. aureus* ATCC 25923, a reference strain produced both lipase and protease enzymes. In the present study, coagulase-negative staphylococcal isolates produced both lipase and protease enzymes more frequently than the coagulase-positive group. The percentages of organisms with enzyme activities in our study focusing on staphylococci isolated from acne lesions are different from other reports. This may be due to the ability of staphylococci to produce enzymes depending on the environment and nutrition availability in different infectious sites. Furthermore, this report clearly indicated that staphylococci isolated from acne lesions are more common among lipase producers than protease producers. Lipolytic enzymes which are produced by *S. epidermidis* and possibly *S. aureus* could demonstrate that lipase enzymes are important to the organisms for their colonization and growth within the lipid-rich environment of the skin (*24*). The site of growth of staphylococci within the sebaceous unit is superficial (*25*). *S. epidermidis* which is coagulase-negative is prevalent in areas with many sebaceous follicles. The organism produces lipase whose activity may be involved in its virulence (*26*).

Production of lipase, a putative virulence determinant, was reported to be up-regulated in the biofilm mode of bacterial growth (*27*). Biofilm formation could be a characteristic of invasive staphylococcal isolates. In the analysis of 85 coagulase-negative staphylococci by the microtiter plate method (Figure 1A), 97.7% were biofilm formers and only 2.3% were non-biofilm producers. On the other hand, of 64 coagulase-positive staphylococci isolates, 68.8% exhibited biofilm formation while 31.2% could not produce biofilm. In the Congo red agar method, slime production was investigated. Similarly, 84.7% of coagulase-negative staphylococci were biofilm producing strains while 62.5% of coagulase-positive staphylococci were biofilm producers (Figure 1B). *S. aureus* ATCC 25923 was considered as a moderate biofilm former and biofilm producer by the microtiter plate method and Congo red agar method, respectively. The results demonstrated that both coagulase-negative and coagulase-positive staphylococci exhibited biofilm formation, but with greater frequency in the coagulase-negative group. Despite their low virulence, coagulase-negative staphylococci, particularly *S. epidermidis*, are well-adapted to adhere to smooth metal and plastic surfaces of foreign bodies such as vascular catheters, cardiac devices, and ventricular catheters (*28*). The results from other workers showed a high percentage of up to 90% of *S. epidermidis* isolated from infections associated with indwelling medical devices were biofilm producers. In contrast, a relatively lower percentage of biofilm producers were present in the skin, 35.7% and 64.3% were non-biofilm formers and weak biofilm producers, respectively (*29*). Similarly, only 32% from skin and nasal swabs showed biofilm production while 70% of invasive staphylococcal strains isolated from blood of patients hospitalized with peripheral intravenous devices exhibited biofilm forming ability (*22*). In contrast, this study demonstrated that up to 85% of staphylococci isolated from acne lesions were biofilm producers.

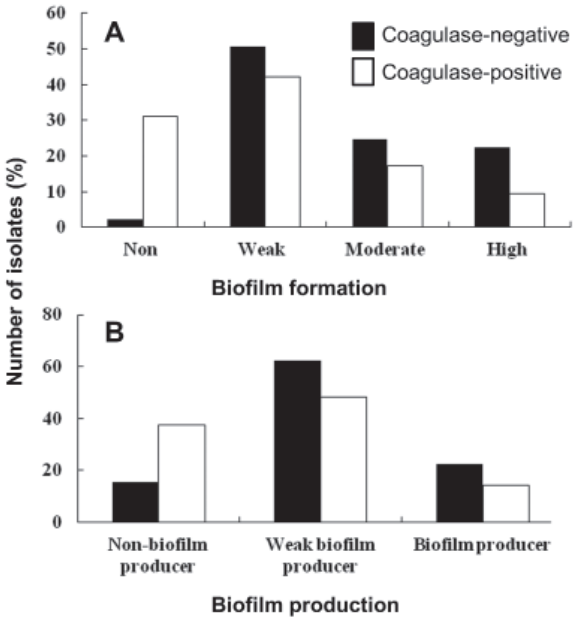

Figure 1. Quantitative screening of biofilm formation by microtiter plate method (A) and qualitative screening of slime production by Congo red agar method (B) from coagulase-negative staphylococci (■) and coagulase-positive staphylococci (□).

Table 1. Comparison of biofilm production of coagulase-negative staphylococci (*n* = 85) and coagulase-positive staphylococci (*n* = 64) by the microtiter plate method and Congo red agar method

Coagulase-negative staphylococci (*n* = 85)				Coagulase-positive staphylococci (*n* = 64)			
	Microtiter plate		Total		Microtiter plate		Total
	Positive	Negative			Positive	Negative	
Congo red agar				Congo red agar			
Positive	71	1	72	Positive	30	10	40
Negative	12	1	13	Negative	14	10	24
Total	83	2	85	Total	44	20	64

Table 2. Statistical evaluation of Congo red agar method for detection of biofilm formation in staphylococci using the microtiter plate method as the standard method

Staphylococci	Test characteristics (%)				
	Sensitivity	Specificity	Positive predictive value	Negative predictive value	Accuracy
Coagulase-negative (*n* = 85)	85.54	50.00	98.61	7.69	84.70
Coagulase-positive (*n* = 64)	68.18	50.00	75.00	41.66	62.50

The microtiter plate method was used as the standard method to evaluate the Congo red agar method. Sensitivity, specificity, positive predictive value, negative predictive value, and accuracy were calculated by analysis of a 2 × 2 table (Table 1). Sensitivities of the Congo red agar method were 85.54% and 68.18% for coagulase-negative and coagulase-positive staphylococci, respectively. Specificity of both staphylococci was 50% while accuracies were 84.70% and 62.50% for coagulase-negative and coagulase-positive staphylococci, respectively (Table 2). A positive predictive value was 98.61% for coagulase-negative staphylococci while the value for coagulase-positive staphylococci was 75%. On the other hand, negative predictive values were 7.69% and 41.66% for coagulase-negative and coagulase-positive staphylococci, respectively.

As sensitivity and accuracy in coagulase-negative staphylococci are much higher than those in the coagulase-positive group, it is suggested that the Congo red agar method is more suitable for the detection of coagulase-negative staphylococci which are capable of producing biofilm more readily than coagulase-positive organisms. This method is easy to perform and takes less time while the microtiter plate method is somewhat more sophisticated. However, the microtiter plate method is a quantitative tool for biofilm detection and can be used as a reliable technique since it can detect the process of biofilm formation, attachment to the surface or secreted extracellular polysaccharide production, while the Congo red agar method can only detect slime production which suggests biofilm formation. Additionally, the quantitative microtiter plate method is more efficient to categorize biofilm formation than the Congo red agar method which depends on chromatic evaluation. The variation from black to red colony color can sometimes result in a difficult decision for investigators.

In conclusion, our results indicate that coagulase-negative staphylococci isolated from acne lesions were demonstrated to present lipase and protease activities as well as biofilm formation more often than coagulase-positive staphylococci.

Acknowledgements

This research was supported by grants under the program Strategic Scholarships for Frontier Research Network for the Joint Ph.D. Program Thai Doctoral degree from the Office of the Higher Education Commission, Thailand and the National Research University Project of Thailand's Office of the Higher Education Commission.

References

1. Pancholi V. Staphylococcal Extracellular/Surface Enzymatic activity. In: Staphylococcus aureus Infection and Disease (Honeyman AL, Friedman H, Bendinellim, eds.). Kluwer Academic/Plenum Publishers, New York, USA, 2001; pp. 137-153.
2. Gordon RJ, Lowy FD. Pathogenesis of methicillin-resistant *Staphylococcus aureus* infection. Clin Infect Dis. 2008; 46:S350-S359.
3. Brook I, Frazier EH, Cox ME, Yeager JK. The aerobic and anaerobic pustular acne lesions. Anaerobe. 1995; 1:305-307.
4. Rosenstein R, Götz F. Staphylococcal lipases: Biochemical and molecular characterization. Biochimie. 2000; 82:1005-1014.
5. Bojar RA, Holland KT. Review: The human cutaneous microflora and factors controlling colonisation. World J Microbiol Biotechnol. 2002; 18:889-903.
6. O'Leary WM, Weld JT. Lipolytic activities of

Staphylococcus aureus. I. Nature of the enzyme producing free fatty acids from plasma lipids. J Bacteriol. 1964; 88:1356-1363.
7. Archer GL. *Staphylococcus aureus*: A well-armed pathogen. Clin Infect Dis. 1998; 26:1179-1181.
8. Dubin G. Extracellular proteases of *Staphylococcus* spp. Biol Chem. 2002; 383:1075-1086.
9. Götz F. *Staphylococcus* and biofilms. Mol Microbiol. 2002; 43:1367-1378.
10. Mah TF, O'Toole GA. Mechanisms of biofilm resistance to antimicrobial agents. Trends Microbiol. 2001; 9:34-39.
11. Cerca N, Martins S, Cerca F, Jefferson KK, Pier GB, Oliveira R, Azeredo J. Comparative assessment of antibiotic susceptibility of coagulase-negative staphylococci in biofilm versus planktonic culture as assessed by bacterial enumeration or rapid XTT colorimetry. J Antimicrob Chemother. 2005; 56:331-336.
12. Nishimura S, Tsurumoto T, Yonekura A, Adachi K, Shindo H. Antimicrobial susceptibility of *Staphylococcus aureus* and *Staphylococcus epidermidis* biofilms isolated from infected total hip arthroplasty cases. J Orthop Sci. 2006; 11:46-50.
13. Frank KL, Reichert EJ, Piper KE, Patel R. *In vitro* effects of antimicrobial agents on planktonic and biofilm forms of *Staphylococcus lugdunensis* clinical isolates. Antimicrob Agents Chemother. 2007; 51:888-895.
14. Miedzobrodzki J, Kaszycki P, Bialecka A, Kasprowicz A. Proteolytic activity of *Staphylococcus aureus* strains isolated from the colonized skin of patients with acute-phase atopic dermatitis. Eur J Clin Microbiol Infect Dis. 2002; 21:269-276.
15. Suzuki T, Kawamura Y, Uno T, Ohashi Y, Ezaki T. Prevalence of *Staphylococcus epidermidis* strains with biofilm-forming ability in isolates from conjunctiva and facial skin. Am J Ophthalmol. 2005; 140:844-850.
16. Mathur T, Singhal S, Khan S, Upadhyay DJ, Fatma T, Rattan A. Detection of biofilm formation among the clinical isolates of staphylococci: An evaluation of three different screening methods. Indian J of Med Microbiol. 2006; 24:25-29.
17. Holt JG. Bergey's Manual of Systematic Bacteriology, Volume 2. Williams & Wilkins, Maryland, USA, 1986; pp. 1015-1022.
18. Karaolis DK, Rashid MH, Chythanya R, Luo W, Hyodo M, Hayakawa Y. c-di-GMP (3'-5'-cyclic diguanylic acid) inhibits *Staphylococcus aureus* cell-cell interactions and biofilm formation. Antimicrob Agents Chemother. 2005; 49:1029-1038.
19. Stepanovic S, Vukovic D, Dakic I, Savic B, Svabic-Vlahovic M. A modified microtiter-plate test for quantification of staphylococcal biofilm formation. J Microbiol Methods. 2000; 40:175-179.
20. Freeman DJ, Falkiner FR, Keane CT. New method for detecting slime production by coagulase negative staphylococci. J Clin Pathol. 1989; 42:872-874.
21. Arciola CR, Campoccia D, Gamberini S, Cervellati M, Donati E, Montanaro L. Detection of slime production by means of an optimised Congo red agar plate test based on a colourimetric scale in *Staphylococcus epidermidis* clinical isolates genotyped for ica locus. Biomaterials. 2002; 23:4233-4239.
22. Jain A, Agarwal A. Biofilm production, a marker of pathogenic potential of colonizing and commensal staphylococci. J Microbiol Methods. 2009; 76:88-92.
23. Cunha Mde L, Rugolo LM, Lopes CA. Study of virulence factors in coagulase-negative staphylococci isolated from newborns. Mem Inst Oswaldo Cruz. 2006; 101:661-668.
24. Longshaw CM, Farrell AM, Wright JD, Holland KT. Identification of a second lipase gene, gehD, in *Staphylococcus epidermidis*: Comparison of sequence with those of other staphylococcal lipases. Microbiology. 2000; 146:1419-1427.
25. Burkhart CG, Burkhart CN, Lehmann PF. Acne: A review of immunologic and microbiologic factors. Postgrad Med J. 1999; 75:328-331.
26. Burkhart CG. Clinical assessment of acne pathogenesis with treatment implications. International Pediatrics. 2003; 18:14-19.
27. Coenye T, Peeters E, Nelis HJ. Biofilm formation by Propionibacterium acnes is associated with increased resistance to antimicrobial agents and increased production of putative virulence factors. Res Microbiol. 2007; 158:386-392.
28. Meskin I. *Staphylococcus epidermidis*. Pediatr Rev. 1998; 19:105-106.
29. Mateo M, Maestre JR, Aguilar L, Gimenez MJ, Granizo JJ, Prieto J. Strong slime production is a marker of clinical significance in *Staphylococcus epidermidis* isolated from intravascular catheters. Eur J Clin Microbiol Infect Dis. 2008; 27:311-314.

(Received January 30, 2012; Revised August 18, 2012; Accepted August 19, 2012)

Original Article

DOI: 10.5582/bst.2012.v6.4.165

The impact of Gonoshasthaya Kendra's Micro Health Insurance plan on antenatal care among poor women in rural Bangladesh

Mohammad Touhidul Islam*, Isao Igarashi, Koichi Kawabuchi

Health Care Economics, Graduate School of Medical and Dental Sciences, Tokyo Medical and Dental University, Tokyo, Japan.

Summary **Low utilization of antenatal care (ANC) by pregnant women, particularly in rural areas, is an obstacle to ensuring safe motherhood in Bangladesh. Currently, Micro Health Insurance (MHI) is being considered in many developing countries as a potential method for assuring greater access to health care, especially for the poor. So far, there is only limited evidence evaluating MHI schemes. This study assesses the impact of MHI administered by Gonoshasthaya Kendra (GK) on ANC utilization by poor women in rural Bangladesh. We conducted a questionnaire survey and collected 321 valid responses from women enrolled in GK's MHI scheme and 271 from women not enrolled in any health insurance plan. We used a two-part model in which dependent variables were whether or not women utilized ANC and the number of times ANC was used. The model consisted of logistic regression analysis and ordinary least squares regression analysis. The main independent variables were dummies for socioeconomic classes according to GK, each of which represented the premiums and co-payments charged by class. The results showed that destitute, ultra-poor, and poor women enrolled in MHI used ANC significantly more than women not enrolled in health insurance. Women enrolled in MHI, except for those who were destitute or ultra-poor, utilized ANC significantly more times than women not enrolled in health insurance. We assume that GK's sliding premium and co-payment scales are key to ANC utilization by women. Expanding the MHI scheme may enhance ANC utilization among poor women in rural Bangladesh.**

Keywords: Antenatal care, Micro Health Insurance (MHI), Gonoshasthaya Kendra (GK), poor women, rural Bangladesh

1. Introduction

Antenatal care (ANC) is an important prerequisite for ensuring safe motherhood. ANC demands that pregnant women deliver under the care of skilled birth attendants (*1*), and its absence is a vital factor in maternal death (*2,3*). It is effective in detecting and preventing many health problems that women suffer and reduces their vulnerability. Thus, health education and awareness achieved through ANC enables pregnant women to identify the symptoms of maternal complications and prepares them to seek proper health services in emergencies, thus helping to save the lives of mothers (*4*).

Even though some progress has been made in maternal health over the past decade through national and global efforts aimed at reaching Millennium Development Goal 5, the number of pregnant women receiving ANC in Bangladesh remains alarmingly low. Impoverished socio-economic conditions interact with cultural and geographical barriers to cause low use of ANC, particularly in rural areas. Moreover, a very inequitable distribution of health facilities and a dearth of medical professionals in rural areas undermine demand for maternal care among pregnant women (*5,6*). As a consequence, only 46.4% of pregnant women in rural areas are likely to receive ANC even once with a medically trained professional compared to 71.3% in urban areas, even though the WHO recommends at

**Address correspondence to:*
Dr. Mohammad Touhidul Islam, Health Care Economics, Graduate School of Medical and Dental Sciences, Tokyo Medical and Dental University, 1-5-45 Yushima, Bunkyo-ku, Tokyo 113-8549, Japan.
E-mail: abir.hce@tmd.ac.jp; abir47@yahoo.com

least 4 ANC visits for safe motherhood (*7,8*).

Of national health expenditures, 71% come from private sources (*9*). Thus, out-of-pocket payment dominates over financed health care in Bangladesh. In theory, there is universal coverage through user fees at public health facilities, but since the government spends only US$3 per capita on health, the health care delivery system cannot offer health services to everyone (US$1 = 74 taka) (*9*). The fee for an outpatient consultation, including ANC, at a rural public health facility is free or 3 taka, depending on the type of facility. Quite frequently, however, unofficial fees, mainly in the form of bribes charged at public facilities, raise the cost so much that poor people often cannot afford care as they are not covered by any type of health insurance or other financial protection (*10,11*). The Household Income and Expenditure Survey 2005 showed that unofficial fees raised the average outpatient consultation fee, including ANC, to 44 taka at public health facilities. Such additional costs further interfere with poor women's use of public health facilities (*12*). Thus, poor women, and particularly those in rural areas, remain excluded from existing public health service arrangements.

Maternal mortality is extremely prevalent among the lower economic group and in rural areas (*13*). Eighty percent of the total population resides in rural areas and 43.8% of the rural population lives under the poverty line (*14*). Maternal improvements will not materialize unless these large, neglected segments are addressed properly by health care intervention. In this context, there is a need to focus on certain pro-poor strategies in rural settings to ensure that poor women have access to maternal care services.

Recently, Micro Health Insurance (MHI) has appeared in many developing countries as a useful tool for making extra financial resources available and elevating demand for health services (*15*). MHI is a social protection program implemented by a community-based organization, rather than government or a private for-profit company, that provides risk-pooling through low pricing and affordable premiums to cover the costs of essential health care services, to a certain extent, for poor people who are unable to afford formal health insurance (*16*). It offers more reliable premiums and co-payments than regular health insurance but is limited to defined health risks. Unlike commercial health insurance, MHIs are voluntary and non-profit in nature.

MHIs are usually designed to be simple, charging flat premiums and providing one-size benefit packages, although some offer sliding premium scales, renewal fees, consultations, and drug co-payments to make them more accessible to the poorest groups. MHI mobilizes extra resources in the community but cannot cover total health costs. Previous studies have shown that enrollment in MHI was associated with higher utilization of modern health care and protected the poor from financial risk (*17-19*). However, in some MHI schemes, sufficiently rich groups may remain absent when pooling required resources. Thus, many MHIs receive financial support from donors, central and local governments, international non-governmental organization (NGOs), micro finance institutes, trade unions, or cooperatives. These external subsidies help sustain these voluntary organizations in the face of low revenue generation and adverse selection (*16*).

Such schemes have successfully increased maternal care utilization in West Africa (*20*). Some MHI schemes have proven beneficial by including the poorest people in developing countries (*19,21*) but others have excluded them (*22,23*). To address whether prepayment schemes are effective tools, the World Health Report 2000 showed the necessity of investigating their effects on poor people (*24*).

MHI is a growing sector in Bangladesh, but is still a new concept. Several NGOs are launching small-scale MHI schemes across the country, particularly in remote areas where conventional health services are unavailable. These schemes mainly provide primary health care services to rural people and prioritize maternal health care services. All of them play the role of both insurer and service provider and only two schemes cover any part of hospitalization costs.

At present, there is little published evidence of the impact of these schemes on maternal care utilization by individuals in Bangladesh. Previous studies of these schemes were mainly conceptual and based on administrative information. The current study focuses on ANC utilization by pregnant rural women under an MHI scheme administered by Gonoshasthaya Kendra (GK), one of the largest health-related NGOs in Bangladesh. An advantage of GK is that it offers health service benefits to the poor with premiums and co-payments on sliding scales. The aim of this study is to evaluate the effect of enrollment in GK's MHI on women, and particularly on poorer women, by examining its ability to enhance ANC utilization in rural areas. The findings are expected to contribute to Bangladesh's health policy.

GK is a pioneering health-related NGO in Bangladesh, established in 1972 in the rural Savar upazila (sub-district) of the Dhaka district, which is 30 km from the capital city. It started a health insurance scheme in 1975 to ensure that poor and marginalized rural people had access to health care services. GK categorizes members into five socioeconomic groups by assessing the socio-economic status of households and provides health services with premiums and co-payments set on sliding scales to protect poor people. Of those enrolled in GK's MHI scheme, 65.5% are destitute, ultra-poor, or poor (*25*). GK never allows health care providers to impose any unofficial fees on its enrollees above regular premiums and co-payments, effectively protecting them against financial risk. The

plan provides health services to rural areas *via* a tertiary hospital with 150 beds in Savar upazila in the Dhaka district, 10 health centers, and 31 sub-centers across the country.

To provide health services at the community level, GK establishes sub-centers (mini-clinics) in rural areas of all the upazilas covered by GK activities. Every sub-center has a normal delivery facility and drug dispensary. Five to eight paramedics, most of whom are females trained in primary health care, work in a typical sub-center. An experienced paramedic heads each sub-center, a skilled birth attendant and a pathology technician are stationed there, and a doctor visits twice a week. Other paramedics provide ANC, immunize mothers, provide postnatal care, encourage health awareness, and promote nutritional diets among rural women during home visits. They are also responsible for recruiting enrollees in health insurance, organizing medical gatherings and community meetings, and conducting community surveys and other related activities in remote areas to treat pregnant women (Table 1).

2. Materials and Methods

2.1. *Data*

A questionnaire survey was conducted from October 2010 to February 2011 to collect primary individual data. At present, GK administers MHI schemes in at least part of the rural areas of 16 upazilas in 11 districts. Among these, there is extensive coverage in the rural areas of Dhaka district. For the current study, two upazilas in Dhaka district and three upazilas in other districts were selected. The number of subjects was chosen in light of the population covered by MHI schemes in these areas. Surveyed were 170 subjects from the rural areas where GK's MHI scheme operates in the two Dhaka district upazilas and 180 subjects from the three upazilas in other districts. Data were collected from GK members utilizing systematic random sampling. The names and addresses of mothers enrolled in MHI were collected from existing GK sub-centers. These names were listed in alphabetical order and numbered from the top. Women with numbers that were multiples of 3 (*i.e.*, 3, 6, 9...) were chosen from the list. The sampling process was repeated if the subject quota was not filled.

For comparison, other rural areas where GK does not operate its MHI or health service activities were chosen from each of the five upazilas noted above (Table 2). Some rural areas where GK operates were saturated with insured households, so a sufficient number of subjects not enrolled in health insurance could not be assembled there. Moreover, GK's MHI scheme had already been in operation in most of the rural areas in the two chosen upazilas in Dhaka district. Additional rural areas where GK's scheme was not in operation were selected from another upazila in Dhaka district to allow selection of a sufficient number of subjects not enrolled in health insurance from the entire Dhaka district. Subjects were 145 individuals in three Dhaka district upazilas and 135 individuals in three upazilas outside Dhaka district. Due to lack of administrative information on births, the addresses of women with infants were collected locally. Data were collected randomly from those rural areas.

Six experienced female interviewers and two field investigators were recruited to conduct this survey. An expert familiar with the designed questionnaire trained these female interviewers to recognize ANC

Table 1. Gonoshasthaya Kendra's Micro Health Insurance

Key features	Characteristics				
Area covered	592 villages in 31 unions of 16 upazilas across 11 districts				
Access status	Voluntary; Entire household				
System providing health service	Tertiary hospital (Dhaka district); Health centers (secondary hospital); Sub-centers (mini-clinics) at the union level; Home visits by health workers; Referral services to public hospitals				
Type of service covered	Curative care; Delivery; Preventive care and family planning				
	Destitue	Ultra-poor	Poor	Middle-class	Rich
Annual premiums (taka/household)	5	6	10	60	80
Co-payments for MHI members (taka)					
Consultation at center	2	3	5	8	12
Consultation in village	Free	Free	2	5	8
Medicine	Free	50%	75%	100%	100%
Normal delivery at mini clinic/center	Free	Free	100	400	500
Caesarean delivery	100	200	1,000	3,600	4,800
Midwife services at home for delivery	Ability-to-pay in all classes				
Financial mechanism	Revenue generation from premiums and hospital profits; Subsidies from commercial GK projects; International donations				

Gonoshasthaya Kendra's socioeconomic classes are defined as Destitute: Widows or abandoned women. Ultra-poor: Very distressed families, beggars, and the physically disabled. Poor: Landless farmers, door-to-door vendors, or others who cannot meet basic needs. Middle-class: Households with 2-3 acres of land and who can meet basic needs. Rich: Households with more than 3 acres of land, owners of big shops, highly paid professionals, and those who have savings at the end of the year.

Table 2. Study sites and number of subjects

Upazila (sub-district)	District	Location from capital city Dhaka	Enrolled in GK		Not enrolled in GK	
			Target	Obtained	Target	Obtained
Kutubdia	Cox's Bazaar	350 km southeast	60	59	45	42
Cox's Bazaar	Cox's Bazaar	350 km southeast	60	57	45	44
Sreepur	Gazipur	65 km northeast	60	58	45	43
Dhamrai	Dhaka	35 km northwest	85	71	45	43
Savar	Dhaka	30 km northwest	85	76	50	50
Keranigonj	Dhaka	20 km southwest	--	--	50	49
Total			350	321	280	271

utilization based on a specific definition and to apply that definition equally for all of the sample population. Women who consulted or participated in any screening by a health professional regarding their pregnancy, either at home or in a facility, were counted as having used ANC. Interviewers were trained to identify ANC involving the services of a health professional by asking respondents several questions. A health professional was defined as a person with formal medical schooling: a doctor, paramedic, skilled birth attendant, midwife, or nurse. On this basis, consultation of a GK's health visitor or a Family Welfare Visitor recruited by the government was also counted as ANC utilization, but traditional birth attendants, village doctors, and drug vendors were not included in this category.

In order to equally survey both literate and illiterate women, data were collected through direct interviews. That is, interviewers asked all questionnaire items and wrote all of their answers on answer sheets. No respondent filled in the sheet personally. In this study, women who had not given birth within 1 year were excluded from analysis. Datasheets with missing information were excluded, so a total of 321 valid data sheets were obtained from GK members and 271 from non-members (Table 2).

The ethical committee of Tokyo Medical and Dental University and the Bangladesh Medical and Research Council approved this study.

2.2. *Statistical model*

The analysis of the data was designed to examine the effect of enrollment in MHI by comparing the ANC utilization by women enrolled in MHI and women not enrolled in health insurance. ANC utilization can be considered as consisting of two parts: a woman's choice of whether she utilizes ANC, and how many times she utilizes it. This approach is similar to that in literature concerning health service utilization (*26,27*). Thus, a two-part model was created (*28*). The first part of the model was logistic regression analysis. The dependent variable was binary and equal to 1 if an individual woman utilized ANC, 0 if not. The second part was an ordinary least squares (OLS) regression analysis with the number of times ANC was used as the dependent variable.

In addition, this study attempted to identify how effectively the sliding premiums and co-payments applied to different socioeconomic classes encouraged poor groups to use ANC. Thus, dummy variables for socioeconomic classes according to GK were entered in the model as the main independent variables. As mentioned above, socioeconomic classes according to GK were destitute, ultra-poor, poor, middle-class, and rich (Table 1). Destitute was, however, combined with ultra-poor and only four dummy variables were prepared since there was only one destitute respondent. The coefficient of the socioeconomic class dummies was designated α_n, with the subscript (n) ranging from 1 (Destitute and Ultra-poor) to 4 (Rich). The dummy variable of the specific class n was equal to 1 if an individual woman belonged to the class or was 0 if the woman belonged to another class. Because socioeconomic classes according to GK were indicated only for women enrolled in MHI, women not enrolled in health insurance were not assigned to any class. All of the latter women were pooled into a reference category for the socioeconomic classes in the model.

Moreover, annual household income was entered in the model to exclude its influence on ANC utilization from the estimates of α_n. Cross terms were also entered in the model. These were the product of enrollment status and household income. Enrollment status was expressed as an enrollment dummy and a non-enrollment dummy. The enrollment dummy was equal to 1 if a woman was enrolled in MHI and 0 otherwise. The non-enrollment dummy was equal to 1 if a woman was not enrolled in MHI and 0 otherwise. For ease of interpretation, the cross term with the enrollment dummy was entered in the first part of the model, while the other cross term with the non-enrollment dummy was entered in the second part. In the first part, the cross term and the non-cross term corresponded to the annual household income of women enrolled in MHI and women not enrolled in health insurance, respectively. In the second part, conversely, the cross term and the non-cross term corresponded to the annual household income of the women not enrolled in health insurance and those enrolled in MHI, respectively. The effect of income could thus be separately addressed for women

enrolled in MHI and women not enrolled in health insurance. In addition, the median (60,000 taka) annual household income of all groups was subtracted from the individual values in the model for ease of interpretation. The coefficients of annual household income (non-cross term) and its cross terms with enrollment and non-enrollment were designated β_1, β_2, and β_3, respectively. Estimates of α_n showed the effect of enrollment in MHI on the utilization of ANC in the first part and the number of times ANC was used in the second part. The effect is associated with a specific socioeconomic class n and is based on the entire pool of respondents not enrolled in health insurance, excluding the effect of income and other independent variables. β_1 and β_2 in the first part of the model show the effect of household income among women not enrolled in health insurance and women enrolled in MHI, respectively; β_1 and β_3 in the second part show the same effect among women enrolled in MHI and those not enrolled in health insurance, respectively.

Data on individual, household, and community level attributes included information on the following control variables that might influence ANC utilization (*29-32*): maternal age (age of woman at last birth), the woman's educational level, and birth order as individual variables; religion and occupation of household head as household variables; and area of residence and distance from a primary health care provider or facility as community level variables. Maternal age, birth order, and distance to a primary health care provider were input as continuous variables. However, women's educational level, occupation of the household head, religion, and area of residence were input as categorical variables. A woman's educational level was categorized by final grade she attended school. Women who had not received a formal education were categorized as having no education. Grades 1 to 5, grades 6 to 10, and grades 11 and above were designated as the primary, secondary, and high education, respectively. The occupations of household heads were farmers, day laborers, providers of services, businessmen, other, or unemployed. Religions in the model were limited to Muslim and Hindu.

The statistical software used in this study was SPSS version 16. Statistical significance was set at $p < 0.05$.

3. Results

3.1. *Descriptive statistics*

The sample population's socio-economic and demographic characteristics are summarized in Table 3. The mean maternal age of surveyed women was 24.3 (Standard Deviation (S.D.) = 4.4) years among enrolled women, which was significantly lower than the 25.2 (S.D. = 4.7) years of among non-enrolled women. The average annual household income of enrolled women was 69.8 (S.D. = 43.2) thousand taka and 74.9 (S.D. = 50.8) thousand taka for non-enrolled women. 28.7% of enrolled women and 28.4% of non-enrolled women

Table 3. Socio-economic and demographic characteristics of the sample population

Variables	Enrolled in MHI (n = 321)		Not enrolled in health insurance (n = 271)	
Continuous variables	Mean	S.D.	Mean	S.D.
Maternal age (years)**	24.3	4.4	25.2	4.7
Annual household income (1,000 taka)	69.8	43.2	74.9	50.8
Birth order*	2.3	1.3	2.5	1.1
Distance to a primary health care provider (km)	2.6	1.8	2.7	1.8
Categorical variables	Frequency	(%)	Frequency	(%)
Women's educational level				
No education	92	(28.7)	77	(28.4)
Primary	90	(28.0)	83	(30.6)
Secondary	117	(36.4)	95	(35.1)
Higher	22	(6.9)	16	(5.9)
Religion				
Muslim	232	(72.3)	203	(74.9)
Hindu	89	(27.7)	68	(25.1)
Occupation of household head				
Farmer	60	(18.7)	63	(23.2)
Day laborer	95	(29.6)	61	(22.5)
Provider of services	62	(19.3)	56	(20.7)
Businessman	67	(20.9)	57	(21.0)
Other	24	(7.5)	25	(9.2)
Unemployed	13	(4.0)	9	(3.3)
Area of residence				
Outside Dhaka district	174	(54.2)	129	(47.6)
Dhaka district	147	(45.8)	142	(52.4)

N: number of observations; S.D.: standard deviation. A two-tailed *t*-test was performed for each case of continuous variables to test for significant differences (** $p < 0.05$, * $p < 0.10$). A lack of significance was determined using a chi-squared test for each categorical variable.

were without any formal education. On the other hand, 6.9% of enrolled women and 5.9% non-enrolled women were in the higher educational category. On average 72.3% of enrolled women and 74.9% of non-enrolled were Muslims and the rest were Hindus. Among household heads, day laborers (29.6%) dominated in the enrolled group, and more of the non-enrolled household heads were farmers (23.2%) than any other occupation. The average birth orders of women were 2.3 (S.D. = 1.3) and 2.5 (S.D. = 1.1) among enrolled and non-enrolled women, respectively. The average distance to a primary health care provider for enrolled women was 2.6 (S.D. = 1.8) kilometers, with non-enrolled women averaging 2.7 (S.D. = 1.8) kilometers. In this study, 54.2% of the enrolled women and 47.6% of non-enrolled were from outside the Dhaka district and the rest were from rural areas of Dhaka district. There was no significant difference in the socio-economic and demographic characteristics of the two groups except maternal age.

The distribution of ANC utilization among the enrolled respondents, grouped by GK's social classes, and the entire non-enrolled group is shown in Table 4. The ratio of those who utilized ANC among all enrolled women formed an arc with a peak of 34.3% with 2 visits. On the other hand, the ratio among all non-enrolled women showed a decreasing trend from 39.5% with no use to 5.9% with 4 or more visits. The average number of ANC visits was 2.3 among enrolled women and 1.1 among non-enrolled women. More precisely, in enrolled women grouped by social class, the average number showed an increasing trend of ANC utilization from 1.2 times with the destitute and ultra poor class to 3.1 times with the rich class. Moreover, since the non-enrolled women were not grouped into classes, the distribution of ANC utilization in both enrolled and non-enrolled women is shown by household income quintile instead of GK's social classes in Table 5. Among both the enrolled and non-enrolled women, the average numbers showed increasing trends from the first household income quintile (poorest) to the fifth (richest). The average number was larger for enrolled women than non-enrolled women in every quintile.

3.2. *Two-part model*

The results of the two-part model are presented in Table 6. The main independent variables of interest are the social class dummies of enrolled women. The results of the first part show that the odds of choosing ANC utilization among destitute and ultra poor enrolled

Table 4. Number and percentage of respondents by times ANC was used by subjects enrolled in MHI by socioeconomic class and for all subjects not enrolled in health insurance

Number of times ANC was used	0	1	2	3	4 or more	Total	Mean
Enrolled in MHI							
Destitute and Ultra-poor	1 (6.7)	11 (73.3)	2 (13.3)	1 (6.7)	0 (0.0)	15 (100.0)	1.2
Poor	10 (5.3)	38 (20.0)	75 (39.5)	43 (22.6)	24 (12.6)	190 (100.0)	2.2
Middle-class	11 (13.6)	8 (9.9)	27 (33.3)	26 (32.1)	9 (11.1)	81 (100.0)	2.3
Rich	2 (5.7)	4 (11.4)	6 (17.1)	10 (28.6)	13 (37.1)	35 (100.0)	3.1
Total	24 (7.5)	61 (19.0)	110 (34.3)	80 (24.9)	46 (14.3)	321 (100.0)	2.3
Not enrolled in health insurance[a]	107 (39.5)	79 (29.2)	51 (18.8)	18 (6.6)	16 (5.9)	271 (100.0)	1.1

[a] Individuals not enrolled in health insurance were not classified into socioeconomic classes. Annual household income for women enrolled in MHI by socioeconomic class according to GK was as follows: Destitute and Ultra-poor: 12,000-36,000 taka, Poor: 25,000-80,000 taka, Middle-class: 60,000-120,000 taka, Rich: 108,000-280,000 taka. Income for women not enrolled in health insurance was 15,000-360,000 taka.

Table 5. Number and percentage of respondents by times ANC was used by subjects enrolled in MHI and subjects not enrolled in health insurance by household income quintile

Number of times ANC was used	0	1	2	3	4 or more	Total	Mean
Enrolled in MHI							
1st quintile (poorest)	5 (6.0)	26 (31.0)	30 (35.7)	16 (19.0)	7 (8.3)	84 (100.0)	2.0
2nd quintile	3 (5.3)	14 (24.6)	23 (40.4)	11 (19.3)	6 (10.5)	57 (100.0)	2.1
3rd quintile	6 (10.7)	8 (14.3)	20 (35.7)	13 (23.2)	9 (16.1)	56 (100.0)	2.3
4th quintile	6 (10.3)	3 (5.2)	22 (37.9)	21 (36.2)	6 (10.3)	58 (100.0)	2.4
5th quintile (richest)	4 (6.1)	10 (15.2)	15 (22.7)	19 (28.8)	18 (27.3)	66 (100.0)	2.8
Total	24 (7.5)	61 (19.0)	110 (34.3)	80 (24.9)	46 (14.3)	321 (100.0)	2.3
Not enrolled in health insurance							
1st quintile (poorest)	33 (61.1)	15 (27.8)	5 (9.3)	1 (1.9)	0 (0.0)	54 (100.0)	0.5
2nd quintile	26 (53.1)	16 (32.7)	6 (12.2)	1 (2.0)	0 (0.0)	49 (100.0)	0.6
3rd quintile	19 (32.2)	27 (45.8)	10 (16.9)	3 (5.1)	0 (0.0)	59 (100.0)	0.9
4th quintile	18 (32.7)	15 (27.3)	13 (23.6)	6 (10.9)	3 (5.5)	55 (100.0)	1.3
5th quintile (richest)	11 (20.4)	6 (11.1)	17 (31.5)	7 (13.0)	13 (24.1)	54 (100.0)	2.2
Total	107 (39.5)	79 (29.2)	51 (18.8)	18 (6.6)	16 (5.9)	271 (100.0)	1.1

Annual household income quintiles were as follows: 1st quintile: 12,000-36,000 taka, 2nd quintile: 40,000-50,000 taka, 3rd quintile: 54,000-70,000 taka, 4th quintile: 72,000-95,000 taka, 5th quintile: 96,000-360,000 taka.

women was a significant 70.9 times more than among the overall group of non-enrolled women, controlling for household income and other independent variables. Similarly, the odds among the poor class of enrolled women were also a significant 29.6 times higher. These results point to enrollment in MHI as being effective in women's choosing ANC utilization for certain poor groups, corresponding to GK's destitute, ultra poor, and poor social classes. On the other hand, the results of the second part show that the number of ANC visits undergone by poor, middle, and rich classes of enrolled women was significantly larger by 0.98, 0.87, and 0.81 visits, respectively, than among whole non-enrolled women. It is possible that enrollment in MHI is effective in increasing the number of ANC visits, except for those in the destitute and ultra poor classes.

Moreover, the first part of the model showed that household income was positively associated with the odds of choosing ANC utilization, and the second showed it to be positively associated with a higher number of ANC visits. These results indicate that with an increase in household income of 1,000 taka, non-enrolled women were 1.01 times more likely to choose ANC utilization at an income level of 60,000 taka, and enrolled women underwent an additional incremental 0.007 visits. Furthermore, the cross term of enrollment status and household income tended to show larger effects than the non-cross term but was not significant in either the first part or the second part. Income effects are always pro-rich in both choice of ANC and the number of visits undergone among both enrolled and non-enrolled women.

The educational level of women was also significant in the first part of the model. Those attaining higher educations had 12.6 times higher odds, and those with secondary educations had 2.2 times higher odds associated with choosing ANC utilization than those with no formal education. The odds of choosing ANC utilization, however, were significantly lower (0.79 times) for an increase of one rank of birth order. In addition, as the results of the second part, the number of ANC use occurrences was significantly lower (by 0.068 visits) for a 1-kilometer increase in distance from their residence to a primary health care provider. Those who were residents of Dhaka district also underwent a larger number (by 0.26 visits) of ANC occasions than those who lived outside the Dhaka district.

4. Discussion

The results of the two-part model showed that higher household income affected both the utilization of ANC and the number of times ANC was used. This is not surprising. The magnitude of the income effect did not differ for women enrolled in MHI and women not enrolled in health insurance because enrollment status was adjusted with socioeconomic class dummies for women enrolled in MHI in the model. However, the odds ratios for the "destitute and ultra-poor" and "poor" dummy variables were significantly greater than 1 in the first part and the coefficients for the "poor", "middle-class", and "rich" dummies were significantly positive in the second part (Table 6). These results suggest that GK's MHI plan could increase women's use of ANC among the destitute, ultra-poor, and poor and the number of ANC visits by all socioeconomic classes except the destitute and ultra-poor. A previous study also showed that MHI schemes contributed substantially towards increasing ANC utilization among women enrolled in MHI (*18*). However, that study did not address the benefits of those schemes for specific socio-economic groups. The ability to encourage ANC utilization by destitute, ultra-poor, and poor women makes GK's MHI plan an advantageous initiative for poor rural women although the plan does not seem to have the effect of increasing the number of ANC visits among the destitute and ultra-poor.

The increase in use of ANC can be attributed to the design of the plan. GK's health insurance program uses sliding premium and co-payment scales based on socioeconomic class. GK offers membership to destitute, ultra-poor, and poor households with much lower premiums and exempts the destitute and ultra-poor from payment for some heath services (Table 1). In fact, even the destitute and ultra-poor tend to use ANC more than women not enrolled in health insurance, although specific classes of women enrolled in MHI and corresponding classes of women not enrolled in health insurance cannot be compared (Table 4).

Another indicator, household income quintile, that served as a proxy for socioeconomic classes according to GK also indicated that the percentage of those who utilized ANC one or more times was higher among women enrolled in MHI than among those not enrolled in GK in every quintile (Table 5). This implies that sliding premiums and co-payments favorable to the destitute, ultra-poor, and poor are effective in persuading them to use ANC, although attention should be paid to the incomplete correlation of income quintile with socioeconomic classes according to GK. Moreover, the odds ratios of socioeconomic class dummies increased substantially from the middle-class to poor and further from poor to destitute and ultra-poor (Table 6). Indeed, there are large discontinuous decreases in the amount of annual premiums and some co-payments from the middle-class to poor and from the poor to ultra-poor (Table 1). Policymakers have argued that sliding premiums and co-payments are key to including people excluded from community society in health service provision, while MHI schemes with flat premiums and coverage have been criticized for their tendency to exclude the poor (*16,22,32*). A previous study noted that women enrolled in MHI might begin using the formal health care system through an MHI

Table 6. Factors affecting antenatal care (ANC) utilization

Independent variables	Logistic regression[a]		OLS[b]	
	Odds ratio	*p* value	Coefficient	*p* value
Constant	0.874	0.902	1.060	0.083
Socioeconomic class (Reference: Not enrolled in health insurance)				
Destitute and ultra-poor [α_1]	70.859	0.001	0.056	0.904
Poor [α_2]	29.605	0.000	0.976	0.002
Middle-class [α_3]	1.746	0.296	0.865	0.001
Rich [α_4]	0.675	0.763	0.805	0.045
Annual household income (1,000 taka) [β_1]	1.013	0.003	0.007	0.015
Enrollment in MHI: Household income (1,000 taka) [β_2]	1.026	0.143	--	--
No enrollment in health insurance: Household income (1,000 taka) [β_3]	--	--	0.004	0.268
Maternal age (years)	1.007	0.803	0.003	0.810
Birth order	0.789	0.023	0.000	0.999
Distance to primary health care provider (km)	0.889	0.074	–0.068	0.019
Women's educational level (Reference: No education)				
Higher	12.648	0.018	0.468	0.065
Secondary	2.247	0.006	0.172	0.246
Primary	1.561	0.126	0.060	0.704
Religion (Reference: Muslim)				
Hindu	0.958	0.875	0.038	0.725
Occupation of household head (Reference: Unemployed)				
Farmer	1.910	0.339	–0.074	0.807
Day laborer	1.353	0.645	–0.030	0.918
Provider of services	1.749	0.410	0.166	0.577
Businessman	2.072	0.286	0.104	0.702
Others	1.983	0.356	0.088	0.786
Area of residence (Reference: Outside Dhaka district)				
Dhaka district	1.162	0.150	0.263	0.012
Number of observations	592		461	
R^2	0.241 (Cox & Snell)			
	0.370 (Nagelkerke)		0.282	

OLS: Ordinary least squares. [a] Dependent variable: ANC utilization (any utilization = 1, no utilization = 0). [b] Dependent variable: Number of times ANC was used. Greek letters in square brackets represent the coefficients of the main independent variables in the model.

plan by using non-maternal health services, which also might result in them seeking maternal health care services for the first time (*20*).

As noted earlier, enrollment in MHI is effective in increasing the number of ANC visits among all classes except the destitute and ultra-poor. The coefficients of the "poor", "middle-class", and "rich" dummies in the second part of the analysis are significant and decreasing in that order (Table 6). This implies that lower premiums and co-payments prompt women in these three classes to undergo more ANC visits. However, the smallest premiums and co-payments, for the destitute and ultra-poor, do not increase the number of times they use ANC. Approximately three-fourths of this class utilized ANC only once while an equal proportion of the other classes did so twice or more (Table 4). That said, a similar proportion of women enrolled in MHI utilized ANC twice (35.7%) as did those who used it once (31.0%) among the first income quintile (Table 5). This suggests that low income may not be the sole factor in a greater number of ANC visits. Other factors may be involved. A study showed that restriction of a woman's mobility during pregnancy is prevalent among the ultra-poor due to deep-rooted cultural beliefs and that they may also be uncomfortable receiving health services due to misconduct and negligence by health professionals. Eventually, the study found that they believe that ANC would not benefit them except to confirm pregnancy (*34*). Such cultural beliefs and norms may override the beneficial economic effects from any social protection program and restrain poorer women from utilizing ANC more than once.

In addition to sliding premiums and co-payments in GK's MHI plan, there may be other factors that influence ANC utilization. First, GK's health workers provide home health care and health education in the areas they service. This type of service may bring about a change in health care-seeking behavior among women enrolled in MHI. Actually, the demand for ANC is very low among rural women as they have limited awareness of its importance in achieving safe motherhood (*7*). In this context, health workers' ability to increase awareness may influence women's health beliefs and lead them to receive the ANC offered by GK paramedics at home or at health facilities. In fact, having a higher or secondary level education was associated with utilization of ANC, which agrees with previous studies (*35,36*). This can be explained by the fact that education develops women's understanding

of better health practices and empowers them to make their own decisions. Thus, a woman's educational level and GK's health education may combine to encourage women to use ANC to improve their health.

In addition, the government of Bangladesh has recruited Family Welfare Visitors to visit door-to-door and provide health education regarding maternal health, but there are not enough of them to cover the whole country (*6*). Moreover, they are not accountable for their activities. GK's health workers, however, are accountable to the representatives of the community for any maternal or child deaths, including family members of victims, at "Death Meetings" – special meetings arranged by GK. Moreover, local GK management is obliged to investigate the cause of death in the field and submit a death report to a higher authority within 72 h. Such accountability may cause GK health workers to encourage rural women to seek maternal services, including ANC (*3*).

Another facet of GK's scheme is that it offers community participation in health service delivery through a village health committee consisting of representatives from different sectors. The committee is headed by an elected female member of the local government (*3*). Moreover, GK, with the involvement of the village health committee, conducts need assessment surveys and arranges community meetings among rural households. These activities help build trust and confidence in GK among rural women. Further, such civic engagement and reciprocal linkages ultimately form social capital among GK members. There is an association between social capital and the use of health services, as previous studies have revealed (*16,37*). Hence, such community cohesiveness might also induce rural women to seek ANC. However, which step this factor influences, utilizing ANC or more frequent ANC visits, cannot be addressed with the variables available in this study.

The current results indicate that women who reside in the rural areas of Dhaka district visited ANC more often than did their counterparts (Table 6). The rural areas of Dhaka district have the benefit of being linked to the capital city. Doctors from the City of Dhaka frequently visit and provide health care in those rural areas. In addition, there are different private and NGO hospitals and clinics, including those run by GK, with better technical equipment, pathology instruments, and facilities than in other areas. Thus, residents of those rural areas have access to better quality treatment. As previous studies have noted, increased quality of care leads to greater patient satisfaction (*38,39*), so better quality may prompt residents to increase their ANC utilization by increasing their overall satisfaction. Due to increased numbers of health campaigns sponsored by different organizations, better access to mass media may have also influenced women to use ANC more often (*31*). There is also a link between the number of ANC visits and the distance from a woman's residence to a primary health care provider (Table 6). This result implies that poor communications and transportation systems in rural areas and transport costs are important obstacles to women wishing to visit ANC more often (*3*).

However, access to health care facilities should be available within each treatment area or control area, whether covered by GK's activities or not, and is equivalent to enrollment status in this study. It is unlikely that the basic health service facilities provided by GK improve overall accessibility to health care since the average distance to a primary health care provider does not differ significantly for treatment and control areas (Table 3). In fact, even in control areas outside the Dhaka district there are many health care facilities on which women can depend for health services. These include a single upazila health complex (secondary level public health facility), a union (sub-upazila) level health center (public), a family welfare center (public), a community clinic (public), other NGO clinics (except in Kutubdia upazila), and a few private health professionals. In control areas within the Dhaka district, there are even more facilities. There are a few private clinics, several NGO clinics, and a higher number of private practitioners, along with public facilities. Although the health care delivery structure is supplemented by GK's sub-centers in treatment areas in districts both inside and outside Dhaka, access to facilities has not improved considerably compared to the existing structure in the control area. Rather, the MHI itself appears to be effective in increasing women's utilization of ANC.

Significantly, women who had borne fewer children (who had a lower birth order) visited ANC at least once. Presumably women are more concerned about their early pregnancies and visit ANC at least once.

The present study showed that 7.5% of women enrolled in MHI did not receive any ANC, and the MHI plan was not effective in increasing the number of ANC visits undergone by destitute and ultra-poor women. The reasons for these problems should be addressed to improve this situation. The impact of MHI schemes on other maternal indicators should also be investigated to justify their potential to ensure safe and healthy maternity. Nevertheless, GK's MHI scheme can be seen as an effective tool in enhancing ANC utilization among rural pregnant women. This study implies that successful implementation of MHI schemes by other NGOs or organizations can complement the government's policy to extend access to ANC to some extent to the poor women of rural Bangladesh.

However, there are several limitations to the findings of this study. First, sliding premium and co-payment scales are decided in accordance with the socioeconomic classes defined by GK, and these classes were not applied to women not enrolled in health insurance. Women enrolled in MHI cannot be

specifically compared with the corresponding classes of women not enrolled in health insurance to determine the effect of the sliding scales. In other words, inferences are made but definitive proof is lacking. Second, analysis with limited cross-sectional data can only show the static state, not dynamic changes. Also, no statistical test can be conducted to directly examine the effect of MHI in reducing the disparity of ANC utilization by socioeconomic class due to a lack of time-series information. Third, self-reporting by respondents may carry some bias. Fourth, women who gave birth within the past year were selected as sample subjects. Thus, a few women who utilized ANC earlier might not report the exact number (over- or under-reporting) of ANC visits due to recall bias. If the over and underreporting biases balance each other out, the regression analysis estimates should be free of bias. If the biases are unequal, the regressions may be biased. Fifth, though ANC utilization and more frequent ANC visits are assumed to bring about better antenatal outcomes, the quality of ANC has not been taken into account in this study. Further study should focus on the components and quality of ANC under MHI schemes.

In conclusion, this study pointed to GK's MHI scheme in Bangladesh as encouraging poor rural women to use ANC. The scheme encourages all women, except for the poorest, enrolled in MHI to use ANC more frequently. Sliding premium and co-payment scales are seen as one of the key features of this scheme. MHI schemes are expected to be part of the solution to ensuring safe motherhood.

Acknowledgements

The authors would like to thank Dr. Rezaul Haque, Rural Health Director, and Dr. Manzur Kadir Ahmed, Senior Director of Health and Training, for their permission to conduct this survey. The authors also wish to thank SM Fardous Kabir of the Statistics and Research Department, Gonoshasthaya Kendra, for providing valuable information and feedback. Finally, the authors wish to sincerely thank all of the rural women who patiently answered this survey.

References

1. Anwar I, Killewo J, Chowdhury ME, Dasgupta SK. Bangladesh: Inequalities in utilization of maternal health care services – evidence from Matlab. Health, Nutrition and Population (HNP) Discussion Paper, Reaching The Poor Program Papers No. 2. The World Bank, Washington DC, USA, 2004. *http://siteresources.worldbank.org/HEALTHNUTRITIONANDPOPULATION/Resources/281627-1095698140167/RPP2Bangladesh.pdf* (accessed December 11, 2011).
2. Bhatia JC. Levels and causes of maternal mortality in southern India. Stud Fam Plann. 1993; 24:310-318.
3. Chaudhury RH, Chowdhury Z. Maternal mortality in rural Bangladesh: Lessons learned from Gonoshasthaya Kendra programme villages. Asia Pac Popul J. 2008; 23:55-78.
4. Bloom SS, Lippeveld T, Wypij D. Does antenatal care make a difference to safe delivery? A study in urban Uttar Pradesh, India. Health Policy Plan. 1999; 14:38-48.
5. Islam MS, Ullah MW. People's participation in health services: A study of Bangladesh's rural health Complex. Bangladesh Development Research Working Paper Series (BDRWPS) 7. Bangladesh Development Research Center (BDRC), Falls Church, USA, 2009. *http://www.bangladeshstudies.org/files/WPS_no7.pdf* (accessed December 11, 2011).
6. Ahmed SM, Hossain MA, Rajachowdhury AM, Bhuiya AU. The health workforce crisis in Bangladesh: shortage inappropriate skill-mix and inequitable distribution. Hum Resour Health. 2011; 9:3.
7. National Institute of Population Research and Training (NIPORT), Mitra and Associates, and Macro International. Bangladesh Demographic and Health Survey 2007. Dhaka, Bangladesh and Calverton, Maryland, USA: NIPORT, Mitra and Associates, and Macro International, 2009. *http://www.measuredhs.com/pubs/pdf/FR207/FR207[April-10-2009].pdf* (accessed December 11, 2011).
8. United Nations Statistics Division. Millennium Development Goals Indicators. United Nations, New York, NY, USA. *http://unstats.un.org/unsd/mdg/Metadata.aspx?IndicatorId=0&SeriesId=763* (accessed December 11, 2011).
9. World Health Organization. Core health indicators, database 2008. *http://apps.who.int/whosis/database/core/core_select_process.cfm?countries=all&indicators=nha* (accessed December 11, 2011).
10. Werner WJ. Micro-insurance in Bangladesh: Risk protection for the poor? J Health Popul Nutr. 2009; 27:563-573.
11. Killingsworth JR, Hossain N, Hedrick-Wong Y, Thomas SD, Rahman A, Begum T. Unofficial fees in Bangladesh: Price, equity and institutional issues. Health Policy Plan. 1999; 14:152-163.
12. Cockcroft A, Andersson N, Milne D, Hossain MZ, Karim E. What did the public think of health services reform in Bangladesh? Three national community-based surveys 1999-2003. Health Res Policy Syst. 2007; 5:1.
13. National Institute of Population Research and Training (NIPORT), ORC Macro, Johns Hopkins University and ICDDR, B. Bangladesh Maternal Health Services and Maternal Mortality Survey 2001. Dhaka, Bangladesh and Calverton, Maryland, USA: NIPORT, ORC Macro, Johns Hopkins University, and ICDDR, B, 2003. *http://www.measuredhs.com/pubs/pdf/FR142/00FrontMatter00.pdf* (accessed December 11, 2011).
14. Asian Development Bank. Bangladesh quarterly economic update Asian Development Bank, Dhaka, Bangladesh, 2006. *http://www.adb.org/documents/economic_updates/BAN/2006/mar-2006.pdf* (accessed December 15, 2011).
15. Preker AS, Carrin G, Dror D, Jakab M, Hsiao W, Arhin-Tenkorang D. Effectiveness of community health financing in meeting the cost of illness. Bull World Health Organ. 2002; 80:143-150.
16. Tabor SR. Community-based health insurance and social protection policy. Social Protection Discussion Paper Series, No. 0503, The World Bank, Washington

DC, USA, 2005. *http://siteresources.worldbank.org/SOCIALPROTECTION/Resources/0503.pdf* (accessed December 15, 2011).
17. Criel B, Kegels G. A health insurance scheme for hospital care in Bwamanda district, Zaire: Lessons and questions after 10 years of functioning. Trop Med Int Health. 1997; 2:654-672.
18. Chankova S, Sulzbach S, Diop F. Impact of mutual health organizations: Evidence from West Africa. Health Policy Plan. 2008; 23:264-276.
19. Ranson MK. Reduction of catastrophic health expenditures by a community-based health insurance scheme in Gujarat, India: Current experiences and challenges. Bull World Health Organ. 2002; 80:613-621.
20. Smith KV, Sulzbach S. Community-based health insurance and access to maternal health services: Evidence from three West African countries. Soc Sci Med. 2008; 66:2460-2473.
21. Yip W, Berman P. Targeted health insurance in a low income country and its impact on access and equity in access: Egypt's school health insurance. Health Econ. 2001; 10:207-220.
22. Bennett S. The role of community-based health insurance within the health care financing system: A framework for analysis. Health Policy Plan. 2004; 19:147-158.
23. Ekman B. Community-based health insurance in low-income countries: A systematic review of the evidence. Health Policy Plan. 2004; 19:249-270.
24. World Health Organization. The World health report 2000 – health systems: Improving performance. World Health Organization, Geneva, Switzerland, 2000. *http://www.who.int/whr/2000/en/whr00_en.pdf* (accessed December 11, 2011).
25. Hassan MR, Surur SH, authors; Labonté R, GK Research Team, editors. Study on GK's comprehensive primary health care (CPHC) model: Social capital, community participation, gender empowerment and health care access for the marginalized. Gonoshasthaya Kendra, 2011. *http://www.globalhealthequity.ca/electronic%20library/Study%20on%20GK%20Comprehensive%20Primary%20Health%20Care%20CPHC%20Model%20September%202011.pdf* (accessed December 15, 2011).
26. Wang H, Yip W, Zhang L, Wang L, Hsiao W. Community-based health insurance in poor rural China: the distribution of net benefits. Health Policy Plan. 2005; 20:366-374.
27. Habibov NN, Fan L. Modeling prenatal health care utilization in Tajikistan using a two-stage approach: Implications for policy and research. Health Policy Plan. 2008; 23:443-451.
28. Smits J. Estimating the Heckman two-step procedure to control for selection bias with SPSS. 2003. *http://home.planet.nl/~smits.jeroen* (accessed May 8, 2012).
29. Collin SM, Anwar I, Ronsmans C. A decade of inequality in maternity care: Antenatal care, professional attendance at delivery, and caesarean section in Bangladesh (1991-2004). Int J Equity Health. 2007; 6:9.
30. Islam MR, Odland JO. Determinants of antenatal and postnatal care visits among indigenous people in Bangladesh: A study of the Mru community. Rural Remote Health. 2011; 11:1672.
31. Simkhada B, van Teijlingen ER, Porter M, Simkhada P. Factors affecting the utilization of antenatal care in developing countries: Systematic review of the literature. J Adv Nurs. 2008; 61:244-260.
32. Magadi MA, Madise NJ, Rodrigues RN. Frequency and timing of antenatal care in Kenya: Explaining the variations between women of different communities. Soc Sci Med. 2000; 51:551-561.
33. Ranson MK, Sinha T, Chatterjee M, Acharya A, Bhavsar A, Morris SS, Mills AJ. Making health insurance work for the poor: Learning from the Self-Employed Women's Association's (SEWA) community-based health insurance scheme in India. Soc Sci Med. 2006; 62:707-720.
34. Choudhury N, Ahmed SM. Maternal care practices among the ultra poor households in rural Bangladesh: A qualitative exploratory study. BMC Pregnancy Childbirth. 2011; 11:15.
35. Raghupathy S. Education and the use of maternal health care in Thailand. Soc Sci Med. 1996; 43:459-471.
36. Cleland JG, van Ginneken JK. Maternal education and child survival in developing countries: The search for pathways of influence. Soc Sci Med. 1988; 27:1357-1368.
37. Hendryx MS, Ahern MM, Lovrich NP, McCurdy AH. Access to health care and community social capital. Health Serv Res. 2002; 37:85-101.
38. Mendoza Aldana J, Piechulek H, al-Sabir A. Client satisfaction and quality of health care in rural Bangladesh. Bull World Health Organ. 2001; 79:512-517.
39. Andaleeb SS, Siddiqui N, Khandakar S. Patient satisfaction with health services in Bangladesh. Health Policy Plan. 2007; 22:263-273.

(Received January 25, 2012; Revised July 19, 2012; Accepted July 25, 2012)

Original Article

DOI: 10.5582/bst.2012.v6.4.176

High quality nutrient intake is associated with higher household expenditures by Japanese adults

Yoshiharu Fukuda [1,*], Ayako Hiyoshi[2]

[1] *Department of Community Health and Medicine, Yamaguchi University School of Medicine, Yamaguchi, Japan;*
[2] *Department of Epidemiology and Public Health, University College London, London, UK.*

Summary **There is little evidence of socioeconomic differences in dietary intake in the Japanese population. This study examined the association between household expenditures and dietary intake using nationally representative surveys of Japan. We analyzed data from the Comprehensive Survey of Living Conditions and National Health and Nutrition Survey, 2003-2007. For subjects ages 18 to 74 years (11,240 men and 11,472 women), the sex-specific association between household expenditure quartiles and selected nutrient intake was examined using comparison of means and prevalence of a healthy intake. Higher household expenditures were associated with an increase in the mean levels of total energy, fat, protein, carbohydrates, calcium, vitamins A and C, niacin, and fiber for both men and women and salt for men. Prevalence comparison indicated that most of the recommendations for dietary intake were met for people with higher household expenditures than for those with lower household expenditures. There was no clear association between fat intake and expenditures. Higher household expenditures were associated with a healthy and balanced nutrient intake in Japanese adults. The findings suggest that socioeconomic differences in dietary patterns contribute to socioeconomic inequalities in mortality and morbidity in Japan.**

Keywords: Health inequalities, socioeconomic factors, household expenditures, nutrient intake, diet quality

1. Introduction

Socioeconomic differences in health are currently a great concern in the field of public health and health policies. Health is determined by a wide range of individual socioeconomic circumstances and social environments that are termed social determinants of health (*1*). Social epidemiology is the branch of epidemiology that seeks to ascertain health inequalities and social determinants of health (*2*). Like in Western countries, prior studies in Japan found that disparities in mortality, morbidity, self-rated health, psychological distress, health behaviors, and other aspects were explained by socioeconomic status such as educational attainment, income, and occupational status (*3*).

The pathways from socioeconomic status to poor health are complicated. One of the important pathways is related to health behaviors including dietary patterns and nutrient intake (*1*). People of a lower socioeconomic status in terms of education, income, occupational status, *etc.* have been found to have a poor quality diet (*4-7*). An unhealthy dietary intake pattern results in increased risk factors particularly for cardiovascular disease, including obesity, diabetes, and dyslipidemia (*8,9*).

Several studies in Japanese populations have examined socioeconomic differences in health, and differences in mortality, morbidity, and health risks were noted (*3*). However, the socioeconomic differences were moderate compared with those in other countries, and the association between socioeconomic status and major diseases and risks was not entirely consistent (*10-14*). In particular, there are

**Address correspondence to:*
Dr. Yoshiharu Fukuda, Department of Community Health and Medicine, Yamaguchi University School of Medicine, 1-1-1 Minamikogushi, Ube, Yamaguchi, 755-8505, Japan.
E-mail: fukuday@yamaguchi-u.ac.jp

limited findings relating to socioeconomic differences in dietary intake by the Japanese population. In a prior study of pregnant Japanese women, a healthy dietary intake was associated with education but not household income (*15*). Another study found that increasing monetary costs of dietary energy were associated with both healthy and unhealthy dietary intake patterns (*16*). Since these studies examined specified populations, nationwide differences in dietary intake need to be examined.

The present study used nationally representative surveys to examine the association between household expenditures as a socioeconomic indicator and the intake of major nutrients by the Japanese population.

2. Methods

2.1. *Data*

Two nationally representative surveys conducted by the Ministry of Health, Labor, and Welfare in Japan were used: the Comprehensive Survey of Living Conditions (CSLC) and the National Health and Nutritional Survey (NHNS), 2003-2007 (*17,18*).

The CSLC began in 1986 and has been conducted every three years since, with smaller surveys in-between. In both types of surveys, the entire land area of Japan was divided into approximately one million enumeration districts (EDs). The large surveys randomly selected around 5,000 EDs while the small surveys selected 1,000 EDs. Interviewers visited all households within the selected areas using lists of households and approached all members of the household. The questionnaires included basic household and individual information regarding demographics, health, illness profiles, lifestyle, monthly household expenditures, and other items. The survey sample was about 280,000 households for the large surveys in 2004 and 2007 and about 57,000 households in 2003, 2005, and 2006. The response rates were about 80%.

The NHNS is an annual nationwide nutrition survey that began in 1948. Using the EDs of the CSLC, around 300 EDs were randomly selected every year, and all members of the household 1 year of age and older were approached. The survey consisted of an anthropometric examination including height, weight, and blood pressure; blood tests; a dietary survey; and health-related behaviors. The subject sample every year from 2003 to 2007 was around 5,000 households and 15,000 members of those households. The response rates were almost 60%.

The dietary survey was carried out using a food weight record method for one day of November, excluding Sunday and national holidays, in each household (*17*). Trained dietitians visited participants, and they were asked to weigh and record all foods and beverages that any of the members of the household consumed. Dietary records were coded using the Standard Tables for Food in Japan, 5th edition, and the intake of nutrients and food groups were tallied for every household. Nutrient intake per person was calculated as intake per household simply divided by the number of members of the household 1 year of age and over.

Since the NHNS and CSLC utilize the same sampling units, survey data were linked using the survey year, regional area, number of households, number of members of the household, age, and sex. These data were narrowed to those from subjects from ages 18 to 74 years with no missing data for relevant variables.

The data from the two surveys were used with permission of the Ministry of Health, Labor, and Welfare.

2.2. *Outcomes*

The following eleven nutrients served to indicate outcomes; total energy, total fat, carbohydrates, protein, calcium, vitamins A, B_1, and C, niacin, fiber, and salt. This nutrient intake was estimated by the Ministry of Health, Labour and Welfare. Total fat and carbohydrates were represented as % energy, and protein, calcium, vitamins A, B_1, and C, niacin, fiber and salt were calculated per 1,000 kcal.

The prevalence of a healthy nutrient intake was determined using the recommended dietary allowance (RDA) or the tentative dietary goals for preventing lifestyle-related disease (DG) according to the Dietary Reference Intakes for Japanese, 2010 (*19*). The values were total fat: 20-30%; carbohydrates: 50-70%; protein: 60 g for men and 50 g for women; calcium: 700 mg for men and 650 mg for women; vitamin A: 850 μg for men and 650 μg for women, vitamin B_1: 1.4 mg for men and 1.1 mg for women; vitamin C: 100 mg; niacin: 15 mg for men and 12 mg for women; fiber: 19 mg for men and 12 mg for women; and salt: 9 g for men and 7.5 g for women. To adjust for total energy intake, the values of calcium to salt were divided by the mean of total energy intake by subjects: 2,197 kcal for men and 1,752 kcal for women. The final cut-offs are shown in Table 1.

2.3. *Analysis*

Equivalent household expenditures were used as a socioeconomic measure in this study. Expenditures were calculated by dividing total household expenditures per month by the square root of household size according to a recent method devised by the OECD (*20*). The study subjects were then grouped into quartiles according to expenditures. Quartile lines were 100, 140, and 180 thousand yen per month.

Statistical analysis was conducted separately by sex. Age-adjusted means of nutrient intake were estimated and compared by household expenditure quartiles using

Table 1. Summary of basic characteristics and nutrient intake by study subjects

Variable	Men (*n* = 11,240)	Women (*n* = 11,472)
Age (years, mean ± standard deviation)	49.5 ± 15.5	49.2 ± 15.5
Marital status (%)		
Married	75.6%	69.0%
Single	20.3%	18.4%
Separated	1.6%	7.5%
Divorced	2.5%	5.1%
Nutrient intake (mean ± standard deviation)		
Total energy (kcal/day)	2,197.4 ± 613.4	1,751.7 ± 462.5
Total fat (% energy)	24.0 ± 7.3	25.9 ± 7.5
Carbohydrates (% energy)	61.4 ± 8.2	58.7 ± 8.3
Protein (g/1,000 kcal)	36.6 ± 7.8	38.4 ± 7.9
Calcium (mg/1,000 kcal)	244.3 ± 113.1	302.4 ± 140.0
Vitamin A (μg/1,000 kcal)	348.6 ± 420.1	433.8 ± 437.9
Vitamin B_1 (mg/1,000 kcal)	0.72 ± 2.69	0.87 ± 3.68
Vitamin C (mg/1,000 kcal)	53.1 ± 71.5	77.5 ± 115.1
Niacin (mg/1,000 kcal)	8.25 ± 3.52	8.32 ± 3.44
Fiber (g/1,000 kcal)	7.07 ± 2.82	8.57 ± 3.32
Salt (g/1,000 kcal)	5.77 ± 2.07	6.15 ± 2.20
Healthy nutrient intake (%)*		
Total fat 20-30% energy	26.5%	24.0%
Carbohydrates 50-70% energy	77.5%	77.6%
Protein ≥ 27.3 (m), 28.5 (w) g/1,000 kcal	90.7%	91.5%
Calcium ≥ 319 (m), 371 (w) mg/1,000 kcal	21.9%	25.8%
Vitamin A ≥ 387 (m), 371 (w) μg/1,000 kcal	27.4%	43.2%
Vitamin B_1 ≥ 0.64 (m), 0.63 (w) mg/1,000 kcal	13.4%	16.5%
Vitamin C ≥ 45.5 (m), 57.1 (w) mg/1,000 kcal	40.4%	46.8%
Niacin ≥ 6.8 mg/1,000 kcal	62.2%	63.6%
Fiber ≥ 8.6 (m), 9.7 (w) g/1,000 kcal	24.8%	43.8%
Salt < 4.1 g/1,000 kcal	20.2%	15.3%

* (m) for men, (w) for women.

Table 2. Nutrient intake by men according to quartiles of household expenditures: age-adjusted mean ± standard error

Nutrient intake	1st (lowest) quartile (*n* = 2,724)	2nd quartile (*n* = 2,523)	3rd quartile (*n* = 2,936)	4th (highest) quartile (*n* = 3,057)
Total energy (kcal/day)	2,173.2 ± 11.8[4]	2,183.3 ± 12.2[4]	2,194.2 ± 11.3[4]	2,233.8 ± 11.1[1,2,3]
Total fat (% energy)	23.2 ± 0.1[2,3,4]	23.8 ± 0.1[1,4]	24.0 ± 0.1[1,4]	24.7 ± 0.1[1,2,3]
Carbohydrates (% energy)	62.6 ± 0.2[2,3,4]	61.6 ± 0.2[1,3,4]	61.1 ± 0.1[1,2,4]	60.4 ± 0.1[1,2,3]
Protein (g/1,000 kcal)	35.6 ± 0.1[2,3,4]	36.4 ± 0.2[1,3,4]	37.2 ± 0.1[1,2]	37.2 ± 0.1[1,2]
Calcium (mg/1,000 kcal)	236.3 ± 2.1[2,3]	240.2 ± 2.2[3,4]	247.0 ± 2.0[1,2]	252.3 ± 2.0[1,2]
Vitamin A (μg/1,000 kcal)	319.6 ± 8.0[2,3,4]	354.5 ± 8.3[1]	351.8 ± 7.7[1]	366.6 ± 7.6[1]
Vitamin B_1 (mg/1,000 kcal)	0.65 ± 0.05	0.73 ± 0.05	0.73 ± 0.05	0.74 ± 0.05
Vitamin C (mg/1,000 kcal)	49.4 ± 1.4[3,4]	51.3 ± 1.4[4]	54.7 ± 1.3[1]	56.4 ± 1.3[1,2]
Niacin (mg/1,000 kcal)	7.84 ± 0.07[2,3,4]	8.11 ± 0.07[1,2,4]	8.48 ± 0.06[1,2]	8.51 ± 0.06[1,2]
Fiber (g/1,000 kcal)	6.92 ± 0.05[3,4]	6.98 ± 0.05[3,4]	7.13 ± 0.05[1,2]	7.22 ± 0.05[1,2]
Salt (g/1,000 kcal)	5.66 ± 0.04[3,4]	5.77 ± 0.04	5.84 ± 0.04[1]	5.79 ± 0.04[1]

[1, 2, 3, 4] significant ($p < 0.05$) compared to the 1st, 2nd, 3rd, and 4th quartiles, respectively.

the General Linear Model and the least significant difference method. The prevalence of a healthy nutrient intake by household expenditure quartiles was also compared *via* the chi-squared test for trends. Then, the odds ratio (OR) of the prevalence for age, household expenditure quartiles, and marital status (being married *vs*. not being married, including being separated or divorced) was estimated using multiple logistic regression analysis. The statistics package SPSS 19 was used for all statistical analyses.

3. Results

The data for 11,240 men and 11,472 women were analyzed. Table 1 shows the basic characteristics of age and marital status. Age and marital status were almost the same for men and women.

A summary of nutrient intake is also shown in Table 1. The prevalence of a healthy nutrient intake ranged from 13.4% for vitamin B_1 to 90.7% for protein in men and from 15.3% for salt to 91.5% for protein in women.

Table 2 shows the age-adjusted mean and the standard error (S.E.) of nutrient intake according to quartiles of household expenditures for men. Intake of all nutrients except carbohydrates and vitamin B_1 trended to increase as household expenditures increased. A significant decrease in carbohydrates in accordance with expenditures was noted. There were no

differences in the intake of vitamin B_1.

As shown in Table 3, men and women had similar results. This was not true for salt intake: the highest (4th) quartile had a significantly lower salt intake than other quartiles.

Table 4 shows the prevalence of a healthy nutrient intake and the odds ratio (OR) for men. Significant gradients of increased prevalence with an increase in household expenditures were noted for carbohydrates, protein, calcium, vitamins A, B_1, and C, niacin, and fiber: the OR for the 4th quartile compared to that for the 1st quartile ranged from 1.20 for vitamin B_1 to 1.82 for protein. For total fat, there was no significant OR among quartiles. For salt, the 2nd and 3rd quartiles had

Table 3. Nutrient intake by women according to quartiles of household expenditures: age-adjusted mean ± standard error

Nutrient intake	1st (lowest) quartile (n = 2,696)	2nd quartile (n = 2,488)	3rd quartile (n = 2,782)	4th (highest) quartile (n = 2,909)
Total energy (kcal/day)	1,702.3 ± 8.9[3,4]	1,727.4 ± 9.2[3,4]	1,765.9 ± 8.7[1,2,4]	1,804.5 ± 8.5[1,2,3]
Total fat (% energy)	25.3 ± 0.1[2,3,4]	25.7 ± 0.1[1,4]	26.0 ± 0.1[1,4]	26.6 ± 0.1[1,2,3]
Carbohydrates (% energy)	59.8 ± 0.2[2,3,4]	58.9 ± 0.2[1,4]	58.5 ± 0.2[1,4]	57.9 ± 0.1[1,2,3]
Protein (g/1,000 kcal)	37.5 ± 0.2[2,3,4]	38.5 ± 0.2[1]	38.7 ± 0.1[1]	38.9 ± 0.1[1]
Calcium (mg/1,000 kcal)	292.0 ± 2.6[3,4]	298.4 ± 2.7[4]	304.4 ± 2.6[1,4]	313.8 ± 2.5[1,2,3]
Vitamin A (μg/1,000 kcal)	398.8 ± 8.4[2,3,4]	437.6 ± 8.7[1]	436.3 ± 8.3[2,4]	460.6 ± 8.1[1,3]
Vitamin B_1 (mg/1,000 kcal)	0.78 ± 0.07	0.88 ± 0.07	0.91 ± 0.07	0.92 ± 0.07
Vitamin C (mg/1,000 kcal)	69.4 ± 2.2[3,4]	73.5 ± 2.3[4]	77.5 ± 2.2[1,4]	88.5 ± 2.1[1,2,3]
Niacin (mg/1,000 kcal)	7.96 ± 0.07[2,3,4]	8.34 ± 0.07[1]	8.46 ± 0.07[1]	8.50 ± 0.06[1]
Fiber (g/1,000 kcal)	8.32 ± 0.06[3,4]	8.59 ± 0.06[1]	8.61 ± 0.06[1]	8.75 ± 0.06[1]
Salt (g/1,000 kcal)	6.14 ± 0.04[4]	6.25 ± 0.04[4]	6.21 ± 0.04[4]	6.02 ± 0.04[1,2,3]

[1, 2, 3, 4] significant ($p < 0.05$) compared to the 1st, 2nd, 3rd, and 4th quartiles, respectively.

Table 4. Prevalence of a healthy nutrient intake by men and the odds ratio (OR) and 95% confidence interval (CI) for quartiles of household expenditures and marital status

Nutrient intake	Total fat 20-30% energy % OR (95% CI)	Carbohydrates 50-70% energy % OR (95% CI)	Protein ≥ 27.3 g/1,000 kcal % OR (95% CI)
Age (per ten-year increase)	1.08 (1.04-1.11)	0.91 (0.87-0.94)	1.14 (1.08-1.19)
Household expenditures			
1st (lowest) quartile	25.7% 1.00 reference	74.4% 1.00 reference	87.2% 1.00 reference
2nd quartile	26.7% 1.04 (0.92-1.17)	76.5% 1.10 (0.97-1.25)	90.4% 1.38 (1.16-1.64)
3rd quartile	27.5% 1.07 (0.95-1.20)	78.4% 1.25 (1.11-1.41)	92.0% 1.63 (1.37-1.95)
4th (highest) quartile	26.0% 0.99 (0.88-1.11)	80.2% 1.42 (1.25-1.60)	92.8% 1.82 (1.53-2.18)
Trend		***	***
Not married (reference = married)	0.94 (0.82-1.07)	0.72 (0.63-0.82)	1.13 (0.94-1.36)

Nutrient intake	Calcium ≥ 319 mg/1,000 kcal % OR (95% CI)	Vitamin A ≥ 387 μg/1,000 kcal % OR (95% CI)	Vitamin B_1 ≥ 0.64 mg/1,000 kcal % OR (95% CI)
Age (per ten-year increase)	1.36 (1.31-1.41)	1.18 (1.14-1.22)	1.03 (0.99-1.08)
Household expenditures			
1st (lowest) quartile	19.2% 1.00 reference	22.8% 1.00 reference	12.2% 1.00 reference
2nd quartile	20.0% 1.05 (0.92-1.21)	26.3% 1.20 (1.05-1.36)	12.9% 1.08 (0.92-1.27)
3rd quartile	20.5% 1.18 (1.04-1.35)	29.8% 1.39 (1.24-1.57)	14.1% 1.19 (1.02-1.39)
4th (highest) quartile	25.3% 1.35 (1.19-1.53)	30.2% 1.40 (1.25-1.58)	14.3% 1.20 (1.03-1.40)
Trend	***	***	*
Not married (reference = married)	1.56 (1.35-1.80)	1.10 (0.97-1.26)	1.21 (1.03-1.43)

Nutrient intake	Vitamin C ≥ 45.5 mg/1,000 kcal % OR (95% CI)	Niacin ≥ 6.8 mg/1,000 kcal % OR (95% CI)	Fiber ≥ 8.6 g/1,000 kcal % OR (95% CI)	Salt < 4.1 g/1,000 kcal % OR (95% CI)
Age (per ten-year increase)	1.64 (1.59-1.70)	1.10 (1.07-1.14)	1.59 (1.53-1.65)	0.86 (0.83-0.89)
Household expenditures				
1st (lowest) quartile	34.9% 1.00 reference	56.4% 1.00 reference	21.4% 1.00 reference	23.4% 1.00 reference
2nd quartile	37.7% 1.12 (1.00-1.26)	60.5% 1.16 (1.04-1.29)	23.3% 1.10 (0.96-1.26)	20.9% 0.88 (0.77-1.00)
3rd quartile	42.8% 1.33 (1.19-1.49)	64.0% 1.33 (1.19-1.48)	25.4% 1.17 (1.03-1.33)	19.1% 0.80 (0.70-0.91)
4th (highest) quartile	45.1% 1.41 (1.26-1.57)	67.1% 1.51 (1.36-1.69)	28.3% 1.32 (1.17-1.50)	17.8% 0.74 (0.65-0.85)
Trend	***	***	***	***
Not married (reference = married)	1.67 (1.47-1.89)	0.76 (0.67-0.85)	1.33 (1.15-1.55)	0.99 (0.87-1.14)

* $p < 0.05$, ** $p < 0.01$, *** $p < 0.001$ with a chi-squared test for trends. % was prevalence of a healthy nutrient intake: *e.g.* total fat 20-25% energy. OR was estimated with multiple logistic regression using age, household expenditure quartile, and marital status. Individuals who were single, separated, or divorced were designated as "not married".

Table 5. Prevalence of a healthy nutrient intake by women and the odds ratio (OR) and 95% confidence interval (CI) for quartiles of household expenditures and marital status

Nutrient intake	Total fat 20-30% energy		Carbohydrates 50-70% energy		Protein ≥ 28.5 g/1,000 kcal	
	%	OR (95% CI)	%	OR (95% CI)	%	OR (95% CI)
Age (per ten-year increase)		1.16 (1.12-1.21)		1.05 (1.02-1.09)		1.24 (1.18-1.32)
Household expenditures						
1st (lowest) quartile	24.4%	1.00 reference	77.2%	1.00 reference	88.3%	1.00 reference
2nd quartile	22.9%	0.93 (0.82-1.06)	77.2%	1.00 (0.88-1.14)	91.5%	1.44 (1.20-1.73)
3rd quartile	24.5%	0.99 (0.88-1.12)	78.0%	1.04 (0.91-0.18)	92.6%	1.60 (1.33-1.93)
4th (highest) quartile	24.3%	0.98 (0.87-1.11)	77.9%	1.03 (0.91-1.17)	93.5%	1.82 (1.51-2.21)
Trend					***	
Not married (reference = married)		0.97 (0.84-1.11)		0.90 (0.79-1.04)		1.46 (1.19-1.80)

Nutrient intake	Calcium ≥ 371 mg/1,000 kcal		Vitamin A ≥ 371 μg/1,000 kcal		Vitamin B_1 ≥ 0.63 mg/1,000 kcal	
	%	OR (95% CI)	%	OR (95% CI)	%	OR (95% CI)
Age (per ten-year increase)		1.35 (1.30-1.40)		1.21 (1.18-1.25)		1.06 (1.02-1.10)
Household expenditures						
1st (lowest) quartile	23.6%	1.00 reference	37.4%	1.00 reference	14.6%	1.00 reference
2nd quartile	24.7%	1.11 (0.97-1.26)	42.0%	1.25 (1.12-1.40)	16.3%	1.15 (0.99-1.34)
3rd quartile	25.9%	1.14 (1.00-1.29)	45.7%	1.41 (1.26-1.57)	17.2%	1.22 (1.06-1.42)
4th (highest) quartile	28.8%	1.32 (1.16-1.49)	47.4%	1.50 (1.35-1.68)	17.8%	1.26 (1.09-1.46)
Trend	***		***		***	
Not married (reference = married)		1.55 (1.34-1.78)		1.22 (1.08-1.38)		1.30 (1.12-1.52)

Nutrient intake	Vitamin C ≥ 57.1 mg/1,000 kcal		Niacin ≥ 6.8 mg/1,000 kcal		Fiber ≥ 9.7 g/1,000 kcal		Salt < 4.1 g/1,000 kcal	
	%	OR (95% CI)	%	OR (95% CI)	%	OR (95% CI)	%	OR (95% CI)
Age (per ten-year increase)		1.66 (1.61-1.72)		1.16 (1.12-1.19)		1.61 (1.56-1.67)		0.83 (0.80-0.87)
Household expenditures								
1st (lowest) quartile	42.2%	1.00 reference	58.0%	1.00 reference	40.1%	1.00 reference	17.1%	1.00 reference
2nd quartile	44.6%	1.18 (1.05-1.32)	63.7%	1.29 (1.15-1.44)	43.6%	1.22 (1.08-1.37)	13.9%	0.78 (0.67-0.90)
3rd quartile	48.1%	1.27 (1.13-1.42)	65.5%	1.36 (1.22-1.52)	44.4%	1.17 (1.04-1.31)	14.2%	0.82 (0.71-0.95)
4th (highest) quartile	51.6%	1.47 (1.31-1.64)	66.8%	1.44 (1.29-1.61)	46.8%	1.29 (1.15-1.44)	15.7%	0.93 (0.80-1.07)
Trend	***		***		***			
Not married (reference = married)		1.91 (1.68-2.17)		1.13 (1.00-1.28)		1.63 (1.43-1.85)		0.85 (0.72-0.99)

* $p < 0.05$, ** $p < 0.01$, *** $p < 0.001$ with a chi-squared test for trends. % was prevalence of a healthy nutrient intake: *e.g.* total fat 20-25% energy. OR was estimated with multiple logistic regression using age, household expenditure quartile, and marital status. Individuals who were single, separated, or divorced were designated as "not married".

a significantly lower OR compared to the 1st quartile. In terms of marital status, not being married was significantly associated with a healthy intake compared to being married; intake of calcium, vitamins B_1 and C, and fiber increased while that of carbohydrates and niacin decreased.

As shown in Table 5, women and men had similar results. There were differences, however. There was no significant OR for carbohydrates, and increased salt intake was associated with lower household expenditures. In terms of marital status, not being married had a significantly increased OR compared to being married for all nutrients except total fat, carbohydrates, and salt.

4. Discussion

This study found an association between socioeconomic status and nutrient intake in a nationally representative sample in Japan. Results indicated that people with higher household expenditures were likely to have a healthier nutrient intake. Different patterns were noted mainly for fat and salt intake.

More favorable nutrient intake was associated with higher household expenditures. This finding was in line with prior studies in Western countries, in which higher socioeconomic position was associated with better dietary quality (*4-7*). These findings suggest that people with higher expenditures and income can select and purchase nutrient-rich food, including vegetables and fruit. In a study of pregnant Japanese women, healthy intake patterns were related to education but not income (*15*). Presumably, food choices are determined based on the ability to understand dietary recommendations rather than on other socioeconomic factors (*e.g.* income). However, the present study found that monetary advantages also promote a healthy diet.

In terms of fat intake, people with higher household expenditures had a higher mean of % energy. This seems to suggest that higher household expenditures are associated with an unhealthy fat intake, since an increase in fat results in cardiovascular risk factors such as obesity and dyslipidemia. However, the prevalence of fat intake in the recommended range (20 to 30%

energy) did not differ among quartiles of household expenditures. Therefore, higher household expenditures were not associated with a detrimental increase in fat intake.

Salt intake was associated with household expenditures for men, while women with the highest quartile of expenditures had the lowest salt intake. A prior study of Japanese women found no association between sodium intake and any socioeconomic indicator of education, occupation, or income (*15*). High salt intake is one of the most critical issues affecting nutrient intake in Japan, and a significant decrease in this intake has not been noted in recent years (*17*). This suggests that individuals have difficulty decreasing their salt intake, even if they are of a higher socioeconomic status.

Socioeconomic status is generally associated with cardiovascular disease and risk, which dietary and nutrient intake contribute to (*8,9*). The association between household expenditures and nutrient quality appears to partly explain the increase in cardiovascular disease and risk in people of a lower socioeconomic status. Fat and salt intake are important contributors to cardiovascular disease, but individuals with lower household expenditures were not found to have an unhealthy fat or salt intake. This finding might relate to the moderate association between socioeconomic status and cardiovascular disease and risk in Japan compared to that in Western countries (*11-14*).

The association between marital status and nutrient intake noted by this study is interesting. Not being married was associated with the healthy intake of most nutrients including vitamins and fiber, particularly for women. Prior studies in Japan found that being married decreased mortality and morbidity (*21,22*), so married people are assumed to have a healthier diet than unmarried people. Several studies in other countries found that married individuals tend to eat healthier diets than unmarried individuals do (*23-26*), while a few studies had inconsistent findings (*27,28*). Although the present study did not explore the background of the relationship, unmarried people might be likely to consume nutrient-rich food outside the home, for example. Another possibility is that the method of nutrient estimation is related to a healthy intake by unmarried people. The nutrient intake per capita is obtained by dividing the whole amount consumed in a household by the number of members of the household, regardless of their age and sex. Therefore, the nutrient intake of married subjects and subjects with children might be underestimated.

The mechanisms by which socioeconomic disadvantage leads to an unhealthy nutrient intake have frequently been discussed (*4,8*). Food choice and nutrition security are influenced by individual knowledge and training, food price and diet cost, food access, and the food environment, including neighborhood context, cultural issues, and other aspects (*4,8*). A few studies in Japan examined neighborhood environment and dietary intake but found no meaningful association (*29-31*). Therefore, individual factors might be better suited to explaining socioeconomic differences in nutrient intake in the Japanese population.

A few limitations should be noted. First, household expenditures were found to be less sensitive as an indicator of socioeconomic status compared to household income (*32*). Since income information was not collected in all of the years covered by the present study, household expenditures were divided by equivalent household size. Equivalent expenditures have been found to be useful for social patterning of risk factors (*32*). The second limitation relates to nutrition survey. Several problems with the NHNS have been noted, including limited accessibility of the original raw data, survey and data quality control, the low response rate, and nutrient estimation as a result of simply dividing by family size (*33*).

The findings of this study emphasize socioeconomic factors in disease prevention and health promotion. As in other industrialized countries, in Japan socioeconomic status is associated with nutrient intake, possibly through food choice and purchase. Disease prevention and health promotion should be targeted at socioeconomically disadvantaged populations. In addition to encouraging people to choose a healthy dietary pattern, accessibility to lower cost and nutrient-rich food should be promoted.

In conclusion, this study using nationally representative surveys found that people with higher household expenditures had a healthier intake of nutrients such as vitamins and fiber. The same association was not evident for fat and salt intake. An unhealthy nutrient intake associated with lower household expenditures might partly result in increased morbidity and mortality in socioeconomically disadvantaged populations.

Acknowledgements

The present study was supported by a Grant-in-Aid for Scientific Research in Innovative Areas (Research in a Proposed Research Area) 2011 (No. 4102-21119003) from the Ministry of Education, Culture, Sports, Science, and Technology, Japan.

References

1. Marmot M, Wilkinson RG. Social Determinants of Health. Oxford University Press, New York, NY, USA, 1999.
2. Berkman LF, Kawachi I. Social Epidemiology. Oxford University Press, New York, NY, USA, 1999.
3. Kagamimori S, Gaina A, Nasermoaddeli A. Socioeconomic status and health in the Japanese population. Soc Sci Med. 2009; 68:2152-2160.

4. Dubois L, Girard M. Social position and nutrition: A gradient relationship in Canada and the USA. Eur J Clin Nutr. 2001; 55:366-373.
5. Friel S, Kelleher CC, Nolan G, Harrington J. Social diversity of Irish adults nutritional intake. Eur J Clin Nutr. 2003; 57:865-875.
6. Galobardes B, Morabia A, Bernstein MS. Diet and socioeconomic position: Does the use of different indicators matter? Int J Epidemiol. 2001; 30:334-340.
7. Groth MV, Fagt S, Brondsted L. Social determinants of dietary habits in Denmark. Eur J Clin Nutr. 2001; 55:959-966.
8. Robertson A, Brunner E, Sheiham A. Food is a political issue. In: Marmot M, Wilkinson RG, editors. Social Determinants of Health. Oxford University Press, New York, NY, USA, 2006; pp. 172-195.
9. Smith GD, Brunner E. Socio-economic differentials in health: The role of nutrition. Proc Nutr Soc. 1997; 56:75-90.
10. Anzai Y, Ohkubo T, Nishino Y, Tsuji I, Hisamichi S. Relationship between health practices and education level in the rural Japanese population. J Epidemiol. 2000; 10:149-156.
11. Fujino Y, Tamakoshi A, Iso H, Inaba Y, Kubo T, Ide R, Ikeda A, Yoshimura T; JACC study group. A nationwide cohort study of educational background and major causes of death among the elderly population in Japan. Prev Med. 2005; 40:444-451.
12. Honjo K, Tsutsumi A, Kayaba K; Jichi Medical School Cohort Study Group. Socioeconomic indicators and cardiovascular disease incidence among Japanese community residents: The Jichi Medical School Cohort Study. Int J Behav Med. 2010; 17:58-66.
13. Martikainen P, Lahelma E, Marmot M, Sekine M, Nishi N, Kagamimori S. A comparison of socioeconomic differences in physical functioning and perceived health among male and female employees in Britain, Finland and Japan. Soc Sci Med. 2004; 59:1287-1295.
14. Nishi N, Makino K, Fukuda H, Tatara K. Effects of socioeconomic indicators on coronary risk factors, self-rated health and psychological well-being among urban Japanese civil servants. Soc Sci Med. 2004; 58:1159-1170.
15. Murakami K, Miyake Y, Sasaki S, Tanaka K, Ohya Y, Hirota Y; Osaka Maternal and Child Health Study Group. Education, but not occupation or household income, is positively related to favorable dietary intake patterns in pregnant Japanese women: The Osaka Maternal and Child Health Study. Nutr Res. 2009; 29:164-172.
16. Murakami K, Sasaki S, Okubo H, Takahashi Y, Hosoi Y, Itabashi M. Monetary costs of dietary energy reported by young Japanese women: Association with food and nutrient intake and body mass index. Public Health Nutr. 2007; 10:1430-1439.
17. Ministry of Health, Labour and Welfare. National Health and Nutrition Survey. *http://www.mhlw.go.jp/bunya/kenkou/kenkou_eiyou_chousa.html* (accessed February 10, 2012).
18. Ministry of Health, Labour and Welfare. Comprehensive Survey of Living Conditions. *http://www.mhlw.go.jp/toukei/list/20-19.html* (accessed February 10, 2012).
19. Committee of Dietary Reference Intakes for Japanese. Dietary Reference Intakes for Japanese, 2010. Daiichi Shuppan, Tokyo, 2009.
20. OECD. Growing unequal? Income distribution and poverty in OECD country. OECD, Paris, 2008.
21. Ikeda A, Iso H, Toyoshima H, Fujino Y, Mizoue T, Yoshimura T, Inaba Y, Tamakoshi A, JACC Study Group. Marital status and mortality among Japanese men and women: The Japan Collaborative Cohort Study. BMC Public Health. 2007; 7:73.
22. Kamon Y, Okamura T, Tanaka T, Hozawa A, Yamagata Z, Takebayashi T, Kusaka Y, Urano S, Nakagawa H, Kadowaki T, Miyoshi Y, Yamato H, Okayama A, Ueshima H; HIPOP-OHP Research Group. Marital status and cardiovascular risk factors among middle-aged Japanese male workers: The High-risk and Population Strategy for Occupational Health Promotion (HIPOP-OHP) study. J Occup Health. 2008; 50:348-356.
23. Ball K, Crawford D, Mishra G. Socio-economic inequalities in women's fruit and vegetable intakes: A multilevel study of individual, social and environmental mediators. Public Health Nut. 2006; 9:623-630.
24. Billson H, Pryer JA, Nichols R. Variation in fruit and vegetable consumption among adults in Britain. An analysis from the dietary and nutritional survey of British adults. Eur J Clin Nutr. 1999; 53:946-952.
25. Roos E, Lahelma E, Virtanen M, Prättälä R, Pietinen P. Gender, socioeconomic status and family status as determinants of food behaviour. Soc Sci Med. 1998; 46:1519-1529.
26. Mondini L, Moraes SA, Freitas IC, Gimeno SG. Fruit and vegetable intake by adults in Ribeirao Preto, Southeastern Brazil. Rev Saude Publica. 2010; 44:686-694.
27. Deshmukh-Taskar P, Nicklas TA, Yang SJ, Berenson GS. Does food group consumption vary by differences in socioeconomic, demographic, and lifestyle factors in young adults? The Bogalusa Heart Study. J Am Diet Assoc. 2007; 107:223-234.
28. Satheannoppakao W, Aekplakorn W, Pradipasen M. Fruit and vegetable consumption and its recommended intake associated with sociodemographic factors: Thailand National Health Examination Survey III. Public Health Nutr. 2009; 12:2192-2198.
29. Murakami K, Sasaki S, Okubo H, Takahashi Y; Freshmen in Dietetic Courses Study II Group. Neighborhood socioeconomic status in relation to dietary intake and body mass index in female Japanese dietetic students. Nutrition. 2009; 25:745-752.
30. Murakami K, Sasaki S, Takahashi Y, Uenishi K. Neighborhood food store availability in relation to food intake in young Japanese women. Nutrition. 2009; 25:640-646.
31. Murakami K, Sasaki S, Takahashi Y, Uenishi K. No meaningful association of neighborhood food store availability with dietary intake, body mass index, or waist circumference in young Japanese women. Nutr Res. 2010; 30:565-573.
32. Fukuda Y, Nakao H, Imai H. Different income information as an indicator for health inequality among Japanese adults. J Epidemiol. 2007; 17:93-99.
33. Sasaki S. The value of the National Health and Nutrition Survey in Japan. Lancet. 2011; 378:1205-1206.

(*Received March 1, 2012; Revised July 27, 2012; Accepted August 3, 2012*)

Original Article

DOI: 10.5582/bst.2012.v6.4.183

Membrane raft disruption results in neuritic retraction prior to neuronal death in cortical neurons

Shawn N. Whitehead[1], Sandhya Gangaraju[1], Amy Aylsworth[1], Sheng T. Hou[1,2,*]

[1] *Experimental Neurotherapeutics Laboratory, NRC-Institute for Biological Sciences, National Research Council Canada, Ottawa, Canada;*
[2] *Department of Biochemistry, Microbiology and Immunology, University of Ottawa,Ottawa, Canada.*

Summary **Membrane rafts, rich in sphingolipids and cholesterol, play an important role in neuronal membrane domain-specific signaling events, maintaining synapses and dendritic spines. The purpose of this study is to examine the neuronal response to membrane raft disruption. Membrane rafts of 8 DIV primary neuronal cultures were isolated based on the resistance to Triton X-100 and ability to float in sucrose gradients. Membrane rafts from primary cortical neurons were also imaged using the membrane raft marker, cholera toxin subunit-B (CTxB), and were co-immunolabelled with the dendritic microtubule associated protein marker, MAP-2, the dendritic and axonal microtubule protein, β-III-Tubulin, and the axonal microtubule protein, Tau. Exposure of cortical neurons to either the cholesterol depleting compound, methyl-beta-cyclodextrin (MBC), or to the glycosphingolipid metabolism inhibiting agent D-threo-1-phenyl-2-decanoylamino-3-morpholino-1-propanol (D-PDMP), resulted in neuritic retraction prior to the appearance of neuronal death. Further investigation into the effects of MBC revealed a pronounced perturbation of microtubule protein association with membrane rafts during neuritic retraction. Interestingly, stabilizing microtubules with Paclitaxel did not prevent MBC-induced neuritic retraction, suggesting that neuritic retraction occurred independently of microtubule disassembly and that microtubule association with membrane rafts is critical for maintaining neuritic stability. Overall, the data indicated that membrane rafts play an important role in neurite stability and neuronal viability.**

Keywords: Membrane raft, neuritic retraction, axonal damage, neuronal death, cortical neurons, time lapse imaging

1. Introduction

The plasma membrane of cells, composed mainly of lipids, is a fluid dynamic structure that has the ability to change its fatty acid composition and density to adjust and react to its external environment. One way to do this is through the formation of specialized membrane microdomains called lipid rafts, or membrane rafts, as the name has been redefined recently (*1*). These specialized membrane microdomains are rich in glycosphingolipids and cholesterol and are known to play an important role in neuronal domain specific signaling events (*2*) and maintaining synapses and dendritic spines (*3*). For example, membrane rafts compartmentalize cellular processes by serving as organizing centers or scaffolds for the assembly of axonal outgrowth signaling molecules (*4,5*), influencing membrane fluidity and membrane protein trafficking, and regulating neurotransmission and receptor trafficking (*3,6*). One key feature distinguishing membrane rafts from the rest of the plasma membranes is lipid composition. Membrane rafts generally contain twice the amount of cholesterol found in the surrounding lipid bilayer and have 50% more of sphingolipids, such as sphingomyelin, compared to the rest of the plasma membrane. Proteins in membrane rafts also undergo lipid modifications such as

**Address correspondence to:*
Dr. Sheng T. Hou, NRC-Institute for Biological Sciences, National Research Council Canada, 1200 Montreal Road, Bldg M54, Ottawa K1A 0R6, Canada.
E-mail: sheng.hou@nrc-cnrc.gc.ca

glycosylphosphatidylinositol anchors and acquire the ability to directly bind cholesterol (*7*).

The role of membrane rafts in maintaining axonal structure and neuritic networks in mature adult neurons is still unclear. Cholesterol rich membrane rafts have been shown to interact with components of the cytoskeleton (*8,9*). Specifically, α-tubulin has been co-immunoprecipitated with Caveolin-1, a marker for membrane rafts, in rat brain extracts (*10*). Also, membrane raft domains have been implicated in stabilizing microtubules within smooth muscle cells (*11*). These studies prompted us to hypothesize that disruption of membrane rafts through perturbing cholesterol may affect the cytoskeleton thereby causing morphological changes in neuritic structures and may ultimately affect membrane raft-mediated signal transduction and neuronal survival. Methyl-beta-cyclodextrin (MBC), a cyclic oligosaccharide with high a affinity to cholesterol, has been widely used to sequester cholesterol from cellular membranes and thus disrupt membrane rafts (*12*). Several studies have examined the effects of cholesterol depletion *via* MBC exposure on signal transduction pathways (*13-17*). D-threo-1-phenyl-2-decanoylamino-3-morpholino-1-propanol (D-PDMP) has also been shown to disrupt membrane raft integrity by inhibiting glycosphingolipid metabolism (*18-20*).

In the present study, the neuronal response to membrane raft disrupting agents MBC and D-PDMP were examined. Continued exposure of cortical neurons to either MBC or D-PDMP resulted in rapid neuritic retraction prior to the appearance of neuronal death. Several microtubule proteins were found to co-localize with membrane rafts indicating that membrane raft stability may be required for maintaining neuritic integrity. These findings shed light on the role of membrane rafts in modulating neuritic stability in mature cortical neurons.

2. Materials and Methods

2.1. *Culture of cerebral cortical neurons*

Primary cortical neurons were cultured from embryonic day 15/16 CD-1 mice as described previously (*21,22*). Briefly, neurons were plated into 24-well plates at a density of 1×10^6 cells/well coated with poly-D-lysine (100 μg/mL) in serum-free medium (N_2/Dulbecco's modified Eagle's medium (1:1) supplemented with 6 mg/mL D-glucose, 100 μg/mL transferrin, 25 μg/mL insulin, 20 nM progesterone, 60 μM putrescine, and 30 nM selenium. Neurons were incubated at 37°C with 5% CO_2. One-third of the medium was exchanged with fresh medium at 3 and 6 days *in vitro* (DIV).

2.2. *Induction of neuritic retraction*

Primary cortical neurons were treated with various concentrations (5 μM, 50 μM, 500 μM, 5 mM and 10 mM) of MBC (Sigma, Toronto, ON, Canada) diluted in ddH_2O for various time points up to 1 h. Neuritic retraction was also examined in primary neuronal cultures following exposure to various concentrations (1 μM, 5 μM, 10 μM and 20 μM) of D-threo-1-Phenyl-2-decanoylamino-3-morpholino-1-propanol (D-PDMP) (Sigma, Toronto, ON, Canada). To establish the effects of microtubule stability on MBC-induced neuritic retraction, primary cortical neurons were incubated with either dimethyl sulfoxide (DMSO) (Sigma, Toronto, ON, Canada) alone or with 100 nM Paclitaxel (Taxol) diluted in DMSO 2 h prior to exposure with MBC, a concentration and time point shown to be effective in protecting neurons against toxicity (*23*).

2.3. *Neuronal viability*

Neuronal viability was determined by an Alamar Blue (AB) assay (BioSource International, Nivelles, Belgium). This compound links to the respiratory chain without affecting the integrity of cells (*24*). When AB is reduced, it becomes fluorescent. Thus, cell metabolic rates can be evaluated proportionally with the fluorescence intensity. Briefly, at the end of the treatment period, 10% v/v AB was added to each well. Plates were then incubated at 37°C for 1 h. Next, for each well, three 100 μL aliquots were transferred to a 96-well plate and the absorbance at 540 nm was spectrophotometrically detected with a Cytofluor 2350 Fluorescent Measurement System. The absorbance of a medium blank with AB was subtracted from the absorbance of the control and test wells with AB to give the absorbance of the oxidized form and AB reduction was calculated. Each well was read in triplicate and experimental data was normalized to controls. All results represent the mean of two separate culture experiments. Neuronal viability was also calculated by detecting nuclei per microscopic field using Hoechst 33258 nuclear stain. Data was represented as percent viability and was calculated from five fields per treatment for two independent cultures.

2.4. *Labeling membrane rafts and fluorescent immunohistochemistry*

Coverslips containing 8 DIV primary cortical neurons were fixed with 4% formaldehyde (VWR, Mississauga, ON, Canada) in 10 mM PBS for 30 min at room temperature, followed by rinsing in 10 mM PBS for 5 times. For membrane raft labeling, coverslips were incubated with 5 μg of CTxB-FITC (Sigma, Toronto, ON, Canada) for 1 h on ice and covered to limit exposure to light. Coverslips to be used for

immunofluorecence were washed 3 times with PBS following CTxB incubation and incubated with the following primary antibodies in a buffer containing 10 mM PBS, 0.3% Triton X-100, 1.5% BSA for 1 h at room temperature: mouse Anti-β-III-tubulin monoclonal antibody (1:100, Millipore Laboratories, Billerica, MA, USA), mouse anti-MAP2a+b monoclonal antibody (1:500, Millipore Laboratories, USA) or mouse anti-Tau monoclonal antibody (1:100, Millipore Laboratories, Billerica, MA, USA). Coverslips were then washed 3 times in 10 mM PBS and were incubated in a donkey anti-mouse Cy-3 conjugated secondary antibody (1:400, Jackson laboratories, Bar Harbor, ME, USA). Following 3 washes in 10 mM PBS, coverslips were briefly dipped in water to prevent PBS crystal formation and mounted with Dako fluorescent mounting media (Sigma, Toronto, ON, Canada) spiked with 5 mg/mL Hoechst 33258 (Sigma, Toronto, ON, Canada). Coverslips containing labeled cells were visualized using a Zeiss inverted microscope with a magnification of 40× and digital images were obtained using the Axiovision v.4.7.2.0 software.

2.5. *Isolation of detergent resistant membranes*

Detergent-resistant membranes were isolated on the basis of their resistance to Triton X-100 at 4°C and their ability to float in sucrose density gradients. Primary cortical neurons were homogenized in 1 ml of PTN 50 buffer (50 mM sodium phosphate, pH 7.4; 1% Triton X-100, 50 mM NaCl) containing 10 mM DTT, 1 mM PMSF, 5 μg leupeptin and 1 μg pepstatin A. Cell lysates were centrifuged at 13,400 × g for 3 min to remove any nuclear material. The remaining supernatant was diluted with equal volumes of 80% sucrose. Samples were carefully overlaid with equal volumes of 30% and 5% sucrose respectively. The gradient was centrifuged at 130,000 × g (average) for 20 h at 4°C in a Beckman L8-70 ultracentrifuge (SW40-400 rotor) and aliquoted into 600 μL fractions. Following fractionation, fractions were collected and the protein concentrations within the fractions were detected using the Biorad protein assay (Biorad, Missisauga, ON, Canada). Membrane raft positive fractions were identified based on a positive western blotting signal with Caveolin-1 and Flotillin-1 (see western blotting for details). Membrane raft and non-raft fractions were then pooled and concentrated using Amicon ultra columns (Millipore Laboratories, Billerica, MA, USA).

2.6. *Western blotting*

Twenty microgramme of protein from each pooled fraction was separated by 6% or 8% SDS-PAGE. Electrophoresis was performed at 100 V and the gel was transferred to pure nitrocellulose membrane (Biorad laboratories, Mississauga, ON, Canada) for 1 h at room temperature at 100 V. The nitrocellulose membrane was blocked for 30 min at room temperature with 5% non-fat milk in TBST buffer containing 10 mM Tris, 150 mM NaCl, and 0.1% Tween-20. Membranes were incubated with the following primary antibodies overnight at 4°C: rabbit anti-Caveolin-1 polyclonal (1:500, Santa Cruz Laboratories, Santa Cruz, CA, USA), mouse anti-Flotillin-1 monoclonal (1:1,000, BD Biosciences, USA), anti-β-III-tubulin monoclonal (1:1,000, Millipore Laboratories, Billerica, MA, USA), mouse anti-MAP2a+b monoclonal (1:1,000, Millipore Laboratories, Billerica, MA, USA) or mouse anti-Tau monoclonal (1:500, Millipore Laboratories, Billerica, MA, USA). All primary antibodies were diluted in 5% non-fat milk. TBST: The primary antibody incubation was followed by 3 × 10 min washes in TBST followed by an incubation with the appropriate secondary antibodies diluted in 5% non-fat milk/TBST: HRP-conjugated secondary goat-anti-mouse (1:2,500, Jackson Laboratories, Bar Harbor, ME, USA) and HRP-conjugated secondary goat-anti-rabbit (1:2,500, Jackson Laboratories, Bar Harbor, ME, USA). Following 3 × 10 min washes in TBST, the blots were developed with ECL (GE Healthcare Life Sciences, Baie d'Urfe, QC, Canada).

2.7. *Time lapse imaging*

Primary cortical neurons were acclimated for 30 min to the time lapse chamber and were maintained at 37°C with 5% CO_2. Cells were then incubated with 30 μg/mL propidium iodide (PI) for 30 min. Following acclimation and incubation with PI, cortical neurons were exposed to 5 mM MBC. Cultures were imaged using time lapse microscopy imaging every 20 sec following MBC exposure for up to 1 h. During each time interval both phase and Cy-3 images were obtained.

2.8. *Data analysis*

All data was analyzed by one way ANOVA and further *post hoc* tests for significant groups using Dunnett's test. Groups were considered significant with a p-value < 0.05.

3. Results

3.1. *Exposure of cortical neurons to MBC or D-PDMP results in dose-dependent neuritic retraction and neuronal death*

To determine the effects of membrane raft disruption on neurons, a dose response curve of MBC was established. Primary cortical neurons at 8 DIV were exposed to 5 μM, 50 μM, 500 μM, 5 mM or 10 mM MBC for up to 30 min. At 20 and 30 min of exposure, cells were fixed. Neuritic length and neuronal viability

were assessed (Figure 1A, red colored lines). Based on Hoechst staining and nuclei morphology, a MBC exposure at 5 μM or 50 μM did not have any effect on neuronal viability (Figure 1A). Neuronal viability was significantly reduced by a 30 min exposure of 500 μM or 5 mM MBC. Neuronal viability was also significantly reduced when neurons were exposed to a higher dose of 10 mM MBC (data not shown). Given that membrane raft disruption from MBC appeared to result in a concentration dependant cell death, it is still possible that lower concentrations, (and earlier time points), may still impact neuronal structure and function. We therefore next examined the dose response of MBC exposure on neuritic retraction (Figure 1A, black colored lines). Neurons significantly retracted their neurites as early as 20 min when exposed to 50 μM, 500 μM, or 5 mM MBC. Therefore, these results demonstrated that exposure to MBC resulted in neuritic retraction followed by neuronal death.

Membrane raft disruption *via* inhibition of glycosphingolipid synthesis has also been documented using D-PDMP (*18-20*). Hoechst staining and nuclei morphology revealed that neurons treated with 10 μM D-PDMP started to die following 60 min of exposure

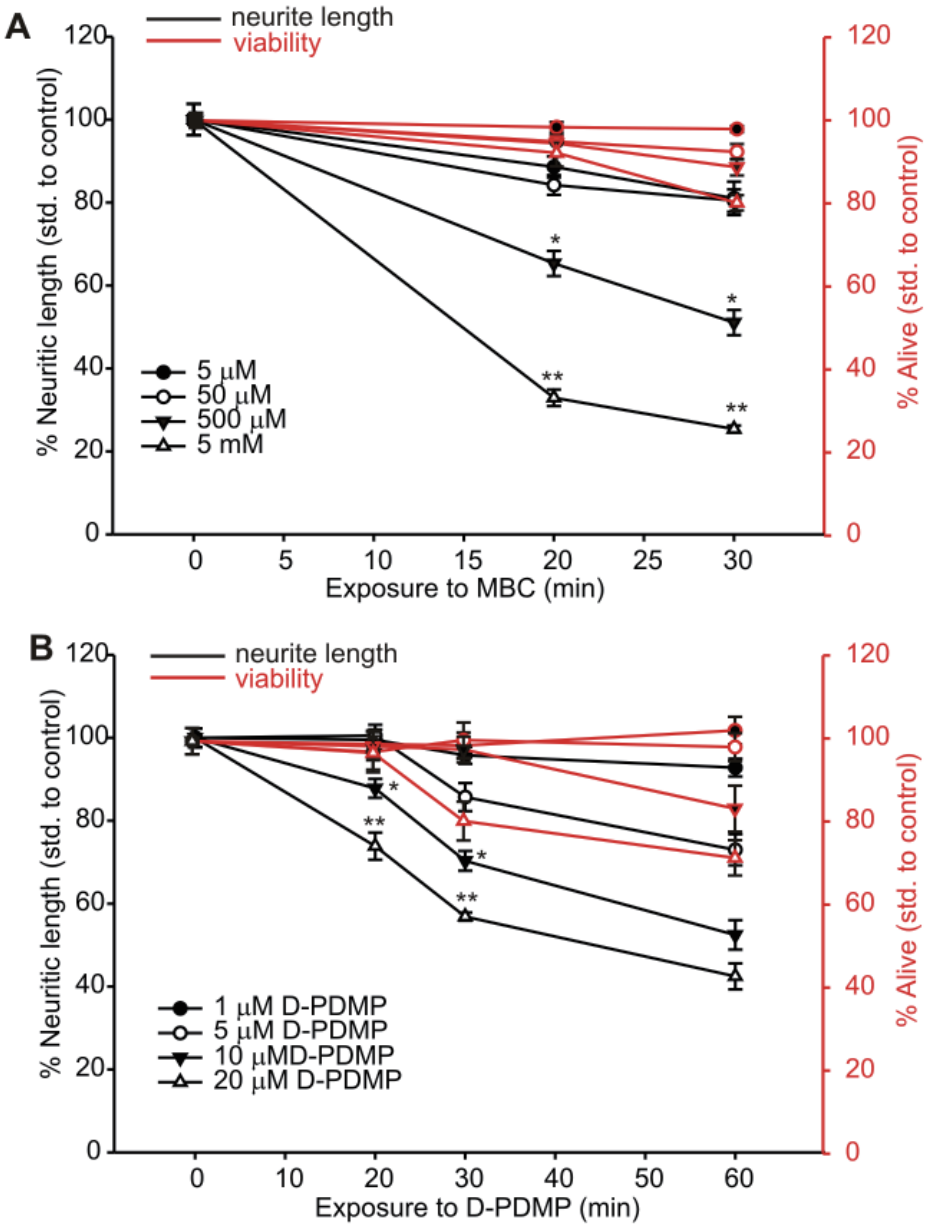

Figure 1. Effects of MBC and D-PDMP on neuritic length and neuronal viability. (A) Primary cortical neurons cultured for 8 DIV were exposed to 5 μM, 50 μM, 500 μM, 5 mM or 10 mM of MBC for 20 and 30 min. **(B)** Primary cortical neurons cultured for 8 DIV were exposed to 1 μM, 5 μM, 10 μM or 20 μM of D-PDMP for 20, 30 or 60 min. In both **(A)** and **(B)**, Neuronal viability (red colored lines) was determined on fixed cells stained with Hoechst 33258. Neuritic length (black colored lines) was measured and quantified using Image J software. Data from two independent experiments were presented as mean% alive from control untreated cells **(A** and **B)** and mean% change in neuritic length **(A** and **B)** ± S.E.M (* indicates statistical significant change at $p < 0.05$ from the control by one-way ANOVA with Dunnett's *post hoc* test, $n = 12$).

while 20 μM D-PDMP treated neurons resulted in cell death by 30 min of exposure (Figure 1B, red colored lines). This level of D-PDMP-induced toxicity was consistent with a previous study demonstrating the toxic effects of D-PDMP in cultured trigeminal sensory neurons whereby neurons died following exposure to 20 μM D-PDMP (*19*). Here, neurons significantly retracted their neurites by 30 min of exposure of 5 μM D-PDMP, and as early as 20 min when exposed to 10 μM and 20 μM D-PDMP (Figure 1A, black colored lines). Results from neurons exposed to D-PDMP demonstrated a similar response pattern and morphology to those treated with MBC, whereby disruption of membrane rafts resulted in neuritic retraction prior to the appearance of cell death. Given that 5 mM of MBC resulted in both neuritic retraction and cell death, and that 5 mM is frequently used experimentally (*14,17,25*), subsequent experiments were performed using this paradigm.

3.2. *Neuritic retraction occurs prior to neuronal death following exposure with MBC*

The relationship between membrane raft integrity, neuritic retraction and neuronal death was further examined using time-lapse microscopy. To do this, cortical neurons were acclimated for 30 min to the time-lapse microscope chamber and followed by incubation with 30 μg/mL PI for 30 min. PI serves as an indicator for changes of membrane permeability and neuronal death. Following acclimation and incubation with PI, cortical neurons were exposed to 5 mM MBC. Cultures were imaged using time-lapse microscopy imaging every 20 sec following MBC exposure for up to 1 h. During each time interval, both phase contrast and PI fluorescent images were obtained in Figure 2A and the supplemental Movie 1 (*http://www.biosciencetrends.com/docindex.php?year=2012&kanno=4*). Neuritic retraction occurred as early as 5 min following exposure to 5 mM of MBC and continued throughout the exposure period. The neurons only became PI positive once the majority of cell retraction occurred (Figure 2A and the supplemental Movie 1). The relationship between neuritic retraction and neuronal cell death was quantified at various time points following exposure to MBC. Neuronal viability was assessed using both a morphometric analysis of Hoechst 33258 stained nuclei and a plate-reader based Alamar blue assay. Both measurements indicated that neuritic retraction preceded neuronal death (Figure 2B). In fact, neurites retracted significantly compared to the controls as early as 5 min following exposure with MBC (70.0 ± 3.8% of control), whereas neuronal death did not occur until 20 min (88.6 ± 1.6% of control by Alamar blue assay) and 30 min (83.4 ± 2.1% of control by Hoechst morphometric analysis) (Figure 2B). Therefore, these results demonstrated that membrane raft destabilization *via* cholesterol extraction resulted in early neuritic retraction prior to the appearance of neuronal death.

3.3. *Cytoskeletal proteins are associated with membrane rafts*

Since membrane raft disruption resulted in neuritic retraction, we sought to examine the potential mechanisms by which the retraction occurred. We hypothesized that perturbation of membrane raft-associated cytoskeleton proteins may be required. To examine this possibility, the presence of neuronal cytoskeletal proteins in the membrane rafts was examined. These proteins are microtubule associated protein 2 (MAP-2), β-III-tubulin and Tau. Membrane raft fractions were isolated using sucrose gradient ultracentrifugation (see Methods section) and confirmed using immunoblotting to detect Caveolin-1 and Flotillin-1, which are makers for membrane rafts (Figure 3A). Both membrane raft and non-membrane-raft fractions were also probed by Western blotting to detect the dendritic expressed MAP-2, dendritic and axonal expressed β-III-tubulin and the axonal expressed Tau. All three microtubule associated proteins were present within the membrane raft fractions (Figure 3A). Quantitative analysis showed that the ratio of β-III-tubulin and Tau within the raft domains compared to the non-raft domains was higher than that of MAP-2. Co-localization of membrane rafts with cytoskeletal proteins was also confirmed using immunostaining of cytoskeletal proteins (red color) combined with CTxB (green color) as shown in Figure 3B.

3.4. *Stabilizing cytoskeleton does not prevent MBC-induced neurite retraction*

Experiments were performed to understand whether the observed neuritic retraction was caused by the general destabilization of microtubules in response to MBC treatment, or caused by the loss of membrane rafts which may serve as anchors for microtubule proteins. To assess these possibilities, neurons were pre-incubated with 100 nM of Paclitaxel (Taxol), a microtubule stabilizing agent, for 2 h (Figure 3C), a concentration and time point that has been shown to be protective against toxic insult (*23*). Cells pre-incubated with or without 100 nM Paclitaxel (and concentrations up to 10 μM, data not shown) demonstrated a similar rapid response with respect to neuritic retraction (Figure 3C, black colored lines) and neuronal viability (Figure 3C, red colored lines), suggesting that neuritic retraction was caused by the loss of membrane rafts serving as anchoring points for microtubule, rather than due to the destabilization of microtubules in response to MBC.

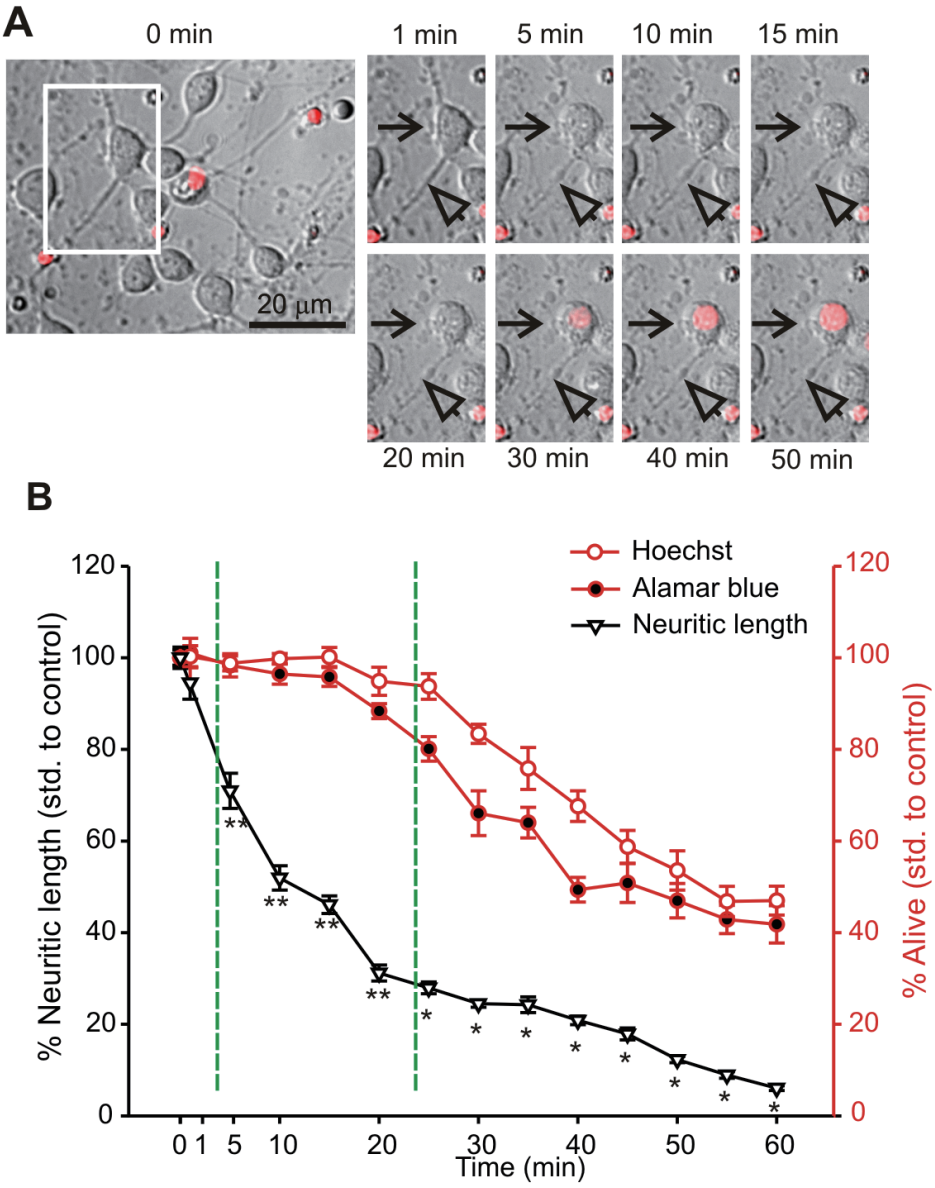

Figure 2. Time lapse imaging neuritic retraction and neuronal death following exposure to MBC. To visualize real time neuritic retraction and neuronal cell death, time-lapse microscopy was performed on 8 DIV cortical neurons treated with 30 μg/mL PI for 30 min prior to exposure with 5 mM MBC for up to 1 h. **(A)** Photomicrographs of the time-lapse imaging demonstrated neuritic retraction as early as 5 min. Cells did not become positive with PI after at least 20 min when the majority of the neurites have retracted (bar represents 20 μm). **(B)** A time course of cell viability was assessed using Hoechst cell counts and the Alamar Blue assay along with corresponding measurements of neuritic length. Cell viability was significantly reduced by 20 min (Alamar blue) and 30 min (Hoechst cell counts) following exposure to MBC. Quantitative data from two independent experiments are represented as mean changes standardized to the control untreated cells. Green lines are to highlight the difference between cell death and neuritoc length with * and ** indicating statistical significant changes from controls at $p < 0.05$ and 0.01, respectively, by one-way ANOVA, Tukey's *post hoc* test, $n = 16$.

4. Discussion

Here, we demonstrated the importance of membrane rafts in mediating neuritic retraction using two membrane raft disruption chemical agents. When membrane rafts are disrupted, perturbations of membrane raft-associated cytoskeleton proteins occur, neurites retract rapidly and neuronal death ensues. Our findings are consistent with a previous study in which inhibition of hydroxymethylglutaryl coenzyme A reductase and cholesterol synthesis in the mevalonate pathway resulted in significant neurite retraction in neuronal differentiated PC12 cells and rat cortical neurons (*26*). These findings are important in the context of understanding the pathogenesis of neuronal injury in several neurodegenerative diseases. Changes in synaptic activity caused by neuritic retraction have been postulated as being an early marker of neuronal dysfunction, commonly found early during the pathogenesis of Alzheimer's disease (*27-29*), Parkinson's disease (*30-32*) and stroke (*33*). It has also been demonstrated that neuritic retraction occurs in response to brain injury

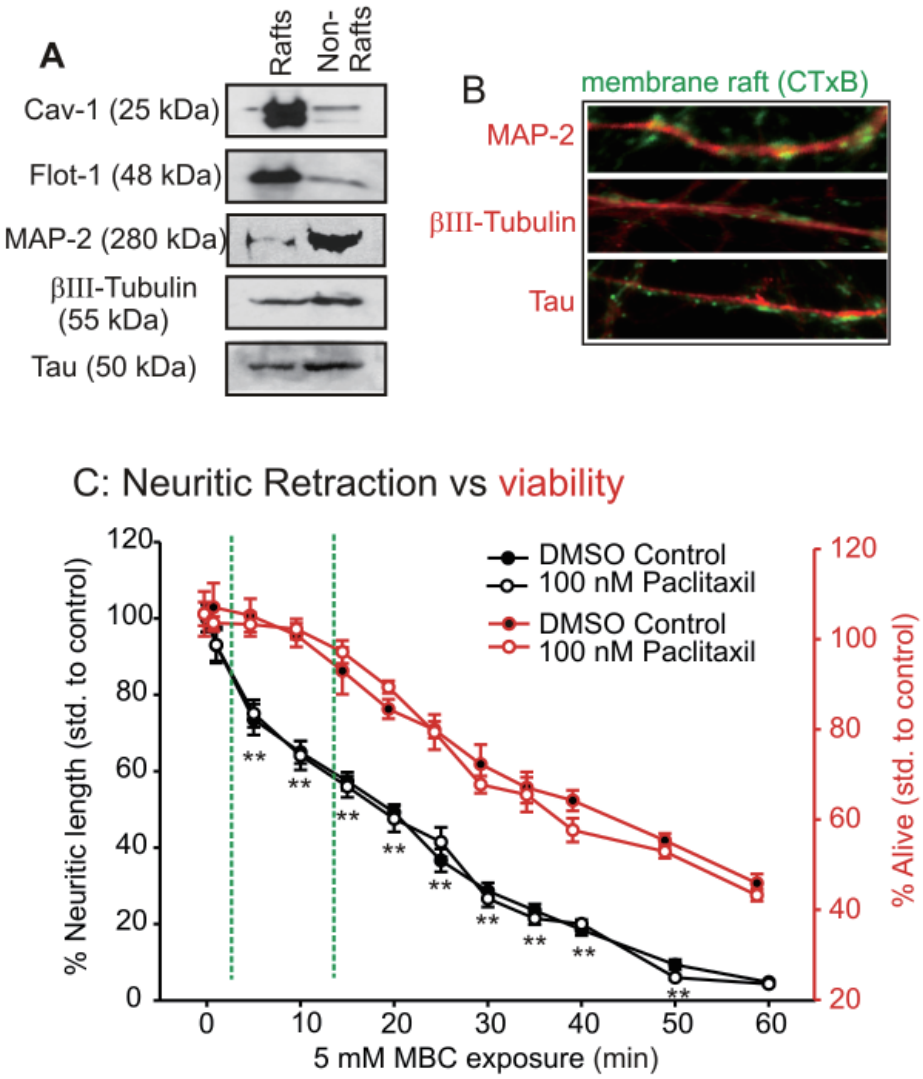

Figure 3. Detection of neuronal microtubule associated proteins within the membrane raft domains of primary cortical neurons. (A) Membrane rafts were isolated (see methods) from (DIV 8) primary cortical neurons. Membrane raft fractions were identified with Caveolin-1 and Flotillin-1 by immunoblotting. Both membrane raft and non-raft fractions were also probed by immunoblotting with the dendritic marker MAP-2, dendritic and axonal marker β-III-tubulin and the axonal marker Tau. All three microtubule associated proteins were present both within the membrane raft and non-raft fractions. The ratio of β-III-tubulin and Tau within the raft fractions compared to the non-raft fractions was higher than MAP-2. **(B)** Primary cortical neurons were also fixed and labelled with CTxB (green color), followed by immunolabelling with antibodies to MAP-2, β-III-tubulin or Tau (red color). **(C)** Effects of MBC on neuritic retraction and viability following treatment with Paclitaxel. Cortical neurons at 8 DIV were pre-incubated with either DMSO or 100 nM Paclitaxel for 2 h. Neurons were then exposed to 5 mM MBC for up to 1 h. Neuritic length was measured at various time points along with corresponding measurements of cell viability assessed using the Alamar Blue. There were no statistical significant differences in neuritic retraction or neuronal viability between neurons pre-incubated with DMSO alone or Paclitaxel (one-way ANOVA with Tukey's *post hoc* test, $n = 10$). Green lines are to highlight the difference between cell death and neurite length with ** indicating statistical significant changes at $p < 0.01$ between neuritic length and percentage of live cells (one-way ANOVA, Tukey's *post hoc* test, $n = 16$).

(*28,34-36*). Together, our data clearly demonstrates that neuritic retraction is mediated by membrane rafts and further suggests that such a mechanism may potentially be common in neuritic response to injury.

Our data clearly established the fact that disruption of membrane rafts results in neuritic retraction prior to neuronal death. Using morphometric analysis and time-lapse imaging, and two membrane raft-disrupting agents, we convincingly showed that neuritic retraction occurred prior to the appearance of PI positivity of the nuclei, confirming neuronal death. Interestingly, some studies have suggested that the inhibition of membrane raft function is neuroprotective (*37,38*). These particular studies suggest that by not allowing clustering of potential harmful receptors such as the N-methyl-D-aspartic acid receptor into rafts, neurons could be protected against excitotoxicity. Our results indicate that MBC caused significant neuritic retraction even at low doses (5 μM). While our results do not refute previous claims that preventing potentially harmful signaling through membrane rafts may provide neuroprotection, they also suggest that a complete disruption of membrane rafts *via*

cholesterol depletion leads to neurodegeneration. This notion that a quantum of membrane rafts are required for neuroprotection following injury is supported by recent studies demonstrating that cytidine 5-diphosphocholine redistributed excitatory amino acid transporters to membrane raft microdomains and improved glutamate uptake in a rat middle cerebral artery occlusion model (*39,40*). More recently, it has been demonstrated that excitatory amino acid transporter 2 localization was significantly reduced within membrane raft domains of Alzheimer's disease patients (*41*). Overall, these studies, together with our results, suggest that membrane rafts are required for neuritic integrity and neuronal viability.

Since MBC exposure resulted in rapid neuritic retraction, examining microtubule associated protein response to MBC was done. Western Blotting results demonstrated that the microtubule proteins, MAP-2, β-III-tubulin and Tau are all present within the membrane raft domains of primary cortical neurons. Using Immunocytochemistry, CTxB-labelled membrane rafts appeared to localize with the dendritic microtubule protein, MAP-2, in roughly equal amounts within the neurites and cell bodies, higher amounts within the neurites with β-III-tubulin, and almost exclusively within the neurites with Tau. The most common preparation for membrane-raft associated protein is the Triton X-100/sucrose density gradient centrifugation method. Cognisant that this technique is not without faults (*42-44*), we were confident that MAP-2, β-III-tubulin and Tau were co-localized within these domains since they were confirmed both using the biochemical Triton X-100/ sucrose density gradient method and by labeling with CTxB.

Disruption of membrane rafts with MBC leads to rapid de-colocalization of membrane rafts, in order of increased rate, with MAP-2, β-III-tubulin and Tau, all of which suggests that axonal microtubules may be more sensitive to membrane raft disruption. The crucial point in this finding lies within the timing. The shift in colocalization between membrane rafts and microtubule associated proteins occurred prior to neuritic retraction and cell death. Our results are consistent with other studies which have demonstrated that cholesterol containing membrane rafts interact with components of the cytoskeleton (*8-10*). To our knowledge, however, this is the first study that has described the presence of both dendritic and axonal microtubule proteins within membrane rafts. Further research needs to be conducted to examine the structural supportive role of membrane rafts in neurites. A clear understanding of the mechanisms involved in this structural support may serve as a novel neuroprotective strategy for neurons exposed to injury.

Acknowledgements

We thank the IBS Animal Facility for the timely supply of experimental animals. This research is supported by the Heart and Stroke Foundation of Ontario grant T5760 and T6706 to S.T.H..

References

1. Pike LJ. Rafts defined: A report on the Keystone Symposium on Lipid Rafts and Cell Function. J Lipid Res. 2006; 47:1597-1598.
2. Pike LJ. The challenge of lipid rafts. J Lipid Res. 2009; 50 (Suppl S):323-328.
3. Hering H, Lin CC, Sheng M. Lipid rafts in the maintenance of synapses, dendritic spines, and surface AMPA receptor stability. J Neurosci. 2003; 23:3262-3271.
4. Guirland C, Suzuki S, Kojima M, Lu B, Zheng JQ. Lipid rafts mediate chemotropic guidance of nerve growth cones. Neuron. 2004; 42:51-62.
5. Simons K, Toomre D. Lipid rafts and signal transduction. Nat Rev Mol Cell Biol. 2000; 1:31-39.
6. Korade Z, Kenworthy AK. Lipid rafts, cholesterol, and the brain. Neuropharmacology. 2008; 55:1265-1273.
7. Simons K, Ikonen E. Functional rafts in cell membranes. Nature. 1997; 387:569-572.
8. Itoh K, Sakakibara M, Yamasaki S, Takeuchi A, Arase H, Miyazaki M, Nakajima N, Okada M, Saito T. Cutting edge: Negative regulation of immune synapse formation by anchoring lipid raft to cytoskeleton through Cbp-EBP50-ERM assembly. J Immunol. 2002; 168:541-544.
9. Foger N, Marhaba R, Zoller M. Involvement of CD44 in cytoskeleton rearrangement and raft reorganization in T cells. J Cell Sci. 2001; 114:1169-1178.
10. Dremina ES, Sharov VS, Schoneich C. Protein tyrosine nitration in rat brain is associated with raft proteins, flotillin-1 and alpha-tubulin: Effect of biological aging. J Neurochem. 2005; 93:1262-1271.
11. Kawabe Ji, Okumura S, Nathanson MA, Hasebe N, Ishikawa Y. Caveolin regulates microtubule polymerization in the vascular smooth muscle cells. Biochemical and Biophysical Research Communications. 2006; 342:164-169.
12. Levitan I, Gooch KJ. Lipid rafts in membrane-cytoskeleton interactions and control of cellular biomechanics: Actions of oxLDL. Antioxid Redox Signal. 2007; 9:1519-1534.
13. Abulrob A, Tauskela JS, Mealing G, Brunette E, Faid K, Stanimirovic D. Protection by cholesterol-extracting cyclodextrins: A role for N-methyl-D-aspartate receptor redistribution. J Neurochem. 2005; 92:1477-1486.
14. Bar-On P, Rockenstein E, Adame A, Ho G, Hashimoto M, Masliah E. Effects of the cholesterol-lowering compound methyl-beta-cyclodextrin in models of alpha-synucleinopathy. J Neurochem. 2006; 98:1032-1045.
15. Huang P, Xu W, Yoon SI, Chen C, Chong PL, Liu-Chen LY. Cholesterol reduction by methyl-beta-cyclodextrin attenuates the delta opioid receptor-mediated signaling in neuronal cells but enhances it in non-neuronal cells. Biochem Pharmacol. 2007; 73:534-549.
16. Gibson NJ, Tolbert LP, Oland LA. Roles of specific membrane lipid domains in EGF receptor activation and cell adhesion molecule stabilization in a developing olfactory system. PLoS One. 2009; 4:e7222.
17. Sjogren B, Csoregh L, Svenningsson P. Cholesterol reduction attenuates 5-HT1A receptor-mediated

signaling in human primary neuronal cultures. Naunyn Schmiedebergs Arch Pharmacol. 2008; 378:441-446.
18. Sillence DJ, Puri V, Marks DL, Butters TD, Dwek RA, Pagano RE, Platt FM. Glucosylceramide modulates membrane traffic along the endocytic pathway. J Lipid Res. 2002; 43:1837-1845.
19. Szoke E, Borzsei R, Toth DM, Lengl O, Helyes Z, Sandor Z, Szolcsanyi J. Effect of lipid raft disruption on TRPV1 receptor activation of trigeminal sensory neurons and transfected cell line. Eur J Pharmacol. 2010; 628:67-74.
20. Sjogren B, Svenningsson P. Depletion of the lipid raft constituents, sphingomyelin and ganglioside, decreases serotonin binding at human 5-HT7(a) receptors in HeLa cells. Acta Physiologica. 2007; 190:47-53.
21. Giovanni A, Keramaris E, Morris EJ, Hou ST, O'Hare M, Dyson N, Robertson GS, Slack RS, Park DS. E2F1 mediates death of B-amyloid-treated cortical neurons in a manner independent of p53 and dependent on Bax and caspase 3. J Biol Chem. 2000; 275:11553-11560.
22. Hou ST, Jiang SX, Desbois A, Huang D, Kelly J, Tessier L, Karchewski L, Kappler J. Calpain-cleaved collapsin response mediator protein-3 induces neuronal death after glutamate toxicity and cerebral ischemia. J Neurosci. 2006; 26:2241-2249.
23. Michaelis ML, Ranciat N, Chen Y, Bechtel M, Ragan R, Hepperle M, Liu Y, Georg G. Protection against beta-amyloid toxicity in primary neurons by paclitaxel (Taxol). J Neurochem. 1998; 70:1623-1627.
24. Fatokun AA, Stone TW, Smith RA. Adenosine receptor ligands protect against a combination of apoptotic and necrotic cell death in cerebellar granule neurons. Exp Brain Res. 2008; 186:151-160.
25. Bruses JL, Chauvet N, Rutishauser U. Membrane lipid rafts are necessary for the maintenance of the (alpha)7 nicotinic acetylcholine receptor in somatic spines of ciliary neurons. J Neurosci. 2001; 21:504-512.
26. Schulz JG, Bosel J, Stoeckel M, Megow D, Dirnagl U, Endres M. HMG-CoA reductase inhibition causes neurite loss by interfering with geranylgeranylpyrophosphate synthesis. J Neurochem. 2004; 89:24-32.
27. Leuba G, Walzer C, Vernay A, Carnal B, Kraftsik R, Piotton F, Marin P, Bouras C, Savioz A. Postsynaptic density protein PSD-95 expression in Alzheimer's disease and okadaic acid induced neuritic retraction. Neurobiol Dis. 2008; 30:408-419.
28. Levin EC, Acharya NK, Sedeyn JC, Venkataraman V, D'Andrea MR, Wang HY, Nagele RG. Neuronal expression of vimentin in the Alzheimer's disease brain may be part of a generalized dendritic damage-response mechanism. Brain Res. 2009; 1298:194-207.
29. Selkoe DJ. Alzheimer's disease is a synaptic failure. Science. 2002; 298:789-791.
30. Plowey ED, Cherra SJ, III, Liu YJ, Chu CT. Role of autophagy in G2019S-LRRK2-associated neurite shortening in differentiated SH-SY5Y cells. J Neurochem. 2008; 105:1048-1056.
31. MacLeod D, Dowman J, Hammond R, Leete T, Inoue K, Abeliovich A. The familial Parkinsonism gene *LRRK2* regulates neurite process morphology. Neuron. 2006; 52:587-593.
32. Farrer MJ. Genetics of Parkinson disease: Paradigm shifts and future prospects. Nat Rev Genet. 2006; 7:306-318.
33. Hou ST, Keklikian A, Slinn J, O'Hare M, Jiang SX, Aylsworth A. Sustained up-regulation of semaphorin 3A, Neuropilin1, and doublecortin expression in ischemic mouse brain during long-term recovery. Biochem Biophys Res Commun. 2008; 367:109-115.
34. Flood DG, Coleman PD. Dendritic regression dissociated from neuronal death but associated with partial deafferentation in aging rat supraoptic nucleus. Neurobiol Aging. 1993; 14:575-587.
35. Terry RD, Katzman R. Life span and synapses: Will there be a primary senile dementia? Neurobiol Aging. 2001; 22:347-348.
36. Terry RD, Masliah E, Salmon DP, Butters N, DeTeresa R, Hill R, Hansen LA, Katzman R. Physical basis of cognitive alterations in Alzheimer's disease: Synapse loss is the major correlate of cognitive impairment. Ann Neurol. 1991; 30:572-580.
37. van der Most PJ, Dolga AM, Nijholt IM, Luiten PG, Eisel UL. Statins: Mechanisms of neuroprotection. Prog Neurobiol. 2009; 88:64-75.
38. Ponce J, de la Ossa NP, Hurtado O, Millan M, Arenillas JF, Davalos A, Gasull T. Simvastatin reduces the association of NMDA receptors to lipid rafts: A cholesterol-mediated effect in neuroprotection. Stroke. 2008; 39:1269-1275.
39. Hurtado O, Moro MA, Cardenas A, Sanchez V, Fernandez-Tome P, Leza JC, Lorenzo P, Secades JJ, Lozano R, Davalos A, Castillo J, Lizasoain I. Neuroprotection afforded by prior citicoline administration in experimental brain ischemia: Effects on glutamate transport. Neurobiol Dis. 2005; 18:336-345.
40. Hurtado O, Pradillo JM, Fernandez-Lopez D, Morales JR, Sobrino T, Castillo J, Alborch E, Moro MA, Lizasoain I. Delayed post-ischemic administration of CDP-choline increases EAAT2 association to lipid rafts and affords neuroprotection in experimental stroke. Neurobiol Dis. 2008; 29:123-131.
41. Tian G, Kong Q, Lai L, Ray-Chaudhury A, Liang Glenn LC. Increased expression of cholesterol 24S-hydroxylase results in disruption of glial glutamate transporter EAAT2 association with lipid rafts: A potential role in Alzheimer's disease. J Neurochem. 2010; 113:978-989.
42. Munro S. Lipid rafts: Elusive or illusive? Cell. 2003; 115:377-388.
43. Hancock JF. Lipid rafts: Contentious only from simplistic standpoints. Nat Rev Mol Cell Biol. 2006; 7:456-462.
44. Babiychuk EB, Draeger A. Biochemical characterization of detergent-resistant membranes: A systematic approach. Biochem J. 2006; 397:407-416.

(*Received July 11, 2012; Revised August 15, 2012; Accepted August 16, 2012*)

Legend for Supplementary Movie 1

Neuritic retraction and neuronal death in response to MBC by time lapse imaging. Primary cortical neurons were acclimated for 30 minutes to the time lapse chamber and were maintained at 37°C with 5 % CO_2. Cells were then incubated with 30 μg/mL propidium iodide (PI) for 30 min. Following acclimation and incubation with PI, cortical neurons were exposed to 5 mM MBC. Cultures were imaged using time lapse microscopy every 20 seconds following MBC exposure for up to 1 h. During each time interval both phase and Cy-3 images were obtained. The appearance of the red color indicates PI positivity and cell death.

Original Article

DOI: 10.5582/bst.2012.v6.4.192

Identification of novel small-molecule inhibitors of glioblastoma cell growth and invasion by high-throughput screening

Lulu Wang[1,2], Hong Zhao[2], Kemi Cui[2,*], Linli Yao[1], Min Ren[3], Aijun Hao[1], Patrick Smollen[2], Fang Nie[2], Guangxu Jin[2], Qian Liu[1,*], Stephen TC Wong[2]

[1] *Key Laboratory of the Ministry of Education for Experimental Teratology, Department of Histology and Embryology, School of Medicine, Shandong University, Ji'nan, Shandong, China;*
[2] *Department of Systems Medicine and Bioengineering, The Methodist Hospital Research Institute, Weill Cornell Medical College, Houston, TX, USA;*
[3] *Department of Traditional Chinese Medicine, Qilu hospital, Shandong University, Ji'nan, Shandong, China.*

Summary **Glioblastoma multiforme (GBM) is the most common and lethal type of primary brain tumor with a very poor prognosis. Current therapies for GBM remain palliative and advances made in decades have resulted in only a slight improvement in treatment outcome. Exploring new therapeutic agents for GBM treatment, therefore, is of prime importance. In the present study, we performed a high-throughput screening for GBM cell growth and invasion, with an attempt to identify novel potential anti-GBM agents. An annotated compound library (LOPAC1280) of 1,280 pharmacologically active compounds was screened and ten compounds were validated and identified as inhibitors of GBM cell growth and invasion. Four of them, *i.e.*, 6-nitroso-1,2-benzopyrone, *S*-(*p*-azidophenacyl) glutathione, phenoxybenzamine hydrochloride, and SCH-28080 have not been implicated in GBM cell growth and invasion previously, suggesting that they may serve as novel potential therapeutic agents for GBM treatment. In conclusion, novel inhibitors of GBM cell growth and invasion were identified in the present study, which provides a basis for the development of therapies for GBM, and may shed light on the molecular mechanisms underlying GBM cell behavior.**

Keywords: Glioblastoma, screening, annotated compound library, cell growth, cell invasion

1. Introduction

Glioblastoma multiforme (GBM) is the most common and most aggressive malignant brain tumor. Current therapeutic approaches for GBM are predominantly palliative, including maximal surgical resection, radiotherapy, and chemotherapy (*1*). However, one of the most important barriers to successful therapy is the diffuse invasion of GBM cells, making them elusive targets for effective surgical management and giving rise to tumor recurrence. Besides, lack of a significant antitumor effect from traditional therapies is frequently observed (*2*), resulting in quite low relative survival (five-year survival rates are less than 5%) (The Central Brain Tumor Registry of the United States, 2012). Therefore, identifying novel effective therapeutic agents for treating GBM is urgently needed.

Etiology and pathophysiology of GBM are complex and currently unclear. Potential molecular targets for GBM therapies are being explored while effective ones are still largely unknown. As GBM is characterized by high proliferation rate and diffuse invasion, regulators targeting these cell behaviors may lead to immediate clinical improvement. The development of experimental technologies to measure cell growth or invasion has made it possible to acquire potential anticancer compounds, while a major obstacle

*Address correspondence to:
Dr. Kemi Cui, The Methodist Hospital Research Institute, Weill Cornell Medical College, 6670 Bertner Avenue, R6-211, Houston, TX 77030, USA.
E-mail: kcui@tmhs.org
Dr. Qian Liu, Key Laboratory of the Ministry of Education for Experimental Teratology,School of Medicine, Shandong University, Ji'nan, 44 Wenhua Xi Road, Ji'nan, Shandong 250012, China.
E-mail: neuroscience.department@gmail.com

is that the current cell invasion assays are difficult to perform in parallel at the scale required to screen large libraries (*3*). High-throughput approaches, which allow simultaneous screening of hundreds to thousands of compounds, are therefore of interest to basic scientists and those in search of therapeutics (*4*). Bioluminescent assays, which are based on the detection of ATP by the luciferin-luciferase reaction, are being studied for high-throughput screening due to their sensitivity, broad linearity, and robustness to library compounds and complex biological samples (*5*). A bioluminescent-based assay for GBM cell growth and invasion was developed in our laboratory previously (*6*), and it was adapted here to allow the possibility of screening regulators of GBM cell behavior in a high-throughput manner.

In the present study, using a high-throughput screening approach, we screened an annotated compound library (LOPAC1280) of 1,280 pharmacologically active compounds that influence most cellular processes and cover all major drug target classes, to identify novel potential therapeutic agents against GBM. LOPAC1280 represents a collection of compounds from 56 pharmacological classes with well-characterized activities and experimentally validated biological mechanisms, and thus, this screening may also provide new insights into the molecular basis of GBM.

2. Materials and Methods

2.1. *Cells, cell cultures and compounds*

Human glioblastoma cell lines U87MG and U251MG were obtained from American Type Culture Collection (Manassas, VA, USA) and maintained in DMEM supplemented with 10% fetal bovine serum (FBS). U87-luc (U87MG glioblastoma cells genetically engineered to express firefly luciferase reporter gene) was kindly provided by Santosh Kesari (Dana-Farber Cancer Institute, Harvard Medical University) and cultured in DMEM containing 10% FBS, 1% penicillin/streptomycin, 1% L-glutamine, and 0.5 mg/mL G418 (Sigma-Aldrich, St. Louis, MO, USA). Cells were maintained in a humidified tissue culture incubator at 37°C with a 5% CO_2 atmosphere.

Compounds from LOPAC1280 (Sigma-Aldrich, St. Louis, MO, USA) were received as 10 mM DMSO stock solutions and stored at –20°C until further use. For validation experiments, active compounds (*i.e.*, "hits") from the primary high-throughput screening were prepared at a concentration ranging between 0.01 and 100 μM.

2.2. *High-throughput screening of LOPAC1280*

For primary screening, a high-throughput screening assay for cell growth and invasion was performed and a library of 1,280 compounds was screened. Briefly, the luciferin-immobilized 96-well black-wall clear-bottom plates (Becton Dickinson, Franklin Lakes, NJ, USA) were prepared following the procedure described in our previous paper (*6*) (Figure 1A). For each plate, the top half (rows A-D) was not coated with luciferin, with the aim of evaluating cell proliferation. Wells in rows E-H were coated with luciferin on the bottom to evaluate cell invasion. Each compound of the LOPAC1280 library was mixed with U87-Luc cell conditioned media and Matrigel Basement Membrane Matrix (BD Biosciences, Bedford, MA, USA), which had been widely used in tumor cell invasion assays or functioned as 3D cell culture platforms (*7,8*), to a final concentration of 10 μM (the DMSO concentration was 0.1% for all samples and controls). Then the mixture was added onto the 96-well plates in triplicate in a cold room at 4°C. Each 96-well plate was placed in an incubator at 37°C for 2 h. Next, luciferin (1 μL) was placed in each of the wells in rows A-D. About 5,000 U87-Luc cells in 5 μL media were loaded onto the Matrigel (0 h) in all wells followed by incubation in a humidified incubator at 37°C in a 5% CO_2 atmosphere for 24 h. The bioluminescent signals were detected at 0 h and 24 h using the IVIS 100 system (Xenogen Co., Alameda, CA, USA). Signal intensity was quantified using Living Image software (version 2.50.1, Xenogen Co., Alameda, CA, USA) (in terms of photon counts).

A good linear correlation between the U87-Luc cell number in Matrigel and bioluminescent signal had been obtained in our previous study (*6*). The photon counts of wells in rows A-D (no luciferin coating) reflected the total number of cells and those in rows E-H (luciferin coated) reflect the cells that moved through the Matrigel. Accordingly, cell growth and invasion were measured. For each 96-well plate, 15 compounds were evaluated. Z' factor was used for quality control of the screening plates, which was defined as described in the following equation: $1 - (3\sigma s + 3\sigma b)/|\mu s - \mu b|$, where σ represents the S.D. of signal (σs) or background (σb) and l is the mean and μ represents the mean (*9*).

2.3. *Cell growth assay*

Cell growth was assessed by CellTiter 96® AQueous cell proliferation assay (MTS) (Promega, Madison, WI, USA) according to the manufacturer's instructions. Briefly, 10,000 U87MG or U251MG cells in 100 μL medium were seeded in triplicate in each well of the 96-well white-wall clear-bottom plates and incubated overnight, followed by 24 h treatment with active compounds at different concentrations (0.01 μM to 100 μM). Cells were then washed and fresh medium was added followed by Cell Titer 96® AQueous One solution (20 μL/well). After 3 h incubation, absorbance at 490 nm was measured using the FLUOstar Omega Microplate Reader (BMG LABTECH, Cary, NC,

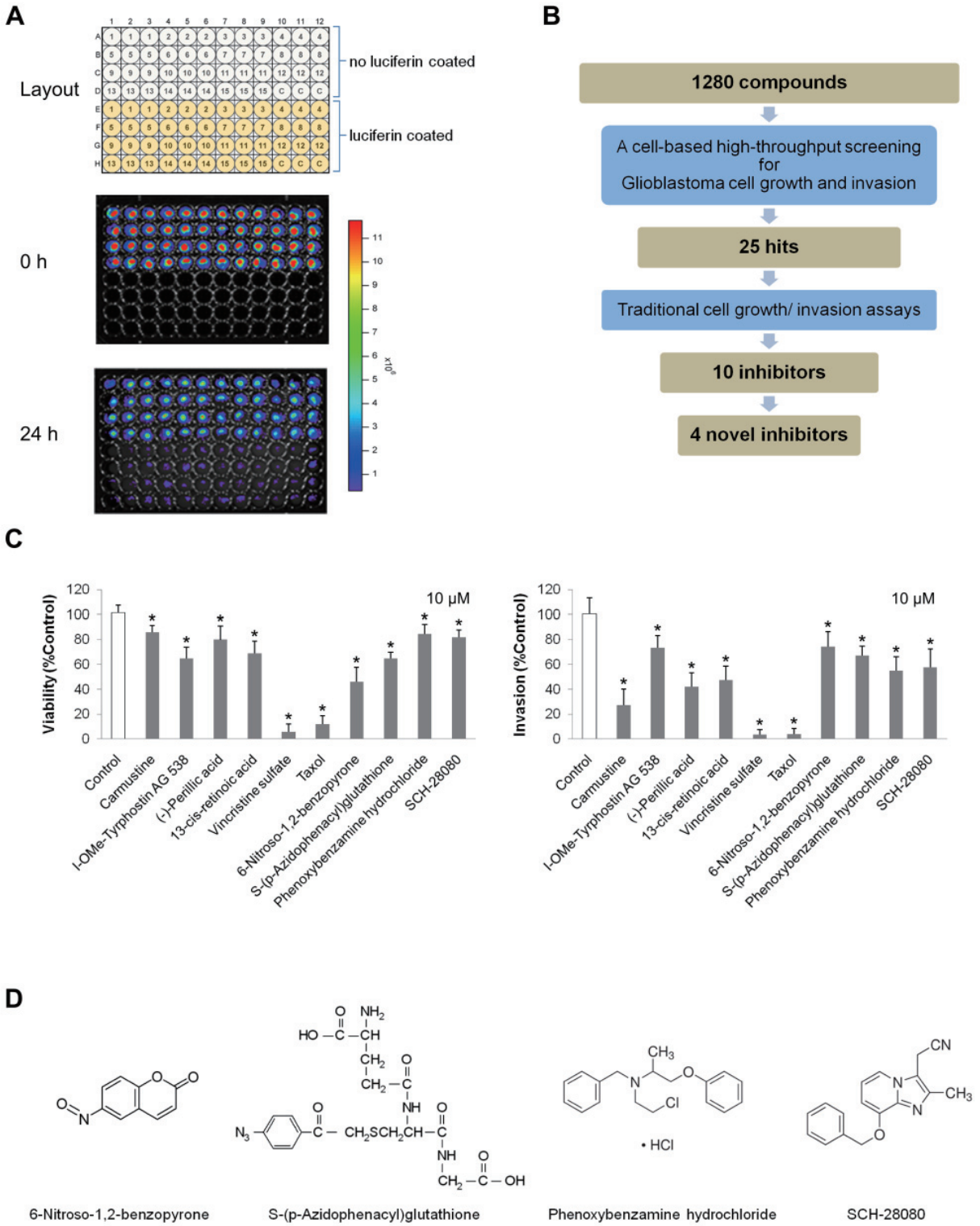

Figure 1. Results of LOPAC1280 high-throughput screening for anti-GBM compounds and chemical structures of the validated novel hits. (A) Layout of the 96-well plate for LOPAC1280 high-throughput screening. Wells in rows A-D have no luciferin coating. U87-Luc cells and luciferin were added simultaneously and cell growth was monitored. Bottom of wells in rows E-H were coated with luciferin. U87-Luc cells alone were added and the bioluminescent signals could be detected only if the cells invade the Matrigel and reached the bottom of wells. Columns 10-12, rows D and H, control cells treated with 0.1% DMSO; Other wells, cells treated with LOPAC1280 compounds (10 μM). Relative luciferase activity of the control was defined as 100% and measurements from other wells were calculated accordingly. For each 96-well plate, 15 compounds were evaluated for their activity in GBM cell growth and invasion. **(B)** Results: 1,280 compounds were screened in triplicate, leading to an initial list of 25 active compounds, of which ten were subsequently validated in traditional assays. The ten validated compounds and their effects on U87-Luc cell growth and invasion as evaluated by the high-throughput screening are shown in **(C)**. Values in bar graphs represent mean ± S.D. of three independent experiments. * $p < 0.05$ *vs.* control. Four (*i.e.*, 6-nitroso-1,2-benzopyrone, *S*-(*p*-azidophenacyl) glutathione, phenoxybenzamine hydrochloride, and SCH-28080) of the ten validated compounds were identified as novel inhibitors of GBM cell growth and invasion. Their chemical structures are shown in **(D)**.

USA).

2.4. *Cell invasion assay*

Cell invasive capacity was evaluated by 24-well Matrigel™ Invasion Chamber according to the manufacturer's instructions (BD Biosciences). Briefly, 25,000 U87MG or U251MG cells in 500 μL medium containing active compounds at different concentrations were added in triplicate to the inserts and incubated for 24 h. After the removal of non-invading cells with a cotton swab, cells on the lower surface of the membrane were stained with a Diff-Quik stain kit (Dade-Behring, Newark, DE, USA). Cells were counted in five chosen microscope fields in each well and the results were numerically averaged. Cell invasion was calculated according to the manufacturer's manual.

2.5. *Cell migration assay*

Cell migration was examined by wound-healing assay as described previously (*10*). Relative migration distance was quantified by measuring the advance of the two opposing wound edges at 0 h and 12 h using Slidebook software (Intelligent Imaging Innovations, Inc., Denver, CO, USA).

2.6. *Statistical analysis*

Data are presented as the mean ± S.D. Statistical significance was determined by one-way ANOVA, followed by Dunnett's *post-hoc* test. All tests were 2-sided and a value of $p < 0.05$ was considered significant. Statistical analyses were performed using GraphPad Prism for Windows (Graphpad Software, San Diego, CA, USA).

3. Results

3.1. *High-throughput screening for novel inhibitors of GBM cell growth and invasion of LOPAC1280*

As an initial step to discover novel potential compounds against GBM, 1,280 pharmacologically active compounds from 56 pharmacological classes were quantitatively assessed for their effects on GBM cell growth and invasion at a concentration of 10 μM (Figure 1A). Assay quality was evaluated using Z′-factors (see Materials and Methods). A Z′-factor of 1 is considered ideal; a Z′-factor between 0.5 and 1.0 represented excellent assays (*9*). For the screen plates, an average Z′ factor of 0.513 was obtained, indicating that the assay was acceptable for cell-based screening (*11*). Outlier wells caused by plate preparation misdispensing were not included in the analysis.

The high-throughput screening of LOPAC1280 resulted in an initial identification of 25 inhibitors (Figure 1B). As will be shown below, ten of them were validated in traditional cell growth, invasion and migration assays. They belong to several pharmacological classes, suggesting that these classes should be paid more attention to in the development of therapies for GBM. It is gratifying that carmustine, I-OMe-Tyrphostin AG 538, (–)-perillic acid, 13-*cis*-retinoic acid, vincristine sulfate, and Taxol, which had been studied in preclinical experiments, evaluated in clinical trials, or used in clinical as chemotherapeutic agents for tumors including GBM (see Discussion for details), were identified in our screening (Table 1). The other four, *i.e.*, 6-nitroso-1,2-benzopyrone, *S*-(*p*-azidophenacyl) glutathione, phenoxybenzamine hydrochloride and SCH-28080, had not been implicated in GBM cell behaviors and were therefore identified as novel potential anti-GBM agents (Table 1, Figure 1D).

Table 1. Potential hit compounds from LOPAC1280 high-throughput screening

LOPAC Cat. #	Name of compound	Pharmacological class	Activity
C 0400	Carmustine	DNA	DNA alkylating agent; causes interstrand crosslinks
T 7697	I-OMe-Tyrphostin AG 538	Phosphorylation	Insulin growth factor 1 (IGF-1) receptor protein tyrosine kinase inhibitor
P 7083	(–)-Perillic acid	G protein	Interferes with activity of p21 ras and other small G proteins by inhibiting post-translational cysteine isoprenylation
R 3255	13-*cis*-Retinoic acid	Transcription	Anti-inflammatory and antitumor actions mediated through RAR-beta and RAR-alpha receptors
V 8879	Vincristine sulfate	Cytoskeleton and ECM	Inhibitor of microtubule assembly
T 7402	Taxol	Cytoskeleton and ECM	Antitumor agent; promotes assembly of microtubules and inhibits tubulin disassembly process
N 8403	6-Nitroso-1,2-benzopyrone	Transcription	Poly (ADP-ribose) polymerase (PARP) ligand which preferentially destabilizes one of the two zinc-fingers, inactivating the enzyme
A 1782	*S*-(*p*-Azidophenacyl) glutathione	Multi-drug resistance	Glyoxalase and glutathione S-transferase inhibitor
B-019	Phenoxybenzamine hydrochloride	Adrenoceptor	Selective alpha adrenoceptor blocking agent; calmodulin antagonist
S 4443	SCH-28080	Ion channels	Potent inhibitor of gastric H^+ and K^+-ATPase.

3.2. *Effects of the active compounds on GBM cell growth*

A traditional cell viability assay (MTS assay) was performed to achieve a dose-response evaluation of the active compounds in two GBM cell lines, U87MG and U251MG. The concentration used in the primary screening was 10 μM (see Materials and Methods). In this part, a concentration ranging between 0.01 and 100 μM was applied (Figure 2). All the four compounds caused a dose-dependent inhibition of GBM cell growth, although the degree of inhibition varied.

3.3. *Effects of the active compounds on GBM cell invasion*

The invasive potential of GBM cells was tested using a Matrigel cell invasion assay and effects of the four novel inhibitors are shown (Figure 3). Compared to the control, 1 μM 6-nitroso-1,2-benzopyrone, 1 μM *S*-(*p*-azidophenacyl) glutathione, 10 μM phenoxybenzamine hydrochloride and 10 μM SCH-28080 significantly reduced the invasion of U87MG cells to 79.8%, 65.2%, 48.6%, and 52.9%, respectively. A similar result was obtained in U251MG cells.

3.4. *Effects of the active compounds on GBM cell migration*

Additionally, we examined whether the reduced invasiveness of GBM cells caused by the hit compounds was accompanied by reduced cell motility. A cell migration assay (wound healing assay) was employed (Figure 4). As shown, compared to the control, 1 μM 6-nitroso-1,2-benzopyrone and 1 μM *S*-(*p*-azidophenacyl) glutathione significantly reduced U87MG cell migration to 86% and 80%, respectively. When treated with 10 μM phenoxybenzamine hydrochloride or 10 μM SCH-28080, U87MG cell migration was reduced to 72% or 82%, respectively. The decreases in U251MG cell migration were also

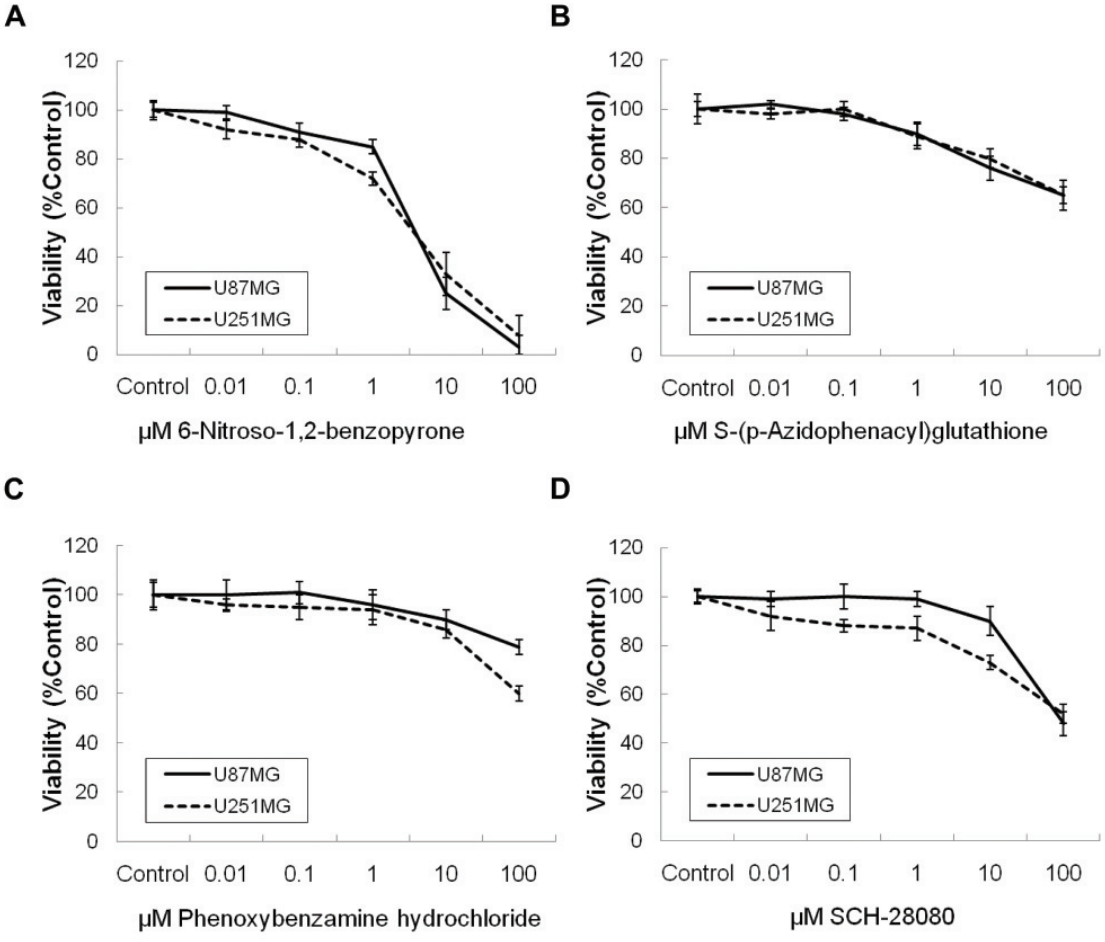

Figure 2. Dose-response curves displaying the activity of the four active compounds in GBM cells. Two GBM cell lines (U87MG and U251MG) were treated with various concentrations of 6-nitroso-1,2-benzopyrone **(A)** *S*-(*p*-azidophenacyl) glutathione **(B)** phenoxybenzamine hydrochloride **(C)** and SCH-28080 **(D)** for 24 h. Cell growth was measured by MTS cell viability assay. Cell viability was calculated as the ratio of the corrected absorbance value of the treated cells to that of untreated control cells. The results are presented as mean ± S.D. of three independent experiments.

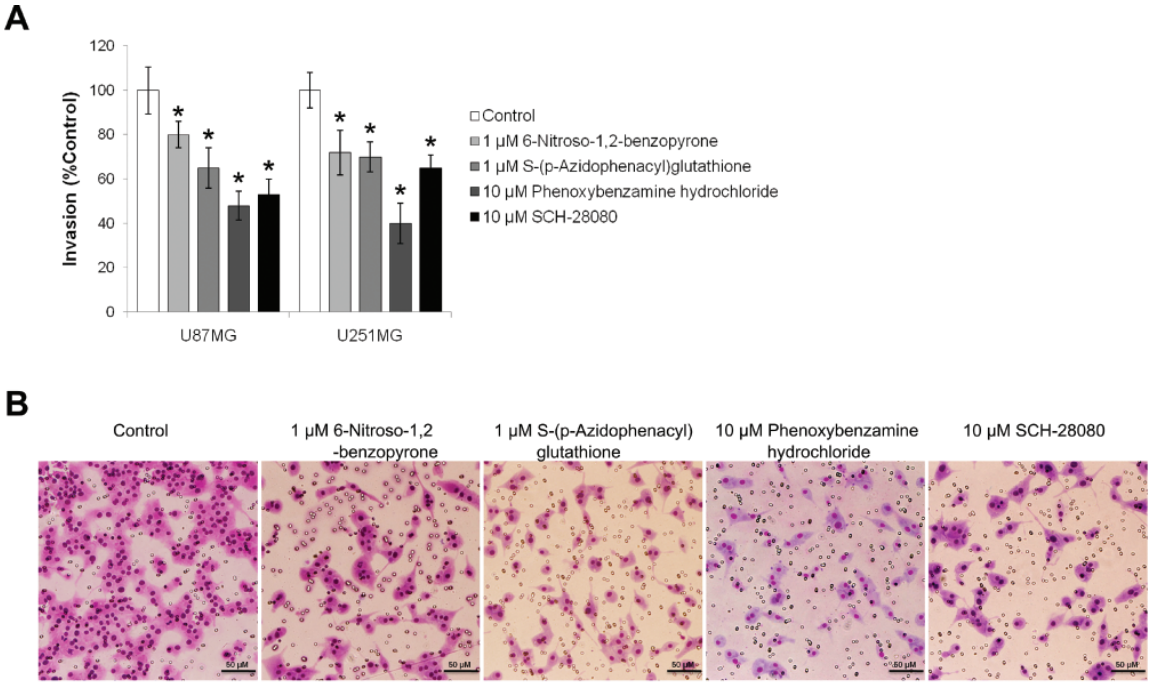

Figure 3. Effects of the four active compounds on GBM cell invasion. (A) U87MG and U251MG cells were treated with the active compounds from the primary high-throughput screening for 24 h. Cell invasion was evaluated by Matrigel cell invasion assay. The invaded cells that adhered to the lower surface of the membrane were counted. The invasive potential of the treated cells is presented as a percentage invasion of control. Data represent mean ± S.D. of three independent experiments. * $p < 0.05$ *vs.* control. **(B)** The representative images of U87MG cells are shown. Scale bar, 50 μm.

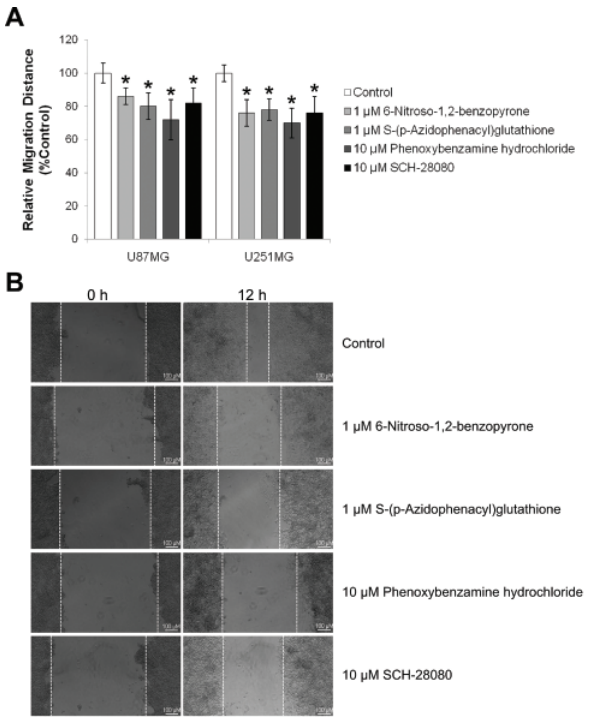

Figure 4. Effects of the four active compounds on GBM cell migration. (A) U87MG and U251MG cells were treated with the active compounds from the primary high-throughput screening for 12 h, and cell migration was measured by wound-healing assay. Cell migration is presented as percentage of relative migration distance divided by that of the control. Each value represents the mean ± S.D. of three independent experiments. * $p < 0.05$ *vs.* control. **(B)** The representative images of U87MG cells are shown. Scale bar, 100 μm.

significant. In other words, as expected, all four compounds caused a statistically significant reduction in the cell migration.

Parallel experiments for evaluating effects of different concentrations of DMSO (used in this study) on GBM cell proliferation, invasion, and migration were performed to rule out the possibility that DMSO might have subtle effects on GBM cell behaviors. No significant difference was observed after DMSO treatment in each experiment (data not shown).

4. Discussion

Mechanisms underlying GBM cell proliferation, invasion, and migration are very complicated. Regulators of these biological behaviors, which hold the promise of effective therapeutic approaches for treating GBM, still have not been well defined. In this study, all compounds of the LOPAC1280, which is a versatile library including the latest drug-like molecules in the fields of cell signaling and neuroscience, and reflects the most commonly screened targets in the drug discovery community, were evaluated in the primary screening assay. The four newly identified potential anti-GBM compounds come from distinct pharmacological classes, some of which have never been implicated in tumor cell behaviors suggesting that these classes may be involved in diverse biological processes of GBM. Other unrevealed compounds from

these classes may also be worth noting in terms of their anticancer effects.

In this study, ten validated active compounds were obtained, of which six have been previously reported to be implicated in GBM cell behaviors (Table 1). Carmustine is a DNA alkylating agent and causes interstrand crosslinks, and it has long been used as a treatment for GBM (*12*). I-OMe-Tyrphostin AG 538 is an insulin growth factor 1 (IGF-1) receptor (IGF-1R) protein tyrosine kinase inhibitor. IGF-1 has been well discussed in GBM (*13*), and targeting IGF-1R has been studied as a treatment option for GBM (*14*). (–)-Perillic acid is a metabolite of perillyl alcohol (POH), which has shown a therapeutic anticancer effect and is currently under phase I and II clinical trials for human cancers including GBM (*15,16*). 13-*cis*-Retinoic acid (cRA) has antitumor actions mediated through RAR-beta and RAR-alpha receptors, which has long been evaluated and has shown therapeutic effectiveness in clinical trials in treatment of brain tumors (*17*). Vincristine sulfate and Taxol, both from the class of cytoskeleton and ECM, are being clinically evaluated alone or combined for use against gliomas (*18,19*). The identification of these compounds is gratifying and may help validate this screen as an effective means to identify compounds that regulate GBM cell behavior. Moreover, the therapeutic effects of these compounds in clinical studies suggest that the four newly identified compounds in our study (*i.e.* 6-nitroso-1,2-benzopyrone, *S*-(*p*-azidophenacyl) glutathione, phenoxybenzamine hydrochloride, and SCH-28080), might benefit patients with GBM and are therefore worth further study (Table 1).

6-Nitroso-1,2-benzopyrone is a poly(ADP-ribose) polymerase (PARP) ligand that has been reported to suppress proliferation of leukemic and other malignant human cells (*20*), while few studies have focused on its effect on GBM cell behavior.

S-(*p*-Azidophenacyl) glutathione is a glyoxalase and glutathione S-transferase (GST) inhibitor. It has been reported that blockage of glyoxalase resulted in an inhibition of proliferation of human leukemia cells (*21*). GSTs have been implicated in the development of drug resistance (*22*), and may be responsible for poor response to alkylating agents in GBM treatment (*23*). In this study, the effects of *S*-(*p*-azidophenacyl) glutathione on GBM cell behavior were examined for the first time.

Phenoxybenzamine hydrochloride is a selective alpha adrenoceptor blocking agent as well as a calmodulin antagonist. The alpha adrenoceptor antagonist has been extensively studied in human prostate cancer and shown to be involved in cell cycle arrest and apoptosis (*24*), whereas it has rarely been studied in GBM cells. Based on the distribution of alpha-adrenoceptors in the human central nervous system, our findings are of concern (*25*). Besides, phenoxybenzamine hydrochloride also reacts irreversibly with calmodulin (*26*), which has been shown to play roles in astrocytoma cell growth (*27*). In this connection, our finding of the effects of phenoxybenzamine hydrochloride in GBM cell behavior is attractive.

SCH-28080 is a potent inhibitor of gastric H^+- and K^+-ATPase, which was considered to exert its antisecretory effect by a competitive interaction with the high affinity K^+-site of the gastric ATPase (*28*). It has been shown to inhibit basal and stimulated aminopyrine accumulation in isolated gastric glands, and to cause relaxation of human airway smooth muscle (*29,30*). Here SCH-28080 exhibited antitumor activity against GBM *in vitro*, whereas the underlying molecular mechanisms still need to be elucidated.

The four active compounds, which have not been previously implicated in GBM cell behavior, are all shown in our study to exert inhibitory effects on GBM cell growth and invasion. This favorable result allows them to be further studied as novel potential therapeutic agents against GBM.

It should be mentioned that although these compounds showed favorable effects on GBM cells *in vitro*, there is still a long way to go before they benefit patients. Their pharmacokinetic and pharmacodynamic activities need to be addressed, and their effectiveness crossing the blood-brain barrier and delivery to a brain tumor area are of vital concern (*31*). Good news is that scientists have never stopped devising innovative approaches to circumvent these obstacles, and strategies for increasing drug delivery are being discovered (*32*). These agents also need further investigation for their cancer-specific action because the toxicity of anticancer agents against normal cells is still one of the major challenges in cancer treatment (*33*). While these uncertainties could not stop this study from providing starting points for anti-GBM drug discovery and design.

In summary, *via* a high-throughput screening, from an annotated compound library, we identified four novel small-molecule inhibitors of GBM cell growth and invasion, with an attempt to provide useful therapeutic leads for GBM treatment. Currently, these four active compounds are being investigated in our laboratory to explore the underlying mechanisms, and their anti-tumor effects are also being evaluated in an intracranial GBM xenograft model. The results will be reported in detail elsewhere.

Acknowledgements

The work was supported by NIH/NCI, U54 CA149196 and Bioinformatics and Bioengineering Program at The Methodist Hospital Research Institute (TMHRI, SWONG) of US. Natural Science Foundation of Shandong University (No. 2012JC006).

References

1. Azizi SA, Miyamoto C. Principles of treatment of malignant gliomas in adults: An overview. J Neurovirol. 1998; 4:204-216.
2. Mariani L, Beaudry C, McDonough WS, Hoelzinger DB, Demuth T, Ross KR, Berens T, Coons SW, Watts G, Trent JM, Wei JS, Giese A, Berens ME. Glioma cell motility is associated with reduced transcription of proapoptotic and proliferation genes: A cDNA microarray analysis. J Neurooncol. 2001; 53:161-176.
3. Decaestecker C, Debeir O, Van Ham P, Kiss R. Can anti-migratory drugs be screened *in vitro*? A review of 2D and 3D assays for the quantitative analysis of cell migration. Med Res Rev. 2007; 27:149-176.
4. Henry S, Bigler S, Wang J. High throughput analysis of neural progenitor cell proliferation in adult rodent hippocampus. Biosci Trends. 2009; 3:233-238.
5. Fan F, Wood KV. Bioluminescent assays for high-throughput screening. Assay Drug Dev. Technol. 2007; 5:127-136.
6. Zhao H, Tang C, Cui K, Ang BT, Wong ST. A screening platform for glioma growth and invasion using bioluminescence imaging. Laboratory investigation. J Neurosurg. 2009; 111:238-246.
7. Justice BA, Badr NA, Felder RA. 3D cell culture opens new dimensions in cell-based assays. Drug Discov Today. 2009; 14:102-107.
8. Terranova VP, Hujanen ES, Loeb DM, Martin GR, Thornburg L, Glushko V. Use of a reconstituted basement membrane to measure cell invasiveness and select for highly invasive tumor cells. Proc Natl Acad Sci U S A. 1986; 83:465-469.
9. Zhang JH, Chung TD, Oldenburg KR. A Simple statistical parameter for use in evaluation and validation of high throughput screening assays. J Biomol Screen. 1999; 4:67-73.
10. Rajasekaran SA, Palmer LG, Quan K, Harper JF, Ball WJ Jr, Bander NH, Peralta Soler A, Rajasekaran AK. Na,K-ATPase beta-subunit is required for epithelial polarization, suppression of invasion, and cell motility. Mol Biol Cell. 2001; 12:279-295.
11. Quintavalle M, Elia L, Price JH, Heynen-Genel S, Courtneidge SA. A cell-based high-content screening assay reveals activators and inhibitors of cancer cell invasion. Sci Signal. 2011; 4:49.
12. Brandes AA, Tosoni A, Basso U, Reni M, Valduga F, Monfardini S, Amistà P, Nicolardi L, Sotti G, Ermani M. Second-line chemotherapy with irinotecan plus carmustine in glioblastoma recurrent or progressive after first-line temozolomide chemotherapy: A phase II study of the Gruppo Italiano Cooperativo di Neuro-Oncologia (GICNO). J Clin Oncol. 2004; 22:4779-4786.
13. Schlenska-Lange A, Knüpfer H, Lange TJ, Kiess W, Knüpfer M. Cell proliferation and migration in glioblastoma multiforme cell lines are influenced by insulin-like growth factor 1 *in vitro*. Anticancer Res. 2008; 28:1055-1060.
14. Yin S, Girnita A, Stromberg T, Khan Z, Andersson S, Zheng H, Ericsson C, Axelson M, Nistér M, Larsson O, Ekström TJ, Girnita L. Targeting the insulin-like growth factor-1 receptor by picropodophyllin as a treatment option for glioblastoma. Neuro oncol. 2010; 12:19-27.
15. Azzoli CG, Miller VA, Ng KK, Krug LM, Spriggs DR, Tong WP, Riedel ER, Kris MG. A phase I trial of perillyl alcohol in patients with advanced solid tumors. Cancer Chemother Pharmacol. 2003; 51:493-498.
16. Liu G, Oettel K, Bailey H, Ummersen LV, Tutsch K, Staab MJ, Horvath D, Alberti D, Arzoomanian R, Rezazadeh H, McGovern J, Robinson E, DeMets D, Wilding G. Phase II trial of perillyl alcohol (NSC 641066) administered daily in patients with metastatic androgen independent prostate cancer. Invest New Drugs. 2003; 21:367-372.
17. Jaeckle KA, Hess KR, Yung WK, Greenberg H, Fine H, Schiff D, Pollack IF, Kuhn J, Fink K, Mehta M, Cloughesy T, Nicholas MK, Chang S, Prados M; North American Brain Tumor Consortium. Phase II evaluation of temozolomide and 13-*cis*-retinoic acid for the treatment of recurrent and progressive malignant glioma: A North American Brain Tumor Consortium study. J Clin Oncol. 2003; 21:2305-2311.
18. Levin VA, Uhm JH, Jaeckle KA, Choucair A, Flynn PJ, Yung WKA, Prados MD, Bruner JM, Chang SM, Kyritsis AP, Gleason MJ, Hess KR. Phase III randomized study of postradiotherapy chemotherapy with alpha-difluoromethylornithine-procarbazine, *N*-(2-chloroethyl)-*N′*-cyclohexyl-*N*-nitrosurea, vincristine (DFMO-PCV) versus PCV for glioblastoma multiforme. Clin Cancer Res. 2000; 6:3878-3884.
19. Terzis AJ, Thorsen F, Heese O, Visted T, Bjerkvig R, Dahl O, Arnold H, Gundersen G. Proliferation, migration and invasion of human glioma cells exposed to paclitaxel (Taxol) *in vitro*. Br J Cancer. 1997; 75:1744-1752.
20. Rice WG, Hillyer CD, Harten B, Schaeffer CA, Dorminy M, Lackey DA 3rd, Kirsten E, Mendeleyev J, Buki KG, Hakam A, Rice WG. Induction of endonuclease-mediated apoptosis in tumor cells by C-nitroso-substituted ligands of poly(ADP-ribose) polymerase. Proc Natl Acad Sci U S A. 1992; 89:7703-7707.
21. Lo TW, Thornalley PJ. Inhibition of proliferation of human leukaemia 60 cells by diethyl esters of glyoxalase inhibitors *in vitro*. Biochem Pharmacol. 1992; 44:2357-2363.
22. Townsend DM, Tew KD. The role of glutathione-S-transferase in anti-cancer drug resistance. Oncogene. 2003; 22:7369-7375.
23. Juillerat-Jeanneret L, Bernasconi CC, Bricod C, Gros S, Trepey S, Benhattar J, Janzer RC. Heterogeneity of human glioblastoma: Glutathione-S-transferase and methylguanine-methyltransferase. Cancer Invest. 2008; 26:597-609.
24. Liou SF, Lin HH, Liang JC, Chen IJ, Yeh JL. Inhibition of human prostate cancer cells proliferation by a selective alpha1-adrenoceptor antagonist labedipinedilol-A involves cell cycle arrest and apoptosis. Toxicology. 2009; 256:13-24.
25. Zilles K, Qü M, Schleicher A. Regional distribution and heterogeneity of alpha-adrenoceptors in the rat and human central nervous system. J Hirnforsch. 1993; 34:123-132.
26. Ning YM, Sánchez ER. Evidence for a functional interaction between calmodulin and the glucocorticoid receptor. Biochem Biophys Res Commun. 1995; 208:48-54.
27. Lee GL, Hait WN. Inhibition of growth of C6 astrocytoma cells by inhibitors of calmodulin. Life Sci. 1985; 36:347-354.
28. Beil W, Hackbarth I, Sewing KF. Mechanism of gastric antisecretory effect of SCH 28080. Br J Pharmacol. 1986; 88:19-23.

29. Wallmark B, Briving C, Fryklund J, Munson K, Jackson R, Mendlein J, Rabon E, Sachs G. Inhibition of gastric H^+,K^+-ATPase and acid secretion by SCH 28080, a substituted pyridyl(1,2a)imidazole. J Biol Chem. 1987; 262:2077-2084.
30. Rhoden KJ, Tallini G, Douglas JS. H^+-K^+ ATPase inhibitors cause relaxation of guinea pig and human airway smooth muscle *in vitro*. J Pharmacol Exp Ther. 1996; 276:897-903.
31. Pardridge WM. The blood-brain barrier: Bottleneck in brain drug development. NeuroRx. 2005; 2:3-14.
32. Groothuis DR. The blood-brain and blood-tumor barriers: A review of strategies for increasing drug delivery. Neuro Oncol. 2000; 2:45-59.
33. Maeda H, Hori S, Ohizumi H, Segawa T, Kakehi Y, Ogawa O, Kakizuka A. Effective treatment of advanced solid tumors by the combination of arsenic trioxide and L-buthionine-sulfoximine. Cell Death Differ. 2004; 11:737-746.

(*Received June 15, 2012; Revised August 3, 2012; Accepted August 7, 2012*)

Original Article

DOI: 10.5582/bst.2012.v6.4.201

Paris saponin II of Rhizoma Paridis – A novel inducer of apoptosis in human ovarian cancer cells

Xue Xiao[1,2,*], Juan Zou[3,*], Tri Minh Bui-Nguyen[4], Peng Bai[5], Linbo Gao[6], Jinsong Liu[2], Shanling Liu[1], Jianguo Xiao[2], Xinlian Chen[7], Xuemei Zhang[7], He Wang[1,]**

[1] *Department of Gynecology and Obstetrics, West China Second University Hospital, Sichuan University, Chengdu, China;*
[2] *Department of Pathology, The University of Texas M. D. Anderson Cancer Center, Houston, Texas, USA;*
[3] *Department of Pathology, West China Second University Hospital, Sichuan University, Chengdu, China;*
[4] *Department of Biochemistry and Molecular Biology, The George Washington University, Washington, DC, USA;*
[5] *West China School of Preclinical and Forensic Medicine, Sichuan University, Chengdu, China;*
[6] *Laboratory of Molecular and Translational Medicine, West China Institute of Women and Children's Health, West China Second University Hospital, Sichuan University, Chengdu, China;*
[7] *Lab of Genetics, West China Second University Hospital, Sichuan University, Chengdu, China.*

Summary **Rhizoma Paridis (dried root and rhizome) has been an essential ingredient in traditional Chinese herbal medicine. In the past decade, active components of Rhizoma Paridis – the Paris saponins have emerged as promising anti-cancer agents. Among these saponins, polyphyllin D (Paris saponin (PS) I), has been extensively studied and proposed to be a potent antitumor agent. In this study, we continue to establish the efficacy and mechanisms underlying the cytotoxic effects of the steroidal PS members, namely formosanin C (PSII) in ovarian cancer treatment. We isolated PSII and evaluated its effects on a panel of ten human cell lines. Isolated PSII has potent inhibitory effects on the growth of tumor cells without deleterious effects to different normal cell types or benign neoplastic derived cells. While PSII, PSI, and etoposide are effective promoting agents for cell cycle arrest and apoptosis, PSII appeared to be marginally more potent than the later two in inhibiting SKOV3 cell growth. In PSII-treated SKOV3 cells, there was an elevation in proapoptotic elements including Bax, cytosolic cytochrome *c*, activated-caspase-3, and activated-caspase-9. The treatment also reduced extracellular signal-regulated kinase (ERK1/2) phosphorylation and anti-apoptotic Bcl-2 expression. We also assessed the antitumor efficacy of intraperitoneal administration of PSII in human SKOV3 ovarian cancer xenografts in athymic mice. PSII treatment significantly inhibited the growth of xenograft tumors relative to controls by 70% ($p < 0.05$). These findings demonstrated that, in addition to the unique selectivity against cancer cells, PSII is a potent antitumor molecule that may be developed as a cancer therapeutic agent.**

Keywords: Asian medicine, cancer, Chinese/Oriental medicine, gynecology, mitogen-activated protein kinase

1. Introduction

Since ancient times, Rhizoma Paridis, a stem of *Paris polyphylla* Smith var. *chinensis* (Franch.) Hare or *Paris polyphylla* Smith var. *yunnanensis* (Franch.) Hand.-Mazz., has been an essential ingredient of traditional Chinese medicine. Rhizoma Paridis can be found in herbal medicines used to treat diseases and conditions including microbial infection, hemorrhage, menometrorrhagia, and venomous poison (*1-4*). The main constituents of Rhizoma Paridis are the steroidal saponins, a family of glycosides with a chemical structure that contains either a steroid or a triterpenoid attached *via* C3 and an ether bond to a sugar side chain (*5-10*). Because of the crucial roles of Rhizoma Paridis in traditional herbal medicines,

* Xiao X and Zou J contributed equally to this paper.
***Address correspondence to:*
Dr. He Wang, Department of Obstetrics and Gynecology, West China Second University Hospital, Sichuan University, No. 20, Block 3, Renmin Road, Chengdu 610041, China.
E-mail: wanghe_cd@126.com

the pharmacologically active components of Rhizoma Paridis, *i.e.*, saponins, have been isolated. Phytochemical and pharmacological studies have further unlocked a novel therapeutic role as an anticancer agent for these steroid saponins (*6,11-17*). Interestingly, like several other traditional herbal products that have gradually been used in conjunction with modern medicine in cancer treatment (*18*), evidence-based research into the mechanism underlying the cytotoxic effects of Paris saponin (PS) remains undefined.

Thirty saponins of the diosgenyl saponin (R1 = H), pennogenyl saponin (R1 = OH) and the prototype saponin sub-group have hitherto been identified from the stem of Rhizoma Paridis (*19,20*). Preliminary screening studies of the isolated saponins from the crude extract of Rhizoma Paridis suggested that steroidal saponins, including Paris Saponin I (PSI) and II (PSII), also known as polyphyllin D and formosanin C, respectively, exhibit comparable inhibitory effects against tumor cell growth. While PSI has been extensively studied for its ability to inhibit tumor growth (*5,11,14,21,22*), PSII has only recently emerged as another potential antitumor agent (*22,23*). Hence, as part of a concerted effort to characterize and develop active constituents of traditional herbal medicines in modern cancer treatment, in this study, we examine the mechanism underlying the cytotoxic effects of PSII and its putative antitumor properties. The effects of PSII on cell viability were examined on ten human cell lines and primary cell types. The mode of action of PSII-induced cell death was further studied using the SKOV3 cell growth model. We also assessed the efficacy of PSII in an ovarian cancer tumor-bearing mouse model. The results from our current experiments not only establish the relationship between structurally similar steroid saponins and antitumor cell proliferation activity but also provide a promising lead for the use of natural products in ovarian cancer treatment.

2. Materials and Methods

2.1. *Materials*

PSI and PSII were obtained from the Department of Pharmacology at Sichuan University (Chengdu, Sichuan, China). PSII was purified as previously described (*19*). Briefly, PSII was isolated from Rhizoma Paridis using a silica gel, macroporous adsorption resin, Sephadex LH-20, and RP-C18 column chromatography. The structure of PSII was determined by electrospray ionization mass spectrometry and ^{1}H and ^{13}C nuclear magnetic resonance spectral analysis (*24*). Etoposide (VP16) and β-actin antibody were purchased from Sigma Chemical Co. (St. Louis, MO, USA). Primary antibodies Bcl-2, Bax, ERK1/2, phospho-ERK1/2 (Thr202/Tyr204), cytochrome *c*, caspase-3, and caspase-9 were obtained from Santa Cruz Biotechnology Inc. (Santa Cruz, CA, USA).

2.2. *Cell lines and cell culture*

SKOV3, a human ovarian cancer cell line; Caski, a cervical epitheloid carcinoma cell line; A549, a human lung adenocarcinoma cell line; HepG2, a hepatocellular carcinoma cell line; SiHa, cervical carcinoma cell lines; and HEC-1A, an endometrial carcinoma cell line; all were purchased from the American Type Culture Collection (Rockville, MD, USA). An ovarian surface epithelial cell (OSE) line, human vascular smooth muscle cells, human bronchial cells, and human meningeal cells were obtained from Sichuan University, China. Cells were cultured using RPMI-1640 medium (Gibco BRL, Life Technologies Gaithersburg, MD, USA) supplemented with 10% fetal bovine serum (FBS) (HyClone, Logan, USA) at 37ºC in 5% CO_2.

2.3. *PSII treatment and determination of cell survivability*

Cells were seeded at a density of 5×10^3 per well in 96-well tissue culture plates for 12 h prior to treatment. Carrier DMSO (< 0.1%) was used as a negative control. Viability was examined using the 3-[4, 5-dimethylthiazol-2-yl]-2, 5-diphenyltetrazolium bromide (MTT; Sigma, USA) assay (*5*). Dose- and time-dependent curves of PSII-treated cells were generated. The cytotoxic effects of tested agents were expressed as the 50% inhibiting concentration (IC_{50}) or total growth inhibiting concentration (TGI). SPSS software version 13.0 (SPSS Inc., China) was used to calculate IC_{50} and TGI.

2.4. *Transmission electron microscopy (TEM)*

SKOV3 cells were treated with 10 μM PSII for 24 h. Harvested cells were then fixed in 5% glutaraldehyde and 3% paraformaldehyde, dehydrated in an ascending acetone series, embedded in PolyBed 812 resin, sectioned into ultra-thin longitudinal sections, and imaged using a transmission electron microscope (JEOL 1010, Jeol, Tokyo, Japan) as previously described (*25*).

2.5. *Flow cytometry analysis*

SKOV3 cells were treated with PSII at various concentrations (1 μM, 5 μM, 10 μM, and 20 μM) or with 10 μM PSII and were harvested at different time points (0, 24 h, and 48 h). Cells were labeled with propidium iodide (PI, 50 μg/mL, Sigma, USA) for 30 min at room temperature in the dark and the DNA content was determined by flow cytometry after filtration with a 300 dialyzer (FACSort, Becton Dickinson, San Jose, CA). Cell apoptotic incidence and distribution of the cell cycle were analyzed using CellQuest software (Becton Dickinson, CA, USA)

and ModFit software (Verity Software House, USA). Experiments were conducted in triplicate.

2.6. *Terminal deoxynucleotidyl transferase-mediated dUTP nick end labeling (TUNEL) assay*

Cells were allowed to grow on cover slides pretreated with poly-(L)-lysine for 12 h prior to PSII treatment. The cell layers were fixed with 4% paraformaldehyde solution for 15 min at room temperature, washed with phosphate buffered saline (PBS), and then permeated with permeabilization solution (Triton X-100, 0.1% and sodium citrate) at 4°C for 2 min. SKOV3 cell samples were labeled with the TUNEL reaction mixture for 1 h at 37°C according to the manufacturer's protocol (Roche Applied Science, USA). Apoptosis was determined as the percentage of TUNEL positive cells per 1,000 DAPI-stained nuclei. Images were recorded using fluorescence microscopy (Confocal Scanning Laser Microscopy, Leica TCS4D, Germany) (*26*).

2.7. *Western blotting analysis*

SKOV3 cells were treated with PSII for 24 h. Harvested cells were collected to determine the apoptotic index and subsequently subjected to Western blot Analysis. Briefly, whole cell lysates were obtained using RIPA Buffer (Sigma, USA) and the protein concentrations were determined using the Bradford assay. Twenty five micrograms of total proteins was resolved in 12% sodium dodecyl sulfate polyacrylamide gel electrophoresis (SDS-PAGE). Proteins of interest were detected by Western blot using primary antibodies (anti-Bcl-2 (1:1,000), anti-Bax (1:3,000), anti-ERK1/2 (1:2,000), anti-phospho-ERK1/2 (Thr202/Tyr204) (1:2,000), anti-cytochrome *c* (1:2,000), anti-pro-caspase-9 (1:1,000), anti-caspase-9 (1:1,000), anti-pro-caspase-3 (1:2,000) and anti-caspase-3 (1:2,000)) and HRP-conjugated secondary antibodies. Blots were developed with enhanced chemiluminescence (ECL, Pierce, USA) and exposed to X-ray film.

2.8. *Immunochemical analysis*

PSII-treated cells were fixed with 3-aminopropyl-triethoxysilane at 60ºC for 60 min. The paraffin sections were treated with 0.3% hydrogen peroxide at room temperature to block endogenous peroxidase activities and incubated with 5% bovine serum albumin to prevent nonspecific binding. Treated sections were exposed to antibodies anti-Bcl-2 (1:100), anti-Bax (1:50), anti-caspase-3 (1:100), and anti-caspase-9 (1:100). After being processed, images of the stained slides were digitized to obtain grey values using a CoolSnap Pro video camera (Meyer Instruments, Houston, TX, USA) interfaced to an Olympus BX2 microscope (Olympus, Center Valley, PA) with a 20× magnification objective.

2.9. *The effect of PSII in a xenograft model of ovarian cancer*

The model has been described previously (*5*). Briefly, 5×10^6 SKOV3 cells were injected subcutaneously into 4- to 6-week-old female BALB/c athymic nude mice (Chengdu Experimental Animal Center, Chengdu, China) and the mice were randomly divided into 6 groups ($n = 5$). PSII and PSI dosages (15 mg/kg and 25 mg/kg) and schedules were established according to preliminary toxicologic and pharmacokinetic studies and from a previous study, respectively (*5*). One week after implantation, treatment groups received their first doses of either PSI or PSII dissolved in a vehicle solution of DMSO (< 0.1%) and diluted in saline solution. Administrations were carried out on 4 consecutive days per week for 4 weeks (between day 8 and 35). Control groups received the vehicle (DMSO, < 0.1%) in saline solution. General clinical observations of the mice and determination of body weight and tumor growth were made twice weekly. Two perpendicular diameters of the xenograft in centimeters were measured to estimate the tumor mass using the formula $(a \times b^2)/2$. At the termination of the study, all mice were euthanized using carbon dioxide asphyxiation. All experiments were conducted based on the guidelines of The Institute for Nutritional Sciences (Shanghai, China).

2.10. *Statistical analysis and reproducibility*

The results were given as standard error of the mean. SPSS software version 13.0 (SPSS Inc., China) was used to calculate IC_{50}. Statistical analysis was performed using the Student's t test. $p < 0.05$ was considered significant.

3. Results

3.1. *Treatment with PSII inhibits the growth of human tumor cell lines*

Figure 1A shows the chemical structural similarity between PSI and PSII. Cell survival curves of the six cancer cell lines (A549, CASki, SiHA, HepG2, HEC-1A, and SKOV3) after exposure to PSII (10 μM) for 4 days show < 50% cell survival compared to nontreated groups. Specifically, the IC_{50}s for PSII in tumor derived cell lines Caski, SiHa, HEC-1A, SKOV3, A549, and HepG2 were 5.7 μM, 3.7 μM, 2.1 μM, 2.4 μM, 4.0 μM, and 2.2 μM, respectively. We also assessed the possibility of PSII to sensitize primary human cells from different origins and benign neoplastic derived cells. As shown in Figure 1B, the growth inhibitory property of PSII is selectively against tumor derived cells. PSII treatment did not suspend the growth of several different normal cell types including human bronchial epithelial cells, human vascular smooth muscle cells,

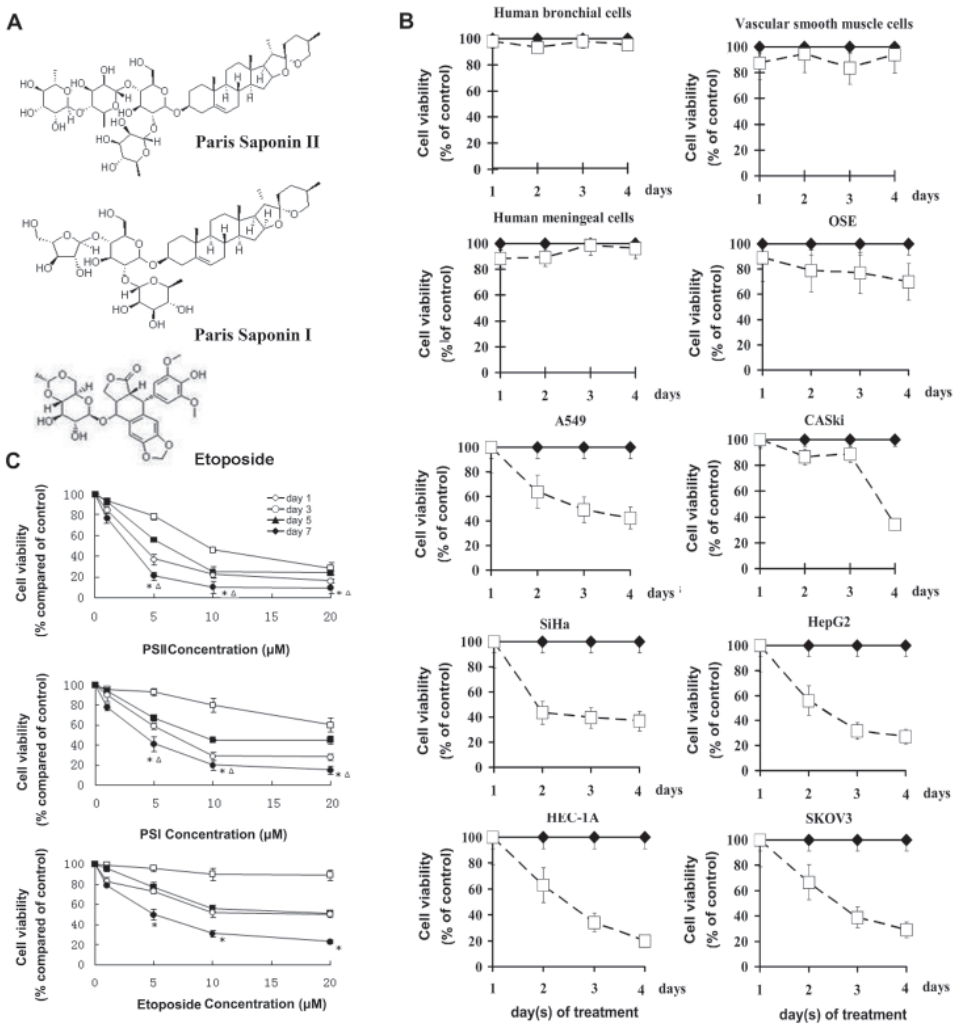

Figure 1. PSII inhibits tumor cell proliferation. (A) The structure of Paris saponin II (PSII), including an α-L-rhamnopyranosyl group at C-2 of the glucosyl moiety that plays an important role in the activity of PSII. The α-L-arabinofuranosyl and β-D-glucopyranoside at C-4 of the inner glucosyl moiety have limited roles. The chemical structure of PSI and etoposide are included. **(B)** Different cell lines were treated with PSII for 4 days. Cell viability was determined by MTT assay. PSII does not have any effect on the survival of normal human meningeal, human vascular smooth muscle, or human bronchial cells. PSII has marginal inhibitory effects on the growth of immortalized ovarian surface epithelial (OSE) cells. In contrast, PSII decreases cell viability of tumor derived cell lines: HEC-1A, A549, HepG2, SKOV3, Caski, and SiHa. Error bars represent standard error of the mean (SEM) ($n = 3$). **(C)** Dose-effect curves for PSII, PSI, and etoposide on the SKOV3 cell line for 1, 3, 5, and 7 days. * $p < 0.05$, *vs*. day 1 group; $\Delta p < 0.05$, *vs*. VP16 group.

and human meningeal cells. Interestingly, we still observed a marginal growth inhibitory effect on the immortalized OSE cell line known to develop sporadic chromosome instability (*27*). Since our primary interest is ovarian cancer, SKOV3, which exhibited the most sensitivity toward PSII treatment, was further studied. The kinetic study demonstrated that PSII treatment inhibits SKOV3 cell growth in a dose- and time-dependent manner. At a concentration of 10 μM, the inhibition index of PSII after 7 days treatment was at a remarkable rate of 90.0% compared to PSI (80.3%) and etoposide (69.2%), a known cytotoxic agent. After a 24-hour treatment, the IC_{50} and TGI values of PSII on treated SKOV3 cells were 2.4 μM and 6.3 μM, respectively compared to those of PSI (3.1 μM and 9.3 μM) and etoposide (3.2 μM and 9.7 μM) (Figure 1C). The results demonstrate potent inhibitory effects on the growth of tumor cells without deleterious effects on different normal cell types or benign neoplastic derived cells of PSII. However, most interestingly, while having marked structural similarities, PSII seemed to render better growth inhibitory effects than PSI on SKOV3 cells at the same concentration and time point.

3.2. *Characterization of PSII-induced apoptosis in solid tumor cells*

To understand the nature underlying PSII's effects on tumor cells' viability, we examined structural changes of treated SKOV3 cells. Tumor cells treated with PSII (10 μM) displayed morphological changes as early as 4 h after initial exposure. After 12 h of PSII treatment, cells shrunk and ensued cell detachment from the culture surface at 24 h suggesting on-going induction of anoikis

(Figure 2A). Ultrastructural electron microscopy analysis of SKOV3 cells demonstrated morphological changes characteristic of apoptosis such as membrane blebbing, fragmentation with apoptotic bodies, swelling of organelles and nuclear condensation (Figure 2B). DNA fragmentation assays showed oligonucleosomal DNA ladders in PSII-treated cells (data not shown), a typical characteristic of cells undergoing apoptosis, confirming that PSII induced apoptosis in SKOV3 cells. The results were complemented by TUNEL staining studies showing an increased percentage of TUNEL positive cells in a concentration dependent manner. Particularly, at 5 μM and 10 μM, PSII induced distinctly high percentages of TUNEL-positive cells (Figure 2C).

To further characterize cell death induced by PSII, the relative portion of DNA contents were assessed by cell cycle analysis by propidium iodide staining using flow cytometry. SKOV3 cells treated with either various concentrations (1 μM, 5 μM, 10 μM, and 20 μM) for 24 h or with 10 μM of PSII for multiple time courses (0 h,

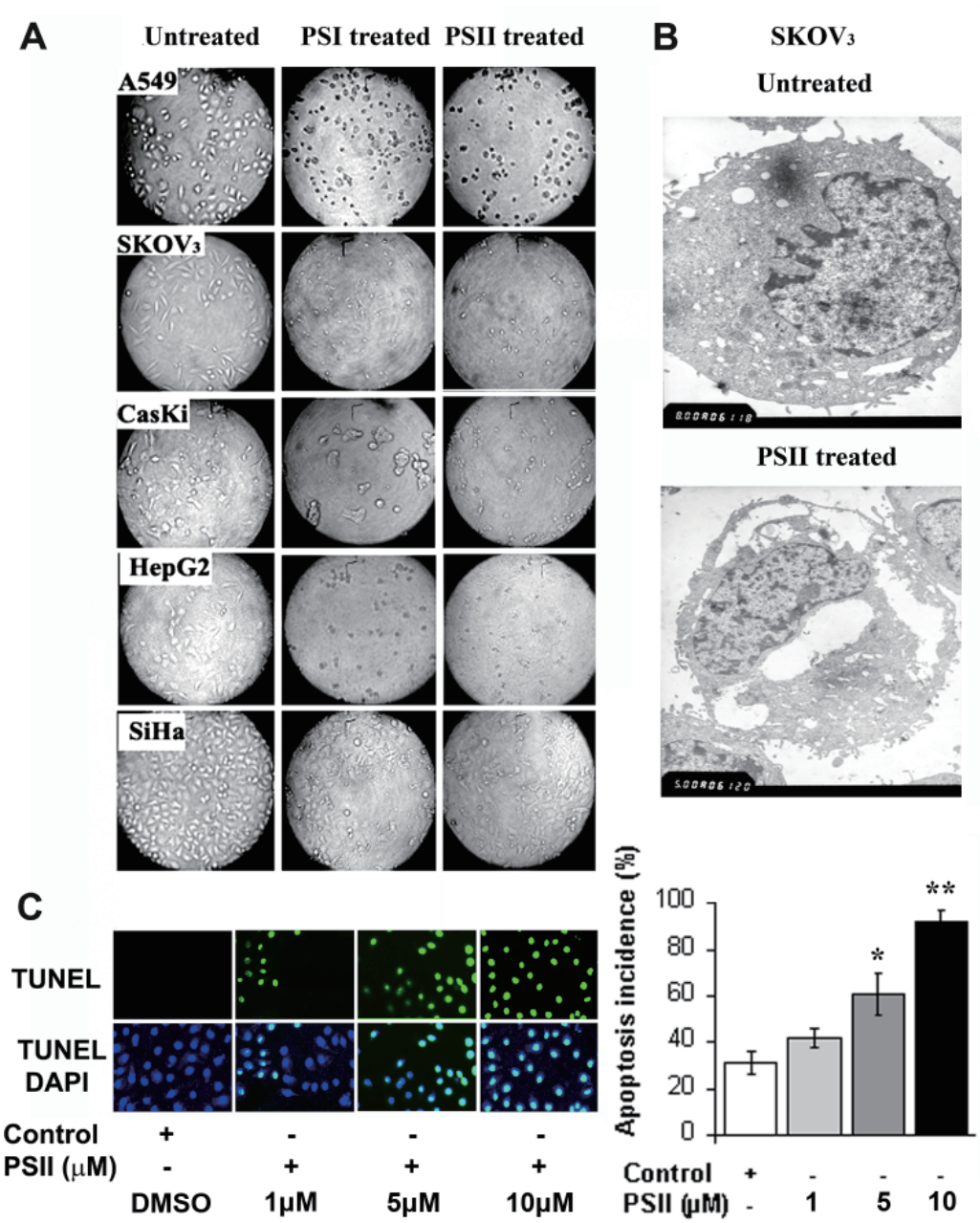

Figure 2. (A) Phase contrast images were recorded at 40× magnification using an Olympus BX60 upright microscope showing PSII (10 μM) and PSI (10 μM) induced morphology changes in A549, SKOV3, CasKi, HepG2, and SiHa cells after a 24 h treatment. Untreated cells (only exposed to DMSO (< 0.1%) in saline) were used as controls. **(B)** Transmission electron microscopy of SKOV3 cells treated with PSII (10 μM) for 24 h (lower panel). Images were recorded at 5,000× magnification using a transmission electron microscope. Displays show structural changes in treated cells compared to control (upper panel). **(C)** SKOV3 cells were treated with different concentrations of PSII and labeled with TUNEL and DAPI after 24 h. Images of random fields ($n = 10$) per slide ($n = 3$) were collected at 400×. Data is presented as the percentage of TUNEL positive cells (green fluorescence) per total number of treated cells (blue-DAPI staining) ($^{*}p < 0.05$, $^{**}p < 0.01$, compared to control). Representative figures of treated cells labeled for TUNEL and counterstained with DAPI are shown.

24 h, 48 h, 72 h) were subjected to analysis. The results indicated PSII treatment induced SKOV3 cell death in a concentration- and time-dependent manner (Figures 3A and 3B). While concentration dependent studies showed only a marginal percentage of cell death after 24 h of PSII (10 μM) exposure, cell cycle analysis indicated a marked increase in the cell population trapped in the G_2 phase as compared to those of the control group. However, cell death was more evident at and after 48 h of treatment (22.1% compared to 2.2% at time 0) (Figures 3C and 3D). Together, the results suggest that PSII treatment caused cell cycle arrest and apoptosis.

3.3. *PSII activates the apoptotic pathway and targets ERK activity*

In a previous study, PSI has been shown to activate the mitochondrial apoptotic pathway (*5*). Thus, to

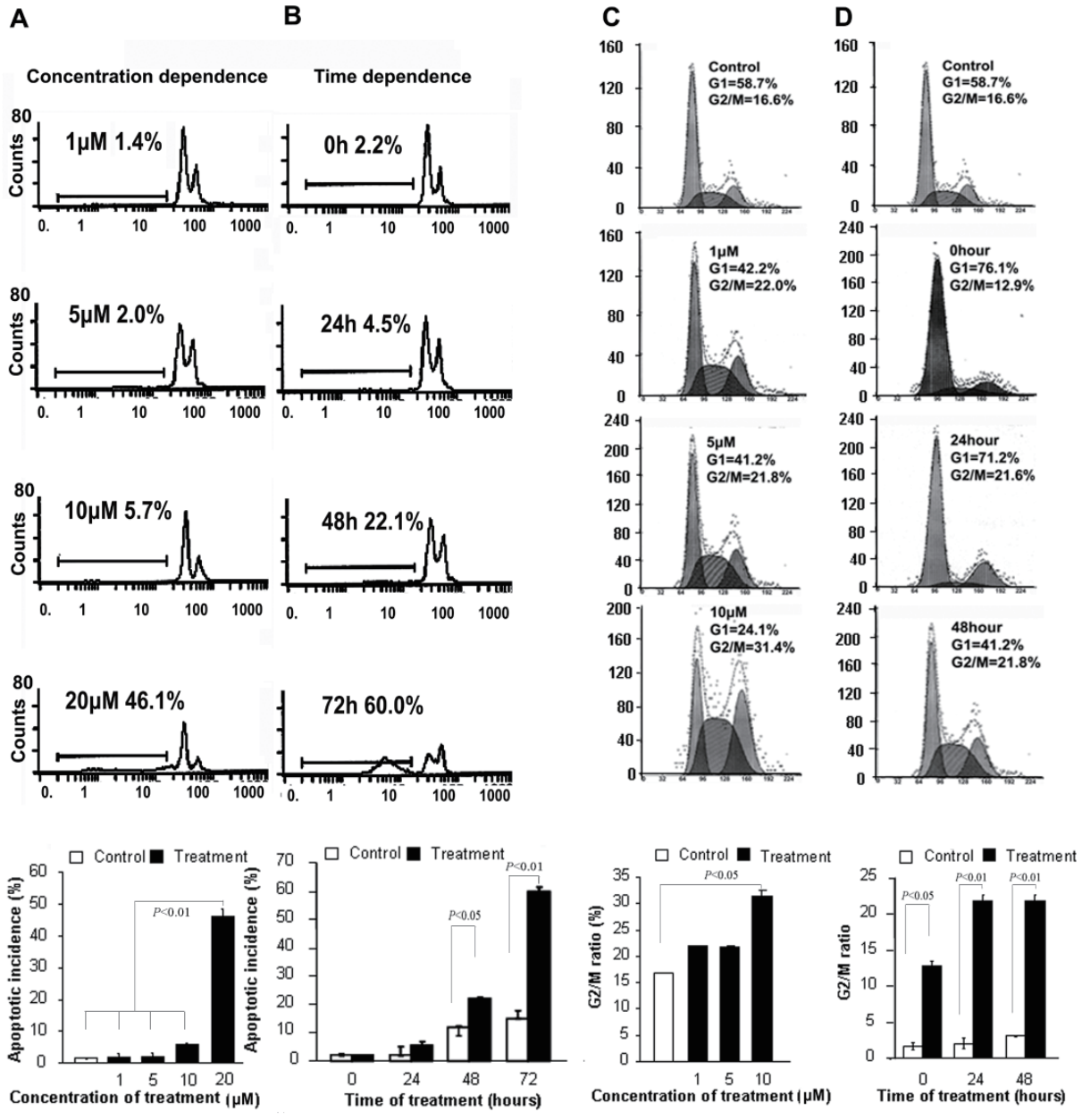

Figure 3. FACS analysis for apoptotic incidence. Special Ap peaks illustrate the characteristics of the cell population committed to apoptosis. (A) SKOV3 cells were treated with different concentrations of PSII for 24 h. The bar chart demonstrates percentage of apoptotic incidence compared to control. **(B)** SKOV3 cells were treated with PSII (10 μM) and were analyzed for percentage of apoptotic incidence at different time points. The bar chart summarizes the results as percentage of apoptotic incidence compared to control. **(C)** PSII induces G_2/M phase arrest in SKOV3 cells in a concentration dependent manner. The SKOV3 cells were treated with different concentrations of PSII (0, 1 μM, 5 μM, and 10 μM) for 24 h and subsequently labeled with propidium iodide staining and analyzed using fluorescence-activated cell sorting analysis. The bar chart summarizes the results as percentage of cells in the G_2/M phase. **(D)** PSII induces G_2/M phase arrest in SKOV3 cells. SKOV3 cells were cultured with or without PSII (10 μM) for 0, 24 h, and 48 h. All treated cells were stained with propidium iodide and analyzed using fluorescence-activated cell sorting analysis. The bar chart shows the percentage of cells in the G_2/M phase. Error bars represent standard error of the mean (SEM) ($n = 3$) ($p < 0.05$ and $p < 0.01$, compared to control to be considered as significant).

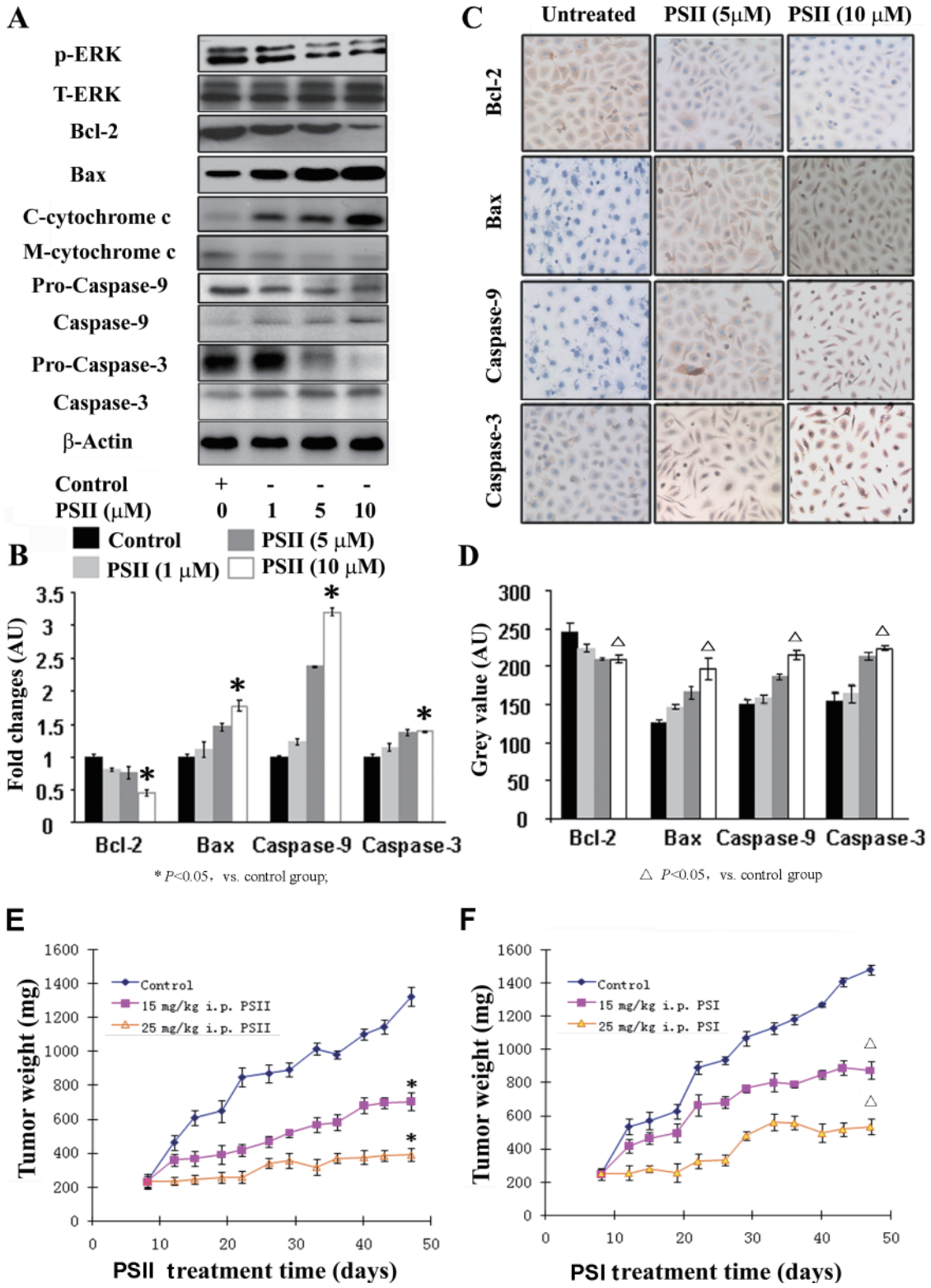

Figure 4. PSII induces caspase activation and cytochrome *c* release and inhibits ERK1/2 phosphorylation in treated SKOV3 cells. (A) Western blot analysis for SKOV3 cells treated with different concentrations of PSII for 24 h. DMSO (< 0.1%) diluted in saline was used as a control. β-Actin was used as a loading control. M-cytochrome c-mitochondrial cytochrome *c* and C-cytochrome c-cytosolic cytochrome *c*. **(B)** Densitometric analysis was performed for Bcl-2, Bax, active caspase-9, and active caspase-3. Values were normalized to β-actin, * $p < 0.05$, compared to control. **(C)** Sections were analyzed by immunohistochemistry for Bax, Bcl-2, caspase-3, and caspase-9. **(D)** Quantification using immunohistochemical staining for Bax, Bcl-2, caspase-3, and caspase-9. Data are presented in arbitrary values ($n = 3$, $^{\Delta}$ $p < 0.05$, compared to control). **(E** and **F)** Paris saponins (PSI and PSII) inhibit tumor growth in a xenograft model of ovarian cancer. Mice were implanted with 5×10^6 SKOV3 cells on day 0 and were randomly divided into various treatment and control groups ($n = 5$). Eight days after implantation, tumor-bearing mice were treated according to the protocols. Briefly, tumor-bearing mice were treated with PSI, PSII, or received the vehicle (DMSO, < 0.1%) in saline solution by intraperitoneal administration for 4 weeks, 4 consecutive days per week with two different doses of either PSI or PSII, 15 mg/kg or 25 mg/kg. Columns, mean; bars, S.D., * $p < 0.05$, $^{\Delta}$ $p < 0.05$, compared to control.

understand the nature of PSII-induced apoptosis on SKOV3 cells, we examined changes in the constituents of the mitochondrial apoptotic pathway. As shown in Figure 4, 24 h PSII treatment led to the expression of proapoptotic protein Bax and the activation of apoptotic proteins such as caspase-3 and caspase-9 in a concentration manner evident by a gradual disappearance of intact pro-caspase-9 and pro-caspase-3 and appearance of proteolytic cleavage bands (Figures 4A and 4B). We also detected increased levels of cytosolic cytochrome *c* and decreased levels of mitochondrial cytochrome *c* in a concentration dependent manner. In contrast, anti-apoptotic Bcl-2 protein levels were markedly reduced in cells being treated with PSII at a concentration as low as 5 μM. Immunochemical studies also confirmed similar observations showing that PSII treatment reduced Bcl-2 expression levels while promoting the expression of Bax and the activation of caspase-3 and caspase-9 (Figures 4C and 4D). Since inhibition of the mitogen-activated protein kinase pathway (MAPK pathway) has been shown to be associated with induction of apoptosis in tumor cells with growth inhibition (*28-30*), to determine whether PSII treatment inhibits tumor cell growth by modulating survival signaling, we also examined the activation status of ERK1/2. As we expected, although PSII treatment did not alter the expression levels of total ERK1/2, prominent reduction of phosphorylated ERK1/2 was observed as we increased the exposure concentration of PSII from 1 μM to 10 μM.

3.4. *PSII inhibits tumor growth in a xenograft mouse model*

To further characterize the antitumor properties of PSII, we assessed its antitumor efficacy in a well established xenograft mouse model of ovarian cancer. Both PSI and PSII did not induce any apparent acute toxic effects in treated mice. Most intriguing, as shown in Figure 4E, PSI and PSII treatment significantly delayed tumor growth. As we have shown that although both PSI and PSII have the same range of efficacy, PSII appeared to be marginally more potent than PSI. We observed the same pattern in the *in vivo* study. At the termination of the experiment, we found that intraperitoneal administration of PSII and PSI at 15 mg/kg and 25 mg/kg dosages led to a 46% and 70% and a 40% and 64% tumor growth inhibition, respectively, compared with that in control mice treated with vehicle solution of DMSO (< 0.1%) diluted in saline solution ($p < 0.05$). However, at a dosage of 15 mg/kg, the antitumor effect of PSII appeared to reach a plateau after 26 days of treatment despite the additional 2 cycles of treatment. In contrast, at the higher dosage (25 mg/kg), the additional cycles of treatment seemed to be beneficial as PSII inhibited 70% tumor growth at day 47 compared to 60% at day 26.

4. Discussion

In attempting to characterize the antitumor effects of active constituents of traditional herbal medicine with diverse therapeutic potential, PSII was isolated from Rhizoma Paridis and characterized (*31,32*). At the time of this writing, eleven steroidal saponins of Rhizoma Paridis have been identified, namely Paris V (3-*O*-Rha(1→2)-Glc), polyphyllin C (3-*O*-Rha(1→3)-Glc), PSI-polyphyllin D (3-*O*-Rha(1→2)[Ara(1→4)]-Glc) (*14,33-36*), PSII-formosanin C (3-*O*-Rha (1→4)-Rha(1→4)[Rha(1→2)]-Glc), prosapogenin B of dioscin (3-*O*-Rha(1→4)-Glc), Paris saponin V (PSV) (3-*O*-Rha(1→3)[Ara(1→4)]-Glc), Paris saponin VI (PSVI))(3-*O*-Rha(1→4)[Ara(1→3)]-Glc), Paris saponin III (3-*O*-Rha(1→4)[Ara(1→2)]-Glc), gracillin (3-*O*-Rha(1→2)[Glc(1→3)]-Glc, polyphyllin E (3-*O*-Rha(1→2)-Rha(1→4)[Rha(1→3)]-Glc), and polyphyllin F (3-*O*-Rha(1→4)-Rha (1→3)[Glc(1→2)]-Rha) (*3,37*). Over the past few decades, the therapeutic properties of the diosgenin-steroid saponins sub-group have been explored for treatments against metabolic diseases, including hypercholesterolemia, dyslipidemia, diabetes and obesity, inflammation, and cancer (*38*). However, the field investigating the antitumor properties of Paris saponin has only become more active in the past five years. Multiple model systems ranging from murine lung adenocarcinoma (*22*), human colon adenocarcinoma grade II (*17*), mouse lung adenocarcinoma (*23*) to zebrafish embryos have demonstrated that several Paris saponins can induce programmed cell death, inhibit cell migration, and inhibit tumor cell growth. Studies from our laboratories have also unraveled PSI mechanisms of action on ovarian cancer cells (*5,24,33,36,39*). While PSII and PSI have remarkable chemical structural similarity, very few studies have been conducted to explore the efficacy and mechanisms underlying the cytotoxic effects of PSII in cancer treatment.

In the present study, we examined the underlying mechanism of action and the antitumor effects of PSII in ovarian cancer cells because they are not completely defined. We also attempted to develop PSII as a systemic treatment strategy for ovarian cancer that remains the fifth-leading cause of death by cancer in the developed world and the most deadly of the gynecologic malignancies (*40*). Here, we showed that PSII selectively inhibits growth of tumor cell lines but not non-neoplastic derived cell lines or normal cell types with relative low IC_{50}s compared with those of PSI. Similar to PSI, PSII appeared to be a more powerful cytotoxic agent than etoposide. Cytotoxic and inhibitory effects of PSII were time- and dose-dependent. Increased concentrations of PSII ensued showing increased levels of cell death signaling evident by DNA fragmentation, the activation of caspase-9 and caspase-3, and reduced levels of active ERK1/2 in treated cells.

PSII treatment also altered the expression levels of anti-apoptotic Bcl-2 and pro-apoptotic protein Bax. Both Bax and Bcl-2 are among the important regulators of cytochrome *c* release from mitochondria; the reduction of Bcl-2 levels promotes cytochrome *c* release, leading to the activation of programmed cell death. It is well known that cross-talk between Bcl-2 and Bax is intimately linked to the fate of the cell; Bax may block Bcl-2 activity and *vice versa*; however, in certain instances, Bcl-2 and Bax function independently to regulate cell death in an exclusive manner. Data from the present studies seem to suggest that PSII induced apoptotic cell death by modulating the expression of both Bcl-2 and Bax. While further studies will be necessary, the dramatic changes in Bcl-2 expression levels corroborated with other clues suggesting PSII may induce ER stress-induced cell death. The first clue was evident from the occurrence of several downstream signals upon PSII treatment such as the collapse of mitochondrial potential (data not shown) and the release of cytochrome *c*. ER stress often triggers release of Ca^{2+} and induces activation of the apoptotic pathway involving collapse of mitochondrial potential, permeabilization of the inner membrane and release of cytochrome *c* (*41*). Another clue came from an observation that increased concentrations of PSII in SKOV3 cell treatment resulted in the upregulation of C/EBP homologous transcription factor (CHOP) protein levels (unpublished data). CHOP is known to regulate ER stress-induced cancer cell death (*33*) and suppress Bcl-2 expression levels leading to a severe irremediable endoplasmic reticulum stress (*42,43*). Here, PSII treatment induced Bax expression in parallel with the dramatic reduction of Bcl-2 expression in PSII-treated tumor cells. While future studies will further determine the nature of PSII-induced apoptosis in ovarian cancer tumor cells, data from the present studies suggest that PSII treatment affects the mitochondrial apoptotic pathways. Indeed, these findings are supported by a study by Lee *et al.* showing PSII-formosanin C induces mitochondria membrane potential collapse and the activation of essential components of the intrinsic apoptosis pathway (*17*).

In addition to activating the apoptotic pathway, PSII also exerts its effect on ERK MAPK. The activation of the MAP-ERK pathway often stimulates cell differentiation, mitosis, and hypertrophy (*44*). In cancer, key events in the cellular transformation process such as proliferation, migration, and tumor development have been linked to the activation of ERK1/2 signaling and its role in relaying communication between growth factor receptors and the cell nucleus (*45*). ERK MAPK also phosphorylates caspase-9 at Thr125 resulting in the inhibition of caspase-9 processing and caspase-3 activation (*46*). Therefore, the effects of PSII treatment on ERK MAPK activation in a dose-dependent manner accompanied with increased levels of activated caspases further suggests that PSII elicits its inhibitory effects *via* modifying ERK activities.

We also demonstrated that PSII has a potent antitumor activity. In a comparative study (*23*), PSII appears to be more effective in inhibiting tumor growth and pulmonary metastasis than cisplatin in a T739 bearing LA795 cells mice. Interestingly, this study also showed that PSII appeared to be marginally more potent than PSI, especially, at the higher dosage (25 mg/kg). It appears that at the higher dosage (25 mg/kg), the additional cycles of treatment seemed to be beneficial compared to the PSI treatment. These results offer an interesting observation that may allow us to develop a strategy for a proper schedule for the administration of PSI and PSII as single agent or in adjunvant therapy. Of note, while Rhizoma Paridis has been used for thousands of years, it is also reasonable to assume that the bioactivity of Rhizoma Paridis is a synergistic effect of multiple active constituents including PSI and PSII.

In conclusion, we have shown that PSII targets tumor cells *via* multiple mechanisms including modulating ERK1/2 activity, inducing cell-cycle arrest, and activating the mitochondrial apoptotic pathway. While the chemical structure of PSI and PSII are markedly similar, the relative higher potency of PSII suggests that further investigations into their structure-functions and associated biological effects may have value for improving the effectiveness of an anti-cancer strategy in a clinical setting.

Acknowledgements

We would like to thank Dr. Hao Zhang and Dr. Hongxiang Yin for PSI, PSII, and PSVI compounds. We also thank Diane Hackett and Maude E. Veech for technical support. This work was supported by the Fund of National Nature Science Foundations (Grant No. 81001159/30571942/C03030401), and National Research Foundation for the Doctoral Program of Higher Education of China (Grant No. 20020610089).

References

1. Vassilopoulos Y. *Paris polyphylla* in medicine. A literary favour to world culture. Newsfinder. 2008.
2. Wang Q, Cheng YB. The bacteriostasis and hermostasis functions of Parispolyphylla Smith var. Chinensis (French.) Hera. The Journal of China Pharmaceutical University. 1989; 20:251-253. (in Chinese)
3. Harborne JB. Saponins used in traditional and modern medicine and Saponins Used in Food and Agriculture. Phytochemistry. 1997; 46:1301-1303.
4. XC ZX. The study and application of Paris plant. Journal of Chinese Herbal Technology. 2000; 7:346-347. (in Chinese)
5. Xiao X, Bai P, Bui Nguyen TM, Xiao J, Liu S, Yang G, Hu L, Chen X, Zhang X, Liu J, Wang H. The antitumoral effect of Paris saponin I associated with the induction of apoptosis through the mitochondrial pathway. Mol

Cancer Ther. 2009; 8:1179-1188.
6. Yan L, Gao W, Zhang Y, Wang Y. A new phenylpropanoid glycosides from *Paris polyphylla* var. *yunnanensis*. Fitoterapia. 2008; 79:306-307.
7. Wang Y, Gao WY, Zhang TJ, Guo YQ. A novel phenylpropanoid glycosides and a new derivation of phenolic glycoside from *Paris polyphylla* var. *yunnanensis*. Chin Chem Lett. 2007; 18:548-550.
8. Wang Y, Gao WY, Liu XQ, Zuo YT, Chen HX, Duan HQ. Antitumor constituents from *Paris polyphylla*. Asian J Tradit Med. 2006; 1:7-10.
9. Cheng ZX, Liu BR, Qian XP, Ding YT, Hu WJ, Sun J, Yu LX. Proteomic analysis of anti-tumor effects by Rhizoma Paridis total saponin treatment in HepG2 cells. J Ethnopharmacol. 2008; 120:129-137.
10. Man S, Gao W, Zhang Y, Yan L, Ma C, Liu C, Huang L. Antitumor and antimetastatic activities of Rhizoma Paridis saponins. Steroids. 2009; 74:1051-1056.
11. Wang Y, Zhang YJ, Gao WY, Yan LL. Anti-tumor constituents from *Paris polyphylla* var. *yunnanensis*. Zhongguo Zhong Yao Za Zhi. 2007; 32:1425-1428.
12. Zhou J. Bioactive glycosides from Chinese medicines. Mem Inst Oswaldo Cruz. 1991; 86 (Suppl 2):231-234.
13. Sun J, Liu BR, Hu WJ, Yu LX, Qian XP. *In vitro* anticancer activity of aqueous extracts and ethanol extracts of fifteen traditional Chinese medicines on human digestive tumor cell lines. Phytother Res. 2007; 21:1102-1104.
14. Lee MS, Yuet-Wa JC, Kong SK, Yu B, Eng-Choon VO, Nai-Ching HW, Chung-Wai TM, Fung KP. Effects of polyphyllin D, a steroidal saponin in *Paris polyphylla*, in growth inhibition of human breast cancer cells and in xenograft. Cancer Biol Ther. 2005; 4:1248-1254.
15. Chiang HC, Wang JJ, Wu RT. Immunomodulating effects of the hydrolysis products of formosanin C and beta-ecdysone from *Paris formosana* Hayata. Anticancer Res. 1992; 12:1475-1478.
16. Wu RT, Chiang HC, Fu WC, Chien KY, Chung YM, Horng LY. Formosanin-C, an immunomodulator with antitumor activity. Int J Immunopharmacol. 1990; 12:777-786.
17. Lee JC, Su CL, Chen LL, Won SJ. Formosanin C-induced apoptosis requires activation of caspase-2 and change of mitochondrial membrane potential. Cancer Sci. 2009; 100:503-513.
18. Liu J, Li X, Liu J, Ma L, Li X, Fønnebø V. Traditional Chinese medicine in cancer care: A review of case reports published in Chinese literature. Forsch Komplementmed. 2011; 18:257-263.
19. Yin HX, Xue D, Bai N, Chen C, Chen Y, Zhang H. Isolation and identification of major steroidal saponins of Paris polyphylla Smith var stenophylla Franch. Sichuan Da Xue Xue Bao Yi Xue Ban. 2008; 39:485-488. (in Chinese)
20. Liu XX, Wang L, Chen XQ, Deng XT, Cao Y, Wang Q. Simultaneous quantification of both triterpenoid and steroidal saponins in various Yunnan Baiyao preparations using HPLC-UV and HPLC-MS. J Sep Sci. 2008; 31:3834-3846.
21. Ma DD, Lu HX, Xu LS, Xiao W. Polyphyllin D exerts potent anti-tumour effects on Lewis cancer cells under hypoxic conditions. J Int Med Res. 2009; 37:631-640.
22. Shuli M, Wenyuan G, Yanjun Z, Chaoyi M, Liu Y, Yiwen L. Paridis saponins inhibiting carcinoma growth and metastasis *in vitro* and *in vivo*. Arch Pharm Res. 2011; 34:43-50.
23. Man S, Gao W, Zhang Y, Liu Z, Yan L, Huang L, Liu C. Formosanin C-inhibited pulmonary metastasis through repression of matrix metalloproteinases on mouse lung adenocarcinoma. Cancer Biol Ther. 2011; 11:592-598.
24. Zhang XF, Cui Y, Huang JJ, Zhang YZ, Nie Z, Wang LF, Yan BZ, Tang YL, Liu Y. Immuno-stimulating properties of diosgenyl saponins isolated from *Paris polyphylla*. Bioorg Med Chem Lett. 2007; 17:2408-2413.
25. Boraks G, Tampelini FS, Pereira KF, Chopard RP. Effect of ionizing radiation on rat parotid gland. Braz Dent J. 2008; 19:73-76.
26. Gavrieli Y, Sherman Y, Ben-Sasson SA. Identification of programmed cell death in situ *via* specific labeling of nuclear DNA fragmentation. J Cell Biol. 1992; 119:493-501.
27. Maeda T, Tashiro H, Katabuchi H, Begum M, Ohtake H, Kiyono T, Okamura H. Establishment of an immortalised human ovarian surface epithelial cell line without chromosomal instability. Br J Cancer. 2005; 93:116-123.
28. Nguyen TT, Tran E, Nguyen TH, Do PT, Huynh TH, Huynh H. The role of activated MEK-ERK pathway in quercetin-induced growth inhibition and apoptosis in A549 lung cancer cells. Carcinogenesis. 2004; 25:647-659.
29. Cusimano A, Foderà D, D'Alessandro N, Lampiasi N, Azzolina A, Montalto G, Cervello M. Potentiation of the antitumor effects of both selective cyclooxygenase-1 and cyclooxygenase-2 inhibitors in human hepatic cancer cells by inhibition of the MEK/ERK pathway. Cancer Biol Ther. 2007; 6:1461-1468.
30. Kunnimalaiyaan M, Ndiaye M, Chen H. Apoptosis-mediated medullary thyroid cancer growth suppression by the PI3K inhibitor LY294002. Surgery. 2006; 140:1009-1014; discussion 1014-1015.
31. Wei J. Determination of steroidal saponins in Rhizoma Paridis by RP-HPLC. Yao Xue Xue Bao. 1998; 33:465-458. (in Chinese)
32. Huang Y, Cui LJ, Liu WN, Wang Q. Quantitative analysis of steroidal saponins in Chinese material medica Rhizoma Paridis by HPLC-ELSD. Zhongguo Zhong Yao Za Zhi. 2006; 31:1230-1233. (in Chinese)
33. Cheung JY, Ong RC, Suen YK, Ooi V, Wong HN, Mak TC, Fung KP, Yu B, Kong SK. Polyphyllin D is a potent apoptosis inducer in drug-resistant HepG2 cells. Cancer Lett. 2005; 217:203-211.
34. Deng S, Yu B, Hui Y, Yu H, Han X. Synthesis of three diosgenyl saponins: Dioscin, polyphyllin D, and balanitin 7. Carbohydr Res. 1999; 317:53-62.
35. Li B, Yu B, Hui Y, Li M, Han X, Fung KP. An improved synthesis of the saponin, polyphyllin D. Carbohydr Res. 2001; 331:1-7.
36. Siu FM, Ma DL, Cheung YW, Lok CN, Yan K, Yang Z, Yang M, Xu S, Ko BC, He QY, Che CM. Proteomic and transcriptomic study on the action of a cytotoxic saponin (Polyphyllin D): Induction of endoplasmic reticulum stress and mitochondria-mediated apoptotic pathways. Proteomics. 2008; 8:3105-3117.
37. Man S, Gao W, Zhang Y, Huang L, Liu C. Identification of chemical constituents in Rhizoma Paridis saponins and their oral administration in rat plasma by UPLC/Q-TOF/MS. Biomed Chromatogr. 2011; 25:712-719.
38. Raju J, Patlolla JM, Swamy MV, Rao CV. Diosgenin, a steroid saponin of *Trigonella foenum-graecum* (Fenugreek), inhibits azoxymethane-induced aberrant

crypt foci formation in F344 rats and induces apoptosis in HT-29 human colon cancer cells. Cancer Epidemiol Biomarkers Prev. 2004; 13:1392-1398.
39. Weizhen K. Identification and clinical application of Paris Polyphylla and Bistort. Journal of China Traditional Chinese Medicine Information. 2010; 2:108-109.
40. Westgren M. Prevention of ovarian cancer − let's do something. Acta Obstet Gynecol Scand. 2012; 91:1009-1010.
41. Wu J, Kaufman RJ. From acute ER stress to physiological roles of the Unfolded Protein Response. Cell Death Differ. 2006; 13:374-384.
42. Oyadomari S, Mori M. Roles of CHOP/GADD153 in endoplasmic reticulum stress. Cell Death Differ. 2004; 11:381-389.
43. McCullough KD, Martindale JL, Klotz LO, Aw TY, Holbrook NJ. Gadd153 sensitizes cells to endoplasmic reticulum stress by down-regulating Bcl2 and perturbing the cellular redox state. Mol Cell Biol. 2001; 21:1249-1259.
44. Provot S, Nachtrab G, Paruch J, Chen AP, Silva A, Kronenberg HM. A-raf and B-raf are dispensable for normal endochondral bone development, and parathyroid hormone-related peptide suppresses extracellular signal-regulated kinase activation in hypertrophic chondrocytes. Mol Cell Biol. 2008; 28:344-357.
45. Svensson S, Jirström K, Rydén L, Roos G, Emdin S, Ostrowski MC, Landberg G. ERK phosphorylation is linked to VEGFR2 expression and Ets-2 phosphorylation in breast cancer and is associated with tamoxifen treatment resistance and small tumours with good prognosis. Oncogene. 2005; 24:4370-4379.
46. Allan LA, Morrice N, Brady S, Magee G, Pathak S, Clarke PR. Inhibition of caspase-9 through phosphorylation at Thr 125 by ERK MAPK. Nat Cell Biol. 2003; 5:647-654.

(*Received February 24, 2012; Revised July 3, 2012; Accepted July 3, 2012*)

Original Article

DOI: 10.5582/bst.2012.v6.4.212

Effects of Chinese herbal medicine Ningdong Granule on regulating dopamine (DA)/serotonin (5-TH) and gamma-amino butyric acid (GABA) in patients with Tourette syndrome

Shuzhen Wang[1], Fanghua Qi[1], Jijun Li[2], Lin Zhao[1], Anyuan Li[1,*]

[1] *Department of Traditional Chinese Medicine, Shandong Provincial Hospital affiliated to Shandong University, Ji'nan, China;*
[2] *Shanghai Children's Medical Center, School of Medicine, Shanghai Jiaotong University, Shanghai, China.*

Summary **Many studies have indicated that a variety of neurotransmitters are implicated in the pathophysiology of Tourette syndrome (TS), including dopamine (DA), serotonin (5-TH), homovanillic acid (HVA), and gamma-amino butyric acid (GABA). Our previous studies found that Ningdong granule (NDG) is effective on a rat model with TS. NDG can regulate the metabolic disturbance of DA, 5-TH and HVA in the rat brain. However, the mechanisms of NDG in patients with TS are still not clear. To further evaluate the efficiency, safety, and possible mechanisms of NDG, a randomized and double-blind study was carried out. One hundred and twenty patients with TS were enrolled in thisstudy, that were randomly divided into 4 groups (NDG group, Haloperidol (Hal) group, NDG + Hal group and Control group). First, the efficiency of NDG was assessed using the Yale Global Tic Severity Score (YGTSS). Second, the concentration of DA, HVA, 5-TH, 5-hydroxyindoleacetic acid (5-HIAA) and GABA in sera were tested by ELISA. In addition, the influence of NDG on liver and renal function was recorded. We found that NDG could ameliorate tics significantly according the YGTSS score. The concentration of HVA and GABA were increased after treatment with NDG. Furthermore, we found that there was no liver or renal damage in children treated with NDG. We also found that the NDG + Hal group was more effective and safe compared with other groups. In conclusion, the current study indicates that NDG might be effective on patients with TS by regulating dopamine (DA)/serotonin (5-TH) and gamma-amino butyric acid (GABA).**

Keywords: Gilles de la Tourette-Syndrome (TS), Ningdong granule (NDG), dopamine (DA), serotonin (5-TH), gamma-amino butyric acid (GABA)

1. Introduction

Tourette syndrome (TS) is a developmental neuropsychiatric disorder, which is characterized by multiple brief, stereotypical and nonrhythmic movements, or vocalizations called tics, with a duration of at least 1 year (*1*). The prevalence of this syndrome is estimated to be four to six per 1,000 children and adolescents (*2*). Initial symptoms of TS usually occur in TS children by 7 years old (*3*). It occurs three to four times more commonly in males than in females (*4*). For some individuals, tics can cause lifelong impairment and about 5% of TS patients have life-threatening symptoms, which are defined as malignant TS (*1*). The detailed etiological and pathophysiological mechanism of TS is currently still unclear. Our previous studies showed that the metabolic disturbance of DA, and 5-TH in the brain was involved in the pathophysiology of TS (*5*). Tian *et al.* found that at least some of these GABA- and acetylcholine-related genes observed in blood that correlate with tics or are alternatively spliced are involved in the pathophysiology of TS and tics (*6*).

Haloperidol is approved by the Food and Drug Administration (USA) for treating TS. It can selectively inhibit the activity of postsynaptic DA receptors, and inhibit the excitability of the cortical motor area through

**Address correspondence to:*
Dr. Li Anyuan, Department of Traditional Chinese Medicine, Shandong Provincial Hospital affiliated to Shandong University, 324 Jinwu Weiqi Road, Ji'nan 250021, China.
E-mail: sdslyy999@163.com

restraining the activity of DA receptors, to weaken TS symptoms (*7*). Although Haloperidol is efficacious for the treatment of TS, a very high proportion of patients eventually discontinue the therapy because of the side effects including sedation, weight gain, extrapyramidal symptoms, and QT prolongation (*8*). Therefore, development of novel drugs for treatment of TS is urgently needed.

Traditional Chinese medicine (TCM) has been widely used in the treatment of various diseases such as nervous system disease, infectious diseases, and cancer, in China for thousands of years (*9-12*). Ningdong granule (NDG), a TCM preparation, has been revealed to tranquilize and allay excitement in TS and ADHD (*12-14*) (Table 1). It could inhibit the stereotypical behavior in TS rats, and the mechanisms might be related to the suppression of the DA system by increasing the content of HVA in sera, decreasing the content of DA and repressing the expression of DRD2 mRNA in the striatum (*13*). Besides, it also indicated that NDG was effective for ADHD children in the short term with increasing the HVA concentration in sera to regulate DA metabolism (*14*). However, the present data are limited and there is a lack of a double-blind and control trial, and the mechanism of NDG on TS patients also remains obscure. In the current study, we evaluated NDG's short-term efficacy and safety in the treatment of TS patients and explored the possible mechanism of NDG on the DA, 5-TH, and GABA system of TS patients.

2. Materials and Methods

2.1. *Participants*

One hundred and twenty patients (6~18 years) were recruited from the outpatient department of integrative medicine in pediatrics, Provincial Hospital Affiliated to Shandong University. All participants clearly met the DSM-IV diagnostic criteria for TS (*15*), and participated in the clinical trial from May 2009 to June 2010. No participants had taken anti-TS medication before being recruited for the research. In addition, we excluded patients who had a past history of seizures, cardiovascular disease, organic brain disorder, current abuse or dependence on drugs within 6 months. After a detailed explanation of the process of our study, both the patients and their parents gave their informed consent. All research procedures were permitted by the medical ethics committee of the Provincial Hospital Affiliated to Shandong University.

2.2. *Study design*

The study was performed using a randomized, and double-blind, 8-week trial. The patients were equally divided into NDG group (n = 30), Haloperidol group (n = 30), NDG + Hal (n = 30) and Control group (n = 30) by a randomized computer-generated code. The NDG group were assigned to receive NDG 5 mg/kg/day (No. 20090412, 999 Co. Ltd., Shenzhen, China) and one kind of placebo with similar appearance and taste with Haloperidol for 8 weeks. Patients in the Haloperidol group were started at a dose of 0.75 mg/day and increased by 1.5~3.0 mg/day increments every 2 weeks to a maximum tolerated dose of 4.5 mg/day and one kind of placebo with similar appearance and taste with NDG (*16*). The NDG + Hal group were assigned both of them at the same dose. The control group were assigned to receive the above two kinds of placebo. These two kinds of placebo were provided by 999 Co. Ltd., Shenzhen, China. All of the medicines were filled by a pharmacist in charge who mastered the data of treatment assignment and the weight and number of the subjects in the trial.

2.3. *The Yale Global Tic Severity Score analysis*

As previously noted, the Yale Global Tic Severity Score (YGTSS) (*17*), used as a Chinese-translated version in the study, is a semi-structured clinical interview designed to assess current tic severity. This scale yields three summary scores, including total motor, total vocal, and total tic scores. We rated the scores at the first clinic visit as the baseline scores and then every 2 weeks vocal for a total of 8 weeks of follow-up. The clinical rating at each visit was recorded by the same clinicians to avoid personal bias in severity evaluation.

Table 1. Composition and active ingredients of Ningdong granule (NDG)

Components	Voucher specimens No.	Part used	Amount used (g)
Uncaria rhynchophylla (Miq.) Jacks	0706011	Ramulus	20
Gastrodia elata Blume	0705081	Root	6
Ligusticum chuanxiong Hort	0704081	Rhizome	6
Buthus martensii Karsch	0704021	Dried body	3
Scolopendra subspinipes mutilans L. Koch.	0707021	Dried body	Single band
Haliotis diversicolor Reeve.	0701041	Shell	20
Haliotis diversicolor Reeve.	0701041	Shell	20
Dried human placenta	0708021	Dried placenta	3
Glycyrrhiza uralensis Fisch.	0706011	Rhizome	3

Table 2. Baseline of case data

Items	Control (n = 28)	Control (n = 28)	Haloperidol (n = 30)	NDG + Hal (n = 30)	Statistical significance
Year (yr)	10.3 ± 1.9	10.2 ± 1.7	10.4 ± 2.1	10.3 ± 2.0	NS
Gender	22:6	22:7	23:7	24:6	NS
weight (kg)	33.2 ± 3.0	33.4 ± 3.2	33.1 ± 3.3	33.2 ± 2.8	NS

Data are expressed as mean ± S.D. NS: not statistically significant ($p > 0.05$).

2.4. *Contents of DA, HVA, 5-TH, 5-HIAA and GABA in sera detected by ELISA*

The serum levels of DA, HVA, 5-TH, 5-HIAA and GABA were measured using a sandwich enzyme-linked immunosorbent assay (ELISA) according to the instructions of the manufacturer (R & D, Shanghai, China). Patient's blood was centrifuged for 10 min at 20,000 × g at 4°C and the serum was used for testing. Briefly, antigen standards and serum samples were added to each well of 96-well plates pre-coated with primary antibodies. After adding biotin conjugate reagent and enzyme conjugate reagent into each well, the plates were incubated at 37°C for 30 min. The plates were then rinsed four times with distilled water. After a chromogenic reaction, the absorbance was measured at 450 nm by a microtiter plate reader within 15 min.

2.5. *Routine analysis and liver and renal function tests*

All of the subjects' blood samples were collected and sent for liver and renal function tests to the Department of Clinical Laboratory, Provincial Hospital Affiliated to Shandong University at end of the trial.

2.6. *Statistical analysis*

All analyses were performed using the SPSS statistical software package (Version 13.0, SPSS Inc. Chicago, IL, USA), and $p < 0.05$ was considered statistically significant. The Yale Global Tic Severity Score from baseline to week 8 was performed using a rank-sum test. The values of routine analysis and liver and renal function week 8 were compared using a paired Student's t-test. Analyses of side effects between the protocols were performed by Fisher's exact test. The levels of DA, HVA, 5-TH, 5-HIAA and GABA in sera were analyzed by repetitive-measure analysis of variance (ANOVA).

3. Results

3.1. *Study population*

No significant difference was identified between NDG group, Haloperidol group, NDG + Hal group and Control group with regard to basic demographic data including age, gender, and weight (Table 2).

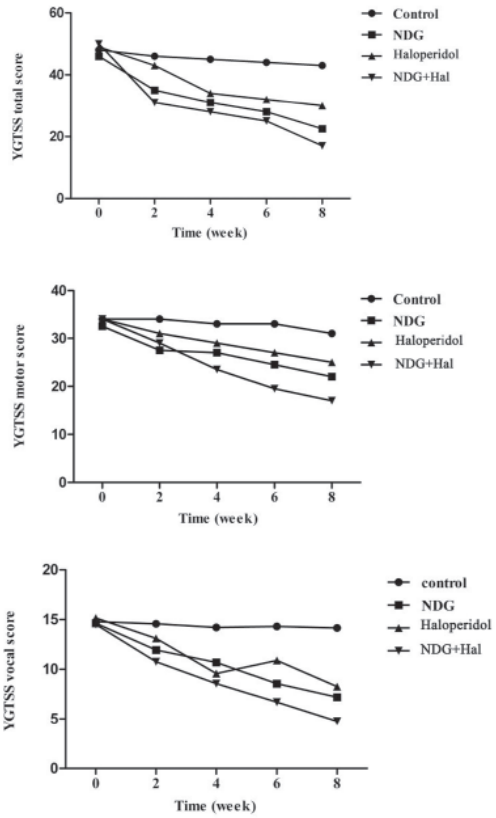

Figure 1. YGTSS score at (0, 2, 4, 6, and 8) week time points. (A) YGTSS total score; **(B)** YGTSS motor score; **(C)** YGTSS vocal score.

3.2. *Assessment of Yale Global Tic Severity Scores*

After treatment, patients in the control group had no significant change in YGTSS motor tic score and YGTSS vocal tic score as well as YGTSS total tic score, at each time point (Compared with the baseline score, $p > 0.05$). However, at the two week time point, patients in the remaining three treatment groups, the YGTSS total tic score, YGTSS motor tic score and as well as YGTSS vocal tic score were significantly reduced ($p < 0.05$), the scores of NDG + Hal group were more significantly reduced ($p < 0.01$) (Figure 1).

3.3. *Levels of DA and HVA in sera detected by ELISA*

The content of DA in sera was not significantly different in the four groups ($p > 0.05$). After treatment the HVA content in the NDG + Hal (67.07 ± 12.01 ng/mL), NDG (64.25 ± 12.88 ng/mL) and Haloperidol

group (60.88 ± 11.71 ng/mL) were increased to a different degree as compared to the control group (47.13 ± 7.58 ng/mL) ($p < 0.05$), The HVA content was higher in the NDG + Hal group than in the NDG ($p < 0.01$) and Haloperidol ($p < 0.05$) group (Figure 2).

3.4. *Levels of 5-TH and 5-HIAA in sera detected by ELISA*

The content of 5-TH and 5-HIAA in sera were not significantly different in the four groups ($p > 0.05$) (Figure 3).

3.5. *Levels of GABA in sera detected by ELISA*

After treatment, the GABA content in the NDG + Hal (166.22 ± 41.91pmol/mL), NDG (123.69 ± 38.47 pmol/mL) and Haloperidol group (113.97 ± 36.23 pmol/mL) were increased to a different degree as compared to the control group (85.63 ± 33.69 pmol/mL) ($p < 0.05$), The content of GABA was higher in the NDG + Hal group than in the NDG ($p < 0.01$) and Haloperidol ($p < 0.05$) group (Figure 4).

3.6. *Analysis of side effects*

No serious adverse effects were detected during the study, while eight kinds of side effects, which were mild and tolerable for the children, were observed as presented in Table 3. In Haloperidol group and NDG + Hal group, the incidence of sedation, extrapyramidal and QT prolongation reactions were higher than that in the NDG and control group ($p < 0.05$). The incidence of nausea and headache reactions in the NDG + Hal group was higher than that in the control group ($p < 0.05$). The incidence of anxiety in the NDG + Hal group was higher than that in the NDG group ($p < 0.05$).

3.7. *Liver and renal function monitoring*

As shown in Table 4, in the NDG + Hal group and Hal group, although the content of alanine in sera were higher than the control group ($p < 0.05$), it was still within the normal range in the Haloperidol group.

4. Discussion

In our previous studies, we found that NDG has the effect of tranquilizing and allaying without obvious side or toxic effects on rats with TS (*12-14*). NDG can regulate the metabolic disturbance of DA, 5-TH and HVA in the rat brain (*13*). However, the mechanisms of NDG in Children with TS are still not clear. To further evaluate the efficiency, safety, and possible mechanisms of NDG, a randomized and double-blind study was carried out in the current study. We found that the effect of NDG was similar to Hal in reducing tic symptoms and NDG might have a synergistic effect on treating TS. The NDG + Hal group was more effective and safe compared to the NDG group and the Hal group. We also found that there was no liver or renal damage in children treated with NDG.

TS is associated with multiple neurotransmitter systems within the basal ganglia-thalamo-cortical circuits (*19,20*). Previous studies showed that the metabolic disturbance of DA, 5-TH and GABA in the brain is involved in the pathophysiology of TS (*21-23*). DA is a key monoamine neurotransmitter in the brain, and numerous studies have shown its regulatory role for motor and limbic functions (*24*), movement (*25*),

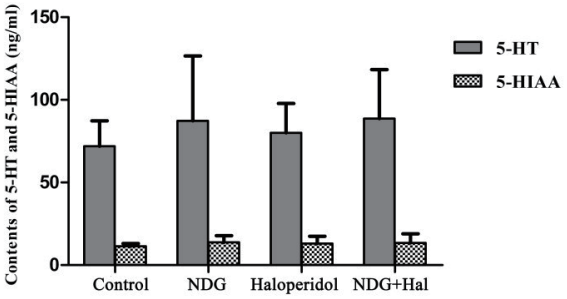

Figure 3. Content of 5-TH and 5-HIAA in sera after treatment with NDG or Hal for 8 weeks. Data are expressed as mean ± S.D.

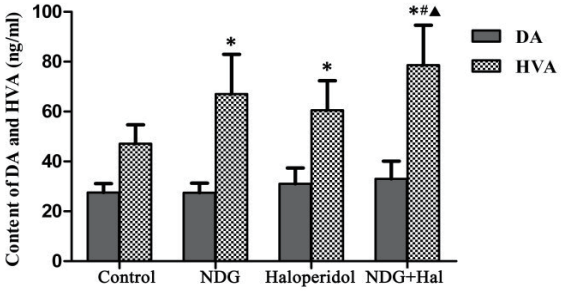

Figure 2. Content of DA and HVA in sera after treatment with NDG or Hal for 8 weeks. Data are expressed as mean ± S.D. * $p < 0.05$ *vs.* Control, # $p < 0.01$ *vs.* NDG, ▲ $p < 0.05$ *vs.* Hal.

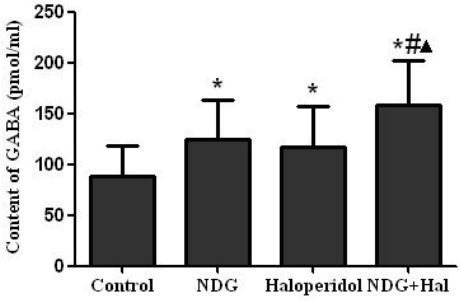

Figure 4. Content of GABA in sera after treatment with NDG or Hal for 8 weeks. Data are expressed as mean ± S.D. * $p < 0.05$ *vs.* Control, # $p < 0.01$ *vs.* NDG, ▲ $p < 0.05$ *vs.* Hal.

Table 3. Clinical complications and side effects

Items	Control (%) (n = 28)	NDG (%) (n = 29)	Hal (%) (n = 30)	NDG + Hal (%) (n = 30)	Statistical significance
Sedation	1 (3.5%)	3 (10.3%)	10 (33.3%)*#	12 (40%)*#	*#
weight gain	2 (7%)	2 (6.9%)	4 (13.3%)	5 (16.7%)	
Extrapyramidal	0	0	5 (16.7%)*#	5 (16.7%)*#	*#
QT prolongation	0	0	5 (16.7%)*#	5 (16.7%)*#	*#
Nausea	0	3 (10.3%)	4 (13.3%)	4 (13.3%)	
Headache	0	1 (3.4%)	4 (13.3%)	6 (20%)*	*
Anxiety	1 (3.5%)	0	6 (20%)#	4 (13.3%)	#
Increased appetite	0	4 (13.8%)	4 (13.3%)	7 (23.3%)*	*

* $p < 0.05$ *vs.* control, # $p < 0.05$ *vs.* NDG.

Table 4. Measure of liver or renal function

Items	Control	NDG	Haloperidol	NDG + Haloperidol	Statistical significance
ALT	24.03 ± 4.43	25.34 ± 5.43	29.87 ± 6.17*	30.23 ± 6.17*	*
AST	24.57 ± 6.53	26.17 ± 5.37	25.90 ± 4.33	26.58 ± 4.98	NS
BUN	24.04 ± 4.43	25.34 ± 5.43	29.87 ± 6.17	30.23 ± 6.17	NS
Cr	75.94 ± 11.18	76.83 ± 10.49	76.64 ± 9.76	77.41 ± 9.79	NS

ALT: alanine transferase, AST: aspartate transaminase, BUN: blood urine nitrogen, NS: not statistically significant ($p > 0.05$), * Significant difference ($p < 0.05$) *vs.* Control.

moods (*26*), neurobehavioral abilities (*27*), and problem solving (*28*). Convergent evidencegave us the signal that dopamine is the final common neurobiological pathway for the expression of TS symptoms (*29*). After reuptake by DA transporters, the DA was transformed into HVA in neurons, and released into the blood, and its concentration in plasma has been widely used to study the function of central DA in psychiatric disorders (*13,30-32*). Therefore, HVA is regarded as the major indicator of DA activity (*13,31*). The current study also revealed that the content of HVA increased in TS patients' sera, while there was no statistical difference in the content of DA after treatment with NDG and Hal. In contrast, neither DA nor HVA concentrations greatly changed for an 8-week period of medication in the placebo group. Based on the hypoactivity of dopamine systems in the brain involved in the pathophysiology of TS, we inferred that NDG could improve the symptoms of TS by enhancing the metabolism of DA *in vivo* and increasing the HVA content in sera. As a dopamine D2 receptor blocker, the mechanism fit for Hal. However, neither NDG nor Hal had an effect on the concentration of DA in sera, which suggested that DA outside the brain has no direct link to the pathophysiological changes in TS.

The research indicates generally that the neurotransmitter serotonin has an inhibitory action in the brain (*33,34*) and it is deeply involved in the regulation of emotion and behavior, including the inhibition of aggression (*35,36*). Serotonergic dysfunction has been reliably associated with the pathology of TS (*18*). As the main metabolite of 5-TH, 5-HIAA is released back into the blood after the metabolism of 5-TH in the central neural system, and 5-HIAA, and therefore, is also regarded as the major indicator of 5-TH activity (*22*). In this research, the results revealed that there was no statistical difference in the content of 5-TH and 5-HIAA after treatment in three groups. So we are unable to infer that NDG improves the symptoms of TS by enhancing metabolism of 5-TH.

From a developmental perspective, many GABAergic interneurons of the cerebral cortex clearly migrate tangentially from the same embryonic regions in the ganglionic eminence that also give rise to the GABAergic medium spiny projection neurons of the striatum (*37*). Could adverse events arising at a specific point in development, the differential loss of medium spiny projection neurons in the matrix compartment – account for the striatal imbalance and intracortical deficits in inhibition seen in some patients with Tourettesyndrome (*38*)? Because of the reported GABA abnormalities in the TS brain, and the possible immune abnormalities in blood and brain of TS subjects (*39*), we postulated that GABA might be involved in the pathophysiology of TS. In this study, we demonstrated that NDG and Hal could increase the level of GABA in sera and improve the symptoms in TS children.

The present study indicates that the symptoms of TS were alleviated and the content of HVA/GABA in sera was increased, but the DA, 5-TH, and 5-HIAA concentrations changed little after treatment with NDG or Hal on TS patients. Based on the above results, it could be inferred that NDG was effective on TS by regulating the DA and GABA system while increasing the content of HVA and GABA in sera, which is valuable for potential pharmacological findings in the clinical application of NDG.

GTSS was widely used to assess the severity of TS, which can be easily mastered for the symptoms

of TS children. For short-term effectiveness, both NDG and Hal can improve the clinical symptoms for TS children by YGTSS at different time points. However, Haloperidol had more side effects than NDG in the form of sedation, weight gain, extrapyramidal symptoms, QT prolongation, Nausea, Headache, and Anxiety. The results suggest that NDG is safe for TS children. NDG is promising to be a safe and effective medication as an alternative therapy for TS.

However, the present study has some limitations as follows. First, only short-term outcomes and adverse effects were observed for 8 weeks, which was limited for NDG as a synthetic therapeutic option pending further study on long-term outcomes. Second, we measured the contents of DA, HVA, 5-TH, 5-HIAA and GABA in sera to deduce the metabolism of neurotransmitters *in vivo*, which was indirect evidence for explaining the metabolism of neurotransmitters in brain. Furthermore, we did not analyze the metabolism of some other kinds of neurotransmitters beyond DA and 5-TH, which might also participate in the pathophysiological course of TS. Therefore, it is a great necessity to explore more meaningful evidenceof pharmacology for an effective and safe alternative treatment.

Acknowledgements

This work was supported by grants from Administration of Traditional Chinese Medicine of Shandong Province (NO.2005064) and Department of Science & Technology of Shandong Province (NO2011GGB14110).

References

1. Du JC, Chiu TF, Lee KM, Wu HL, Yang YC, Hsu SY, Sun CS, Hwang B, Leckman JF. Tourette syndrome in children: An updated review. Pediatr Neonatol. 2010; 51:255-264.
2. Cortese S, Lecendreux M, Bernardo BD, Mouren MC, Sbarbati A, Konofal E. Attention-deficit/hyperactivity disorder, Tourette's syndrome, and restless legs syndrome: The iron hypothesis. Medical Hypotheses. 2008; 70:1128-1132.
3. Grimaldi BL. The central role of magnesium deficiency in Tourette's syndrome: Causal relationships between magnesium deficiency, altered biochemical pathways and symptoms relating to Tourette's syndrome and several reported comorbid conditions. Med Hypotheses. 2002; 58:47-60.
4. Peterson BS, Leckman JF. The temporal dynamics of tics in Gilles de la Tourette syndrome. Biol Psychiatry. 1998; 44:1337-1348.
5. Oades RD. Differential measures of 'sustained attention' in children with attention-deficit hyperactivity or tic disorders: Relations to monoamine metabolism. Psychiatry Res. 2000; 93:165-178.
6. Tian Y, Gunther JR, Liao IH, Liu D, Ander BP, Stamova BS, Lit L, Jickling GC, Xu H, Zhan X, Sharp FR. GABA- and acetylcholine-related gene expression in blood correlate with tic severity and microarray evidence for alternative splicing in Tourette syndrome: A pilot study. Brain Res. 2011; 228-236.
7. Fachinetto R, Villarinho JG, Wagner C, Pereira RP, Avila DS, Burger ME, Calixto JB, Rocha JB, Ferreira J. Valeriana officinalis does not alter the orofacial dyskinesia induced by haloperidol in rats: Role of dopamine transporter. Prog Neuropsychopharmacol Biol Psychiatry. 2007; 31:1478-1486.
8. Yoo HK, Kim JY, Kim CY. A pilot study of aripiprazole in children and adolescents with Tourette's disorder. J Child Adolesc Psychopharmacol. 2006; 16:505-506.
9. Cui XY, Wang YL, Kokudo N, Fang DZ, Tang W. Traditional Chinese medicine and related active compounds against hepatitis B virus infection. Biosci Trends. 2010; 4:39-47.
10. Baeza I, Castro-Fornieles J, Deulofeu R, de la Serna E, Goti J, Salva J, Bernardo M. Plasma homovanillic acid differences in clinical subgroups of first episode schizophrenic patients. Psychiatry Res. 2009; 168:110-118.
11. Qi FH, Li AY, Inagaki Y, Gao JJ, Li JJ, Kokudo N, Li XK, Tang W. Chinese herbal medicines as adjuvant treatment during chemo- or radio-therapy for cancer. Biosci Trends. 2010; 4:297-307.
12. Zhao L, Li AY, Lv H, Liu FY, Qi FH. Traditional Chinese medicine Ningdong granule: The beneficial effects in Tourette's disorder. J Int Med Res. 2010; 38:169-175.
13. Lv H, Li A, Ma H, Liu F, Xu H. Effects of Ningdong granule on the dopamine system of Tourette's syndrome rat models. J Ethnopharmacol. 2009; 124:488-492.
14. Li JJ, Li ZW, Wang SZ, Qi FH; Zhao L, Lv H, Li AY. Ningdong granule: A complementary and alternative therapy in the treatment of attention deficit/hyperactivity disorder. Psychopharmacology. 2011; 216:501-509.
15. American Psychiatric Association (1994) Diagnostic and statistical manual of mental disorders, 4th ed. (DSM-IV). American Psychiatric Association, Washington, DC, USA.
16. Shapiro E, Shapiro AK, Fulop G, Hubbard M, Mandeli J, Nordlie J, Phillips RA. Controlled study of haloperidol, pimozide and placebo for the treatment of Gilles de la Tourette's syndrome. Arch Gen Psychiatry. 1989; 46:722-730.
17. Leckman JF, Riddle MA, Hardin MT, Ort SI, Swartz KL, Stevenson J, Cohen DJ. The Yale Global Tic Severity Scale: Initial testing of a clinician-rated scale of tic severity. J Am Acad Child Adolesc Psychiatry. 1989; 28:566-573.
18. Wong DF, Brasić JR, Singer HS, Schretlen DJ, Kuwabara H, Zhou Y, Nandi A, Maris MA, Alexander M, Ye W, Rousset O, Kumar A, Szabo Z, Gjedde A, Grace AA. Mechanisms of dopaminergic and serotonergic neurotransmission in Tourette syndrome: Clues from an in vivo neurochemistry study with PET. Neuropsychopharmacology. 2008; 33:1239-1251.
19. Albin RL, Mink JW. Recent advances in Tourette syndrome research. Trends Neurosci. 2006; 29:175-182.
20. Jimenez-Shahed J. Tourette syndrome. Neurol Clin. 2009; 27:737-755.
21. Müller-Vahl KR, Meyer GJ, Knapp WH, Emrich HM, Gielow P, Brücke T, Berding G. Serotonin transporter binding in Tourette Syndrome. Neurosci Lett. 2005; 385:120-125.

22. Seo D, Patrick CJ, Kennealy PJ. Role of Serotonin and Dopamine System Interactions in the Neurobiology of Impulsive Aggression and its Comorbidity with other Clinical Disorders. Aggress Violent Behav. 2008; 13:383-395.
23. Grados MA, Walkup JT. A new gene for Tourette's syndrome: A window into causal mechanisms. Trends Genet. 2006; 22:291-293.
24. Nieoullon A. Dopamine and the regulation of cognition and attention. Prog Neurobiol. 2002; 67:53-83.
25. Bohnen NI, Cham R. Postural control, gait, and dopamine functions in parkinsonian movement disorders. Clin Geriatr Med. 2006; 22:797-812.
26. Nutt D, Demyttenaere K, Janka Z, Aarre T, Bourin M, Canonico PL, Carrasco JL, Stahl S. The other face of depression reduced positive affect: The role of catecholamines in causation and cure. J Psychopharmacol. 2007; 21:461-471.
27. Staller JA, Faraone SV. Targeting the dopamine system in the treatment of attention-deficit/hyperactivity disorder. Expert Rev Neurother. 2007; 7:351-362.
28. Brooks DJ. Dopaminergic action beyond its effects on motor function: Imaging studies. J Neurol. 2006; 253: IV8-IV15.
29. Singer HS. Tourette's syndrome: From behavior to biology. Lancet Neurol. 2005; 4:149-159.
30. Baeza I, Castro-Fornieles J, Deulofeu R, de la Serna E, Goti J, Salva J, Bernardo M .Plasma homovanillic acid differences in clinical subgroups of first episode schizophrenic patients. Psychiatry Res. 2009; 168:110-118.
31. Dhir A, Kulkarni SK. Involvement of dopamine (DA)/ serotonin (5-HT)/sigma (sigma) receptor modulation in mediating the antidepressant action of ropinirole hydrochloride, a D2/D3 dopamine receptor agonist. Brain Res Bull. 2007; 74:58-65.
32. Soderstrom H, Blennow K, Sjodin AK, Forsman A. New evidence for an association between the CSF HVA/5-HIAA ratio and psychopathic traits. J Neurol Neurosurg Psychiatry. 2003; 74:918-921.
33. Daw N D, Kakade S, Dayan P. Opponent interactions between serotonin and dopamine. Neural Network. 2002; 15:603-616.
34. Yan, Z. Regulation of GABAergic inhibition by serotonin signaling in prefrontal cortex: Molecular mechanisms and functional implications. Mol Neurobiol. 2002; 26:203-216.
35. Davidson RJ, Putnam KM, Larson CL. Dysfunction in the neural circuitry of emotion regulation-A possible prelude to violence. Science.2000; 289:591-594.
36. Volavka, J. The neurobiology of violence: An update. J Neuropsychiatry Clin Neurosci. 1999; 11:307-314.
37. Anderson SA, Eisenstat DD, Shi L, Rubenstein JL. Interneuron migration from basal forebrain to neocortex: dependence on Dlx genes. Science. 1997; 278:474-476.
38. Ziemann U, Paulus W, Rothenberger A. Decreased motor inhibition in Tourette's disorder: Evidence from transcranial magnetic stimulation. Am J Psychiatry. 1997; 154:1277-1284.
39. Martino D, Dale RC, Gilbert DL, Giovannoni G, Leckman JF.Mov Disord. Immunopathogenic mechanisms in tourette syndrome: A critical review. Mov Disord. 2009; 24:1267-1279.

(*Received March 19, 2012; Revised April 10, 2011; Accepted April 24, 2012*)

BST
BioScience Trends

Guide for Authors

1. Scope of Articles

BioScience Trends is an international peer-reviewed journal. BioScience Trends devotes to publishing the latest and most exciting advances in scientific research. Articles cover fields of life science such as biochemistry, molecular biology, clinical research, public health, medical care system, and social science in order to encourage cooperation and exchange among scientists and clinical researchers.

2. Submission Types

Original Articles should be well-documented, novel, and significant to the field as a whole. An Original Article should be arranged into the following sections: Title page, Abstract, Introduction, Materials and Methods, Results, Discussion, Acknowledgments, and References. Original articles should not exceed 5,000 words in length (excluding references) and should be limited to a maximum of 50 references. Articles may contain a maximum of 10 figures and/or tables.

Brief Reports definitively documenting either experimental results or informative clinical observations will be considered for publication in this category. Brief Reports are not intended for publication of incomplete or preliminary findings. Brief Reports should not exceed 3,000 words in length (excluding references) and should be limited to a maximum of 4 figures and/or tables and 30 references. A Brief Report contains the same sections as an Original Article, but the Results and Discussion sections should be combined.

Reviews should present a full and up-to-date account of recent developments within an area of research. Normally, reviews should not exceed 8,000 words in length (excluding references) and should be limited to a maximum of 100 references. Mini reviews are also accepted.

Policy Forum articles discuss research and policy issues in areas related to life science such as public health, the medical care system, and social science and may address governmental issues at district, national, and international levels of discourse. Policy Forum articles should not exceed 2,000 words in length (excluding references).

Case Reports should be detailed reports of the symptoms, signs, diagnosis, treatment, and follow-up of an individual patient. Case reports may contain a demographic profile of the patient but usually describe an unusual or novel occurrence. Unreported or unusual side effects or adverse interactions involving medications will also be considered. Case Reports should not exceed 3,000 words in length (excluding references).

News articles should report the latest events in health sciences and medical research from around the world. News should not exceed 500 words in length.

Letters should present considered opinions in response to articles published in BioScience Trends in the last 6 months or issues of general interest. Letters should not exceed 800 words in length and may contain a maximum of 10 references.

3. Editorial Policies

Ethics: BioScience Trends requires that authors of reports of investigations in humans or animals indicate that those studies were formally approved by a relevant ethics committee or review board.

Conflict of Interest: All authors are required to disclose any actual or potential conflict of interest including financial interests or relationships with other people or organizations that might raise questions of bias in the work reported. If no conflict of interest exists for each author, please state "There is no conflict of interest to disclose".

Submission Declaration: When a manuscript is considered for submission to BioScience Trends, the authors should confirm that 1) no part of this manuscript is currently under consideration for publication elsewhere; 2) this manuscript does not contain the same information in whole or in part as manuscripts that have been published, accepted, or are under review elsewhere, except in the form of an abstract, a letter to the editor, or part of a published lecture or academic thesis; 3) authorization for publication has been obtained from the authors' employer or institution; and 4) all contributing authors have agreed to submit this manuscript.

Cover Letter: The manuscript must be accompanied by a cover letter signed by the corresponding author on behalf of all authors. The letter should indicate the basic findings of the work and their significance. The letter should also include a statement affirming that all authors concur with the submission and that the material submitted for publication has not been published previously or is not under consideration for publication elsewhere. The cover letter should be submitted in PDF format. For example of Cover Letter, please visit http://www.biosciencetrends.com/downcentre.php (Download Centre).

Copyright: A signed JOURNAL PUBLISHING AGREEMENT (JPA) form must be provided by post, fax, or as a scanned file before acceptance of the article. Only forms with a hand-written signature are accepted. This copyright will ensure the widest possible dissemination of information. A form facilitating transfer of copyright can be downloaded by clicking the appropriate link and can be returned to the e-mail address or fax number noted on the form (Please visit Download Centre). Please note that your manuscript will not proceed to the next step in publication until the JPA Form is received. In addition, if excerpts from other copyrighted works are included, the author(s) must obtain written permission from the copyright owners and credit the source(s) in the article.

Suggested Reviewers: A list of up to 3 reviewers who are qualified to assess the scientific merit of the study is welcomed. Reviewer information including names, affiliations, addresses, and e-mail should be provided at the same time the manuscript is submitted online. Please do not suggest reviewers with known conflicts of interest, including participants or anyone with a stake in the proposed research; anyone from the same institution; former students, advisors, or research collaborators (within the last three years); or close personal contacts. Please note that the Editor-in-Chief may accept one or more of the proposed reviewers or may request a review by other qualified persons.

Language Editing: Manuscripts prepared by authors whose native language is not English should have their work proofread by a native English speaker before submission. If not, this might delay the publication of your manuscript in BioScience Trends.

The Editing Support Organization can provide English proofreading, Japanese-English translation, and Chinese-English translation services to authors who want to publish in BioScience Trends and need assistance before submitting a manuscript. Authors can visit this organization directly at http://www.iacmhr.com/iac-eso/support.php?lang=en. IAC-ESO was established to facilitate manuscript preparation by researchers whose native language is not English and to help edit works intended for international academic journals.

4. Manuscript Preparation

Manuscripts should be written in clear, grammatically correct English and submitted as a Microsoft Word file in a single-column format. Manuscripts must be paginated and typed in 12-point Times New Roman font with 24-point line spacing. Please do not embed figures in the text. Abbreviations should be used as little as possible and should be explained at first mention unless the term is a well-known abbreviation (*e.g.* DNA). Single words should not be abbreviated.

Title Page: The title page must include 1) the title of the paper (Please note the title should be short, informative, and contain the major key words); 2) full name(s) and affiliation(s) of the author(s), 3) abbreviated names of the author(s), 4) full name, mailing address, telephone/fax numbers, and e-mail address of the corresponding author; and 5) conflicts of interest (if you have an actual or potential conflict of interest to disclose, it must be included as a footnote on the title page of the manuscript; if no conflict of

interest exists for each author, please state "There is no conflict of interest to disclose"). Please visit Download Centre and refer to the title page of the manuscript sample.

Abstract: A one-paragraph abstract consisting of no more than 250 words must be included. The abstract should briefly state the purpose of the study, methods, main findings, and conclusions. Abbreviations must be kept to a minimum and non-standard abbreviations explained in brackets at first mention. References should be avoided in the abstract. Key words or phrases that do not occur in the title should be included in the Abstract page.

Introduction: The introduction should be a concise statement of the basis for the study and its scientific context.

Materials and Methods: The description should be brief but with sufficient detail to enable others to reproduce the experiments. Procedures that have been published previously should not be described in detail but appropriate references should simply be cited. Only new and significant modifications of previously published procedures require complete description. Names of products and manufacturers with their locations (city and state/country) should be given and sources of animals and cell lines should always be indicated. All clinical investigations must have been conducted in accordance with Declaration of Helsinki principles. All human and animal studies must have been approved by the appropriate institutional review board(s) and a specific declaration of approval must be made within this section.

Results: The description of the experimental results should be succinct but in sufficient detail to allow the experiments to be analyzed and interpreted by an independent reader. If necessary, subheadings may be used for an orderly presentation. All figures and tables must be referred to in the text.

Discussion: The data should be interpreted concisely without repeating material already presented in the Results section. Speculation is permissible, but it must be well-founded, and discussion of the wider implications of the findings is encouraged. Conclusions derived from the study should be included in this section.

Acknowledgments: All funding sources should be credited in the Acknowledgments section. In addition, people who contributed to the work but who do not meet the criteria for authors should be listed along with their contributions.

References: References should be numbered in the order in which they appear in the text. Citing of unpublished results, personal communications, conference abstracts, and theses in the reference list is not recommended but these sources may be mentioned in the text. In the reference list, cite the names of all authors when there are fifteen or fewer authors; if there are sixteen or more authors, list the first three followed by *et al.* Names of journals should be abbreviated in the style used in PubMed. Authors are responsible for the accuracy of the references. Examples are given below:

Example 1 (Sample journal reference):
Inagaki Y, Tang W, Zhang L, Du GH, Xu WF, Kokudo N. Novel aminopeptidase N (APN/CD13) inhibitor 24F can suppress invasion of hepatocellular carcinoma cells as well as angiogenesis. Biosci Trends. 2010; 4:56-60.

Example 2 (Sample journal reference with more than 15 authors):
Darby S, Hill D, Auvinen A, *et al.* Radon in homes and risk of lung cancer: Collaborative analysis of individual data from 13 European case-control studies. BMJ. 2005; 330:223.

Example 3 (Sample book reference):
Shalev AY. Post-traumatic stress disorder: diagnosis, history and life course. In: Post-traumatic Stress Disorder, Diagnosis, Management and Treatment (Nutt DJ, Davidson JR, Zohar J, eds.). Martin Dunitz, London, UK, 2000; pp. 1-15.

Example 4 (Sample web page reference):
Ministry of Health, Labour and Welfare of Japan. Dietary reference intakes for Japanese. *http://www.mhlw.go.jp/houdou/2004/11/h1122-2a.html* (accessed June 14, 2010).

Tables: All tables should be prepared in Microsoft Word or Excel and should be arranged at the end of the manuscript after the References section. Please note that tables should not in image format. All tables should have a concise title and should be numbered consecutively with Arabic numerals. If necessary, additional information should be given below the table.

Figure Legend: The figure legend should be typed on a separate page of the main manuscript and should include a short title and explanation. The legend should be concise but comprehensive and should be understood without referring to the text. Symbols used in figures must be explained.

Figure Preparation: All figures should be clear and cited in numerical order in the text. Figures must fit a one- or two-column format on the journal page: 8.3 cm (3.3 in.) wide for a single column, 17.3 cm (6.8 in.) wide for a double column; maximum height: 24.0 cm (9.5 in.). Please make sure that the symbols and numbers appeared in the figures should be clear. Please make sure that artwork files are in an acceptable format (TIFF or JPEG) at minimum resolution (600 dpi for illustrations, graphs, and annotated artwork, and 300 dpi for micrographs and photographs). Please provide all figures as separate files. Please note that low-resolution images are one of the leading causes of article resubmission and schedule delays. All color figures will be reproduced in full color in the online edition of the journal at no cost to authors.

Units and Symbols: Units and symbols conforming to the International System of Units (SI) should be used for physicochemical quantities. Solidus notation (*e.g.* mg/kg, mg/mL, mol/mm^2/min) should be used. Please refer to the SI Guide www.bipm.org/en/si/ for standard units.

Supplemental data: Supplemental data might be useful for supporting and enhancing your scientific research and BioScience Trends accepts the submission of these materials which will be only published online alongside the electronic version of your article. Supplemental files (figures, tables, and other text materials) should be prepared according to the above guidelines, numbered in Arabic numerals (*e.g.*, Figure S1, Figure S2, and Table S1, Table S2) and referred to in the text. All figures and tables should have titles and legends. All figure legends, tables and supplemental text materials should be placed at the end of the paper. Please note all of these supplemental data should be provided at the time of initial submission and note that the editors reserve the right to limit the size and length of Supplemental Data.

5. Submission Checklist

The Submission Checklist will be useful during the final checking of a manuscript prior to sending it to BioScience Trends for review. Please visit Download Centre and download the Submission Checklist file.

6. Online Submission

Manuscripts should be submitted to BioScience Trends online at http://www.biosciencetrends.com. The manuscript file should be smaller than 5 MB in size. If for any reason you are unable to submit a file online, please contact the Editorial Office by e-mail at office@biosciencetrends.com.

7. Accepted Manuscripts

Proofs: Galley proofs in PDF format will be sent to the corresponding author via e-mail. Corrections must be returned to the editor (proof-editing@biosciencetrends.com) within 3 working days.

Offprints: Authors will be provided with electronic offprints of their article. Paper offprints can be ordered at prices quoted on the order form that accompanies the proofs.

Page Charge: Page charges will be levied on all manuscripts accepted for publication in BioScience Trends ($140 per page for black white pages; $340 per page for color pages). Under exceptional circumstances, the author(s) may apply to the editorial office for a waiver of the publication charges at the time of submission.

(*Revised October 2011*)

Editorial and Head Office:
Pearl City Koishikawa 603
2-4-5 Kasuga, Bunkyo-ku
Tokyo 112-0003 Japan
Tel: +81-3-5840-8764
Fax: +81-3-5840-8765
E-mail: office@biosciencetrends.com

BST
BioScience Trends

JOURNAL PUBLISHING AGREEMENT (JPA)

Manuscript No.:

Title:

Corresponding Author:

The International Advancement Center for Medicine & Health Research Co., Ltd. (IACMHR Co., Ltd.) is pleased to accept the above article for publication in BioScience Trends. The International Research and Cooperation Association for Bio & Socio-Sciences Advancement (IRCA-BSSA) reserves all rights to the published article. Your written acceptance of this JOURNAL PUBLISHING AGREEMENT is required before the article can be published. Please read this form carefully and sign it if you agree to its terms. The signed JOURNAL PUBLISHING AGREEMENT should be sent to the BioScience Trends office (Pearl City Koishikawa 603, 2-4-5 Kasuga, Bunkyo-ku, Tokyo 112-0003, Japan; E-mail: **office@biosciencetrends.com**; Tel: **+81-3-5840-8764**; Fax: **+81-3-5840-8765**).

1. Authorship Criteria

As the corresponding author, I certify on behalf of all of the authors that:

1) The article is an original work and does not involve fraud, fabrication, or plagiarism.
2) The article has not been published previously and is not currently under consideration for publication elsewhere. If accepted by BioScience Trends, the article will not be submitted for publication to any other journal.
3) The article contains no libelous or other unlawful statements and does not contain any materials that infringes upon individual privacy or proprietary rights or any statutory copyright.
4) I have obtained written permission from copyright owners for any excerpts from copyrighted works that are included and have credited the sources in my article.
5) All authors have made significant contributions to the study including the conception and design of this work, the analysis of the data, and the writing of the manuscript.
6) All authors have reviewed this manuscript and take responsibility for its content and approve its publication.
7) I have informed all of the authors of the terms of this publishing agreement and I am signing on their behalf as their agent.

2. Copyright Transfer Agreement

I hereby assign and transfer to IACMHR Co., Ltd. all exclusive rights of copyright ownership to the above work in the journal BioScience Trends, including but not limited to the right 1) to publish, republish, derivate, distribute, transmit, sell, and otherwise use the work and other related material worldwide, in whole or in part, in all languages, in electronic, printed, or any other forms of media now known or hereafter developed and the right 2) to authorize or license third parties to do any of the above.

I understand that these exclusive rights will become the property of IACMHR Co., Ltd., from the date the article is accepted for publication in the journal BioScience Trends. I also understand that IACMHR Co., Ltd. as a copyright owner has sole authority to license and permit reproductions of the article.

I understand that except for copyright, other proprietary rights related to the Work (*e.g.* patent or other rights to any process or procedure) shall be retained by the authors. To reproduce any text, figures, tables, or illustrations from this Work in future works of their own, the authors must obtain written permission from IACMHR Co., Ltd.; such permission cannot be unreasonably withheld by IACMHR Co., Ltd.

3. Conflict of Interest Disclosure

I confirm that all funding sources supporting the work and all institutions or people who contributed to the work but who do not meet the criteria for authors are acknowledged. I also confirm that all commercial affiliations, stock ownership, equity interests, or patent-licensing arrangements that could be considered to pose a financial conflict of interest in connection with the article have been disclosed.

Corresponding Author's Name (Signature):

Date: